Synthesis of Nano-scale Materials through Miniemulsion Polymerization Method and their Application in Textiles

vorgelegt von
Master of Science – Chemistry
Mahmoud Elgammal
Aus Monofyia, Ägypten

Von der Fakultät II – Mathematik und Naturwissenschaften
der Technischen Universität Berlin
zur Erlangung des akademischen Grades

Doktor der Naturwissenschaften
Dr. rer. nat.

genehmigte Dissertation

Promotionsausschuss:

Vorsitzender:	Prof. Dr. rer. nat. Reinhard Schomäcker	(TUB, Berlin)
Gutachter:	Prof. Dr. rer. nat. Michael Gradzielski	(TUB, Berlin)
Gutachter:	Prof. Dr. rer. nat. André Laschewsky	(University of Potsdam)

Tag der wissenschaftlichen Aussprache: 01. April 2015

Berlin 2016

“To my Mother”

This thesis is dedicated to my mother, who passed away suddenly and unexpectedly in the last day of Febraury 2015. She was one of the most inspiring and strong women I ever knew. I attribute all my success in my life to the moral, inntelctual and physical education I received from her.

Acknowledgements

First, I would like to express my sincere gratitude to my supervisor, Prof. Dr. Michael Gradzielski, who gave me the opportunity to accomplish my thesis at TU Berlin. His support and proficient guidance gave me a great inspiration and motivation. I would like to particularly acknowledge the members of the doctoral board, Prof. Dr. André Laschewsky for the review of the present work. In addition, my gratitude goes to Prof. Dr. Reinhard Schomäcker for taking the chair of the examination board.

My deep thanks to the Institute of Textile Chemistry and Chemical Fibers Denkendorf (ITCF) and particularly Dr. Reinhold Schneider and his group members, Mrs. Angelika Lenz, Mrs. Sabine Frick and Mrs. Stefanie Brenner for the great support to implement the textile printing application and assessment part.

Prof. Dr. Conxita Solans (CSIC, Barcelona, Spain) is gratefully acknowledged for her support and her enlightening thoughts on nanoemulsions during my internship in Barcelona.

I would also like to acknowledge the financial support by the German Academic Exchange Service (DAAD) and the Egyptian Ministry of Higher Education without which this thesis would not have been possible.

I am deeply thankful to all my colleagues within the Stranski Laboratories for their kindness and encouragements. Special thanks go to Dr. Sylvain Prevost, Dr. Ingo Hoffmann, Dr. Katharina Bressel, Dr. Peggy Heunemann, Carolin Ganas, Leonardo Chiappisi and Andreas Klee, for their valuable help and fruitful discussions. I am also grateful to Dr. Rastko Joksimovic for the proof correction and for all Stranski laboratories members for their friendly support and scientific inputs.

I would like to express my sincere gratitude to the secretaries, Christiane, Petra, Maria and CTA's, Michaela, Gabriele, Jana, Monika and René, for their help with the administrative and experimental work, and their easy-going way of accommodating everything.

I am also very grateful to all members of my family and specially my wife for her unconditional support and encouragement. My deepest gratitude goes to my daughters Rawda and Nour who gave me the spirit and self-motivation to keep going and finish up my thesis.

I am particularly thankful to my parents and specially my mother, who gave me and taught me unconditional love and to whom I would like to dedicate this work.

Abstract

The present work deals with the preparation of nanosized copolymer latexes by the polymerization in miniemulsions prepared by the classical high energy and the low energy phase inversion concentration (PIC) methods. In addition, the encapsulation of various organic pigments with copolymer latex layers was carried out on the basis of miniemulsion polymerization. The obtained nanosized copolymer particles or encapsulated pigments have been successfully used as binders or hybrid binders for textile printing applications.

The first part deals with the preparation of nanosized copolymer latexes in a diameter size range between (50-100 nm) by the classical miniemulsion polymerization method. The copolymer latexes composed mainly of a high content of the soft butyl acrylate monomer (BA) and a low content of the hard methyl methacrylate (MMA) monomer. The addition of small amounts of functional monomers such as methacrylic acid MAA and N-methylol acrylamide NMA to some miniemulsion recipes allowed to impart cross-linking sites and functionality to the copolymer chains. The particle size analysis, structure characterization and thermal properties of the latexes were investigated by many analytical techniques such as dynamic light scattering (DLS), small angle neutron scattering (SANS), transmission electron microscopy (TEM), gel permeation chromatography (GPC), and differential scanning calorimetry (DSC). The optimized miniemulsion latexes were applied successfully as binders for the pigment printing and inkjet printing of cotton fabrics. The main objective of this part was to examine the application of the miniemulsion latexes as binders in the textile printing processes in order to reduce the risk of agglomeration and cloaking of the printer screens and nozzles during the printing process. The evaluation of the printed fabrics showed that the miniemulsion binders with their smaller size offered technological advantages over the conventional processes for the conventional and inkjet printing processes as well as the better print properties. Accordingly by optimized use of the miniemulsion method one is not only able to control the particle size but also to improve the properties of these latexes for textile applications.

In the second part, we studied the encapsulation of organic pigments with polymer latex layers by miniemulsion polymerization. Such polymer-encapsulated pigments then can be applied for inkjet printing without addition of separate binder additives, thereby reducing the risk of unfavorite interactions between the separate latex and pigment particles. The encapsulation of C.I. Pigment red 112 was systematically studied by a miniemulsion polymerization of pigment/butyl acrylate-co-methyl methacrylate (BA-MMA) or styrene-co-butyl acrylate (St-BA) copolymers. The ratio of monomer to pigment was varied in order to find optimum conditions for the preparation of self-curable hybrid pigment inks for the textile inkjet printing application. The particle size and polydispersity of the pigment dispersions and pigment hybrid latex particles were investigated by dynamic light scattering (DLS), disc centrifuge particle size analyzer and transmission electron microscopy (TEM). The efficiency of the polymer encapsulation and the thermal properties of the hybrid inks were studied by thermogravimetric analysis (TGA) and differential scanning calorimetry (DSC). The evaluation of the inkjet printing of cotton fabrics with different encapsulated and non-encapsulated pigment colors showed that the encapsulated inks without addition of separate polymer latex binder generate fully satisfying values that compare favourably in terms of color strength, rubbing and washing fastness to the non-encapsulated conventional inks, while avoiding problems of clogging and colloidal instability.

In the last part, the low energy phase inversion composition (PIC) method was used for the formation of monomer based nanoemulsions from a system composed of monomer/Brij78/water. These nanoemulsions were used as templates for generating polymer and copolymer nanoparticles. Styrene was used as monomer for studying the phase diagram, where parameters such as the O/S ratio and water addition rate influence the formation of the nanoemulsion and the structure of the final polymer particles. Hexadecane was added to the oil phase with a concentration 4 wt% (relative to the oil) to achieve stability against Oswald ripening. Nanoemulsions with a fixed water content of 80 wt% and O/S ratios from 0.25 to 9 generated polymer particles with diameters between 30 to 110 nm as determined from dynamic light scattering and transmission electron microscopy. The polydispersity of the polymer nanoparticles was found to be dependent on the O/S ratio. Different copolymer latexes based on styrene, butyl acrylate and methyl methacrylate were prepared with a fixed O/S ratio 9 and water content 80 %, applied successfully as binders for the inkjet printing of cotton fabrics and compared to corresponding copolymer latexes prepared by the high-energy methods or the conventional methods. The results indicated that PIC method constitutes a very interesting and innovative way to generate nanosized polymer latex particles using a simple setup of emulsification experiments.

Zusammenfassung

In der vorliegenden Arbeit wurden die Herstellung von Copolymer Latices durch die klassische Miniemulsionspolymerisation und die bisher hierfür noch wenig eingesetzte Phase Inversion Concentration (PIC) Methode untersucht. Zudem wurde die Verkapselung verschiedener Pigmentfarben über das Konzept der Miniemulsionspolymerisation durchgeführt. Die durch die verschiedenen Methoden hergestellten Copolymer Teilchen bzw. die verkapselten Pigmente wurden erfolgreich als Bindemittel für Textildruckanwendungen angewendet.

Das erste experimentelle Kapitel beschäftigt sich mit der Herstellung von Copolymer Latices im Größenbereich von 50-100 nm hergestellt durch die klassische Miniemulsionspolymerisation. Diese Copolymer Latices bestehen hauptsächlich aus einem hohen Anteil an weichem Butylacrylat-Monomers (BA) und einem niedrigen Gehalt an hartem Methylmethacrylat (MMA) Monomer. Die strukturelle Charakterisierung und die thermischen Eigenschaften der Latex Teilchen erfolgte durch viele analytische Verfahren, wie dynamische Lichtstreuung (DLS), Kleinwinkelneutronenstreuung (SANS), Transmissionselektronenmikroskopie (TEM), Gel-Permeations-Chromatographie (GPC) und Registrierende Differentialkalorimetrie (DSC). Die optimierten Miniemulsion Latices wurden dann erfolgreich als Bindemittel für den Pigmentdruck und Tintenstrahldruck von Gewebe aus Baumwolle eingesetzt. Das Hauptziel dieser Teil der Arbeit war es, die Anwendung der Miniemulsion Latices als Bindemittel in Textildruckverfahren zu untersuchen, wobei diese das Risiko von Agglomeration und damit das Verstopfen der Düsen während des Druckprozesses verringern sollen. Dieser Nachteil resultiert meist aus unerwünscht hohen Partikelgrößen, der Form der herkömmlichen Bindemitteln oder auch anderen Bestandteilen. Die Auswertung der Druckexperimente ergaben, dass die Miniemulsion basierten Bindemittel mit ihrer geringeren Größe technologische Vorteile gegenüber den herkömmlichen Verfahren bieten, sowohl für das konventionelle Druckverfahren als auch für das Tintenstrahldruckverfahren und dabei auch zu verbesserten Druckeigenschaften führen.

Der zweite Teil der Dissertation befasst sich mit der Verkapselung des organischen Pigments durch Polymerlatex Schichten, um die Agglomeration der Pigmentpartikel zu minimieren und ihre Stabilität und Dispergierbarkeit zu verbessern, was zu deren verbesserten Anwendbarkeit beitragen soll. Die Verkapselung der Pigmente wurde durch Miniemulsionspolymerisation mit verschiedenen Monomeren wie Styrol, Methylmethacrylat oder Butylacrylat durchgeführt. Die Analyse der Partikelgröße sowie der Einkapselungseffizienz der verkapselten Pigmente wurde mit Hilfe vieler analytischer Methoden untersucht und mit den nicht verkapselten Pigmenten verglichen. Die verkapselten Pigmente wurden dann erfolgreich als Tinten formuliert und ohne technische Probleme, wie das Verstopfen der Düsen der Druckmaschinen, für das Tintenstrahldrucken von Gewebe aus Baumwolle verwendet.

Der letzte Teil des Projektes beschäftigte sich mit der Herstellung von Latex Teilchen mit einem Durchmesser von ca. 30-100 nm, die durch Nanoemulsionspolymerisation hergestellt wurden, wobei die Nanoemulsionen durch die Phase Inversion Concentration (PIC) Methode hergestellt wurden. Die monomerhaltigen Nanoemulsionen waren Systemen bestehend aus Wasser, Monomer und nichtionischen Tensids. Wir verwendeten Styrol als Monomer für die systematische Untersuchung des Phasenverhaltens und der Bildung der Monomer-Nanoemulsion sowie deren anschließender Polymerisation. Das Phasenverhalten des Systems aus Wasser / Brij 78 (Polyoxyethylen (20) Stearylether) / Styrol ergab den geeigneten Bereich, in dem mit Monomer Nanoemulsionen gebildet werden können. Die Polymerisation in den PIC Nanoemulsionen wurde dann mit verschiedenen Monomeren durchgeführt, um entsprechend unterschiedliche Copolymerpartikel zu synthetisieren. Die Nanoemulsion Latices wurden dann wiederum für die Anwendung als Bindemittel für die normale Bedruckung und den Tintenstrahldruck von Gewebe aus Baumwolle getestet und verglichen mit Copolymeranaloga die über das klassische Miniemulsionsverfahren erhalten worden waren. Diese zeigte, dass die Untersuchung solcher PIC Nanoemulsionen und deren anschließende Polymerisation eine sehr interessante und innovative Möglichkeit darstellt, um neuartige Nanopolymerlatexpartikel für Druckanwendungen zu erzeugen.

Table of Contents **iv**

1. Motivation, objectives and thesis outline

1.1. Motivation

In the last decade, impressive application prospects of the colloidal nanosized materials in a wide variety of technical applications and consumer products (e.g. pharmaceutical, biomedical, cosmetic, electronic, agrochemical, coating and paint, food and energy) have led to a significant increase in production and manufacture of nanomaterials [1]. Nowadays, the application of nano-structured materials in textile-wet processes opened new opportunities to improve the performances and properties of the existing material and develop fibers, composites, and novel finishing methods [2]. Recent reports and publications revealed that nanoparticles, due to their diverse functions, might impart flame retardation, UV-blocking, water repellence, self-cleaning, and antimicrobial properties to the textile fabrics [3-5]. In addition, colloidal polymer particles, so-called polymer latexes, are commonly used for textile processes and in practice, as binding agents in the pastes and formulations of textile pigment and inkjet printing, an industrially enormously important process [6-9]. The properties of these colloid systems are largely controlled by their particle size and surface characteristics and are of fundamental importance for their potential applications. Several processes, many of which involve an initial oil in water (O/W) emulsion in which the stabilization of the particles is maintained by a surfactant molecule, can obtain the preparation of polymeric nanoparticles with well-defined size distributions. The polymer latexes start out as monomer emulsions, i.e., monomer droplets immiscibly dispersed in water. The emulsions are subsequently polymerized to form the latex particles. Usually, conventional (macro) emulsion or microemulsion polymerization is used to prepare these latexes. However, even though these types of heterophase polymerization are widely applied, one has to be aware that a restricted set of polymer reactions can be performed in this way. On the other hand, miniemulsion polymerization, sometimes called nanoemulsion polymerization, represents a convenient method to generate and control the size distributions of polymer particles in the colloidal systems [10, 11]. Miniemulsion polymerization provides many distinct advantages over the conventional emulsion polymerization because the monomer droplets are directly polymerized, whereas in the case of emulsion polymerization, the monomer is polymerized in the micelles and needs to travel through the aqueous phase. The polymerization of very hydrophobic monomers is thus difficult in the case of emulsion polymerization owing to limited diffusion through the aqueous phase. The miniemulsion polymerization does not suffer from these limitations and can lead to the polymerization of very

hydrophobic as well as very hydrophilic monomers [10]. The amount of surfactant used for stabilizing miniemulsions against collision is efficiently used resulting in an incomplete coverage of the droplets and are thus dubbed critically stabilized systems. Moreover, in a miniemulsion system, no free micelles exist [11]. The classical aqueous miniemulsions are obtained via a high energy input to a mixture of monomer, water, surfactant and a highly water-insoluble compound (added in the monomer), the so-called hydrophobe. On a laboratory scale, ultrasonication is used most often, while on industrial scale, high-pressure homogenizers are applied. Because of the high shear, fission and fusion of the droplets occur until a steady state is reached [12]. The role of the hydrophobe, which is housed in the oil phase, is to prevent the growth of the large droplets at the expense of the smaller droplets via diffusion, which is known as Ostwald ripening, while the surfactant prevents droplet coalescence [13-14]. The polymerization of these droplets leads to particles which ideally keep their size (with only a slight reduction in size because of density variation) [15]. Wide ranges of ionic and nonionic surfactants have been used, leading to polymer latexes with different surface charges and colloidal stability [16-19]. Therefore, miniemulsion polymerization could be an effective method for the generation of polymer or copolymer latex nanoparticles with desired particle size range and high degree of monodispersity. Moreover, the miniemulsion approach can be used for the polymer encapsulation of nanoparticles that are more hydrophobic than the miniemulsion monomer. In this method, the nanoparticles are dispersed in the monomer phase without any former treatment in which the nanoparticles dispersion and monomer miniemulsion are subjected together to co-sonication and subsequently polymerized to produce effective particle encapsulation [20]. Using this method, organic and inorganic pigment particles can be encapsulated efficiently by different types of polymer. The polymer encapsulation of organic pigments enhances the stability and dispersibility of the particles in ink formulations by reducing the pigment particle–particle interactions and thereby lowering the risk of the agglomeration of the pigment particles. Additionally, the ratio of pigments to polymer can be varied over a wide range, producing polymer encapsulated pigment inks with self-curable function without addition of separate polymer binders. On the other hand, the generation of polymer nanoparticles by the polymerization in miniemulsion/nanoemulsion templates prepared by the low energy condensation method may be considered as a competitive approach for the classical miniemulsion method due to the required energy input for the preparation of such miniemulsions. The low energy methods depend on the phase transition that takes place spontaneously during the emulsification as a result of the changes in the curvature of the surfactant molecules, mostly non-ionic surfactants [21]. The phase transition could be achieved

at constant composition by changing the curvature of surfactants with temperature, which is well known as phase inversion temperature method, (PIT) [22-23], or at constant temperature by varying, the composition of the system and that is known as phase inversion composition (concentration) method, (PIC) [24-26].

1.2 Objectives and thesis outline

Although many previous publications and reports have dealt with the synthesis of polymer latex nanoparticles and polymer encapsulated hybrid particles through the classical miniemulsion polymerization, the design and orientation of these nano-structured materials for the textile applications may be considered as a novel approach and need further investigations. On the other hand, the formation of monomer-nanoemulsion/miniemulsion templates by means of low energy input methods is a very interesting approach, not only from a fundamental scientific point of view but also for many practical applications. Using this method, O/W miniemulsion/nanoemulsion shall be achieved by a simple experimental method, where polymer nanoparticles are generated upon subsequent polymerization. To the best of our knowledge, the generation of monodisperse polymer nanoparticles by the low energy methods and in particular the phase inversion composition (concentration) is considered as a novel synthetic approach as well as their potential application for textile processes.

In the first part of the thesis, we are particularly interested to prepare monodisperse nanosized copolymer latexes in diameter size range between 50-100 nm by the classical miniemulsion polymerization method. The main objective of this part was to examine the application of the synthesized monodisperse miniemulsion latexes as binders in the textile printing and inkjet printing processes and to compare their properties to conventional binders prepared by the (macro) emulsion polymerization. The miniemulsion copolymer latexes composed mainly of a high content of the soft butyl acrylate monomer (BA) and a low content of the hard methyl methacrylate (MMA) monomer. The particle size analysis, structure characterization and thermal properties of the latexes were investigated by many physico-chemical characterization methods such as dynamic light scattering (DLS), small angle neutron scattering (SANS), transmission electron microscopy (TEM), gel permeation chromatography (GPC), proton nuclear magnetic resonance (^{1}H-NMR) and differential scanning calorimetry (DSC).

In the second part of the project, we studied the encapsulation of the organic pigments with polymer latex layers by the miniemulsion polymerization with different monomers such as styrene, methyl methacrylate, butyl acrylate. The particle size analysis as well as the encapsulation efficiency of the encapsulated pigments were studied by many analytical methods and compared to the non-encapsulated pigment. The general aim of these investigations was to

optimize, by a miniemulsion based polymerization in a systematic way, the conditions for preparing latex encapsulated pigments with long-time stability and low tendency of clogging of printing nozzles, which are essential prerequisites for their successful application in inkjet printing.

In the final part, we studied a novel approach for the synthesis of polymer latex nanoparticles by subsequent polymerization in monomer-nanoemulsion templates obtained by phase inversion composition (PIC) method. The monomer-nanoemulsions were prepared from systems consisting of water, monomer and non-ionic surfactant. We used styrene as monomer for the systematic study of the monomer-nanoemulsion formation and their subsequent polymerization. The phase behavior study of system consisting of water/ Brij 78 (Polyoxyethylene (20) stearyl ether)/ styrene was investigated in order to study the evolution of the system and reach to the suitable region at which monomer nanoemulsions could be formed. The polymerization in the PIC nanoemulsion systems using different monomers was performed to synthesize different copolymer nanoemulsion particles. The nanoemulsion copolymer latexes were then tested for application as binding agents for the printing and inkjet printing of cotton fabrics and compared to their miniemulsion copolymer analogs prepared by the high energy method. In general, the study of such PIC nanoemulsions and their subsequent polymerization constitutes a very interesting and innovative way to produce nanosized polymer latex particles using a simple setup of emulsification experiments.

2. Introduction and theoretical background

2.1. Emulsion principles

The focus of this thesis is on the generation of polymer nanoparticles and hybrid particles from mini (nano) emulsion systems. Therefore, it is important to point out the fundamental principles of emulsions, their definition and structural characteristics, stabilization and method of preparation.

2.1.1. Definition and stabilization of emulsions

Emulsions are classes of disperse systems consisting of two immiscible liquids. The liquid droplets (the disperse phase) are dispersed in a liquid medium (the continuous phase). Several classes of emulsion may be distinguished, namely oil-in-water (O/W) (e.g. milk), water-in-oil (W/O) (e.g. margarine) and oil-in-oil (O/O). The latter class may be exemplified by an emulsion consisting of a polar oil (e.g. propylene glycol) dispersed in a non-polar oil (paraffinic oil), and vice versa. In order to disperse two immiscible liquids a third component is required, namely the emulsifier; the choice of emulsifier is crucial not only for the formation of the emulsion but also for its long-term stability [27–29]. It should be noted that beside this simple emulsion phase even more sophisticated structures are known (e.g. w/o/w or o/w/o) that are irrelevant for this thesis.

Several processes related to the breakdown of emulsions may occur upon storage, which depend on many parameters such as, the particle size distribution and the density difference between the droplets and the medium, the magnitude of the attractive versus repulsive forces (which determines flocculation), the solubility of the disperse droplets and the particle size distribution, which in turn determines Ostwald ripening and the stability of the liquid film between the droplets, which determines coalescence and phase inversion. A summary of the various breakdown processes are illustrated schematically in Figure 2.1. However, to suppress the break down processes, such as coalescence, phase separation and flocculation, surface-active agents, known as surfactants, are required to stabilize the emulsions. Such compounds lower surface tension between the dispersed and continuous phases; thus, they favor the formation of kinetically stable emulsion droplets, according to the amphiphilic character of the surfactant molecules. Amphiphiles are chemical compounds that possess both a hydrophilic (water loving) and lipophilic (fat-loving) part in the overall molecular structure, whereas generally the hydrophilic head group is oriented towards the water and the lipophilic tail in oil-direction. Their head group as anionic, cationic, and nonionic or amphoters usually classify surfactants.

However, the addition of a highly water insoluble and low molecular weight hydrophobe in the oil phase acts to prevent the diffusional degradation of the droplets i.e. Ostwald ripening [30].

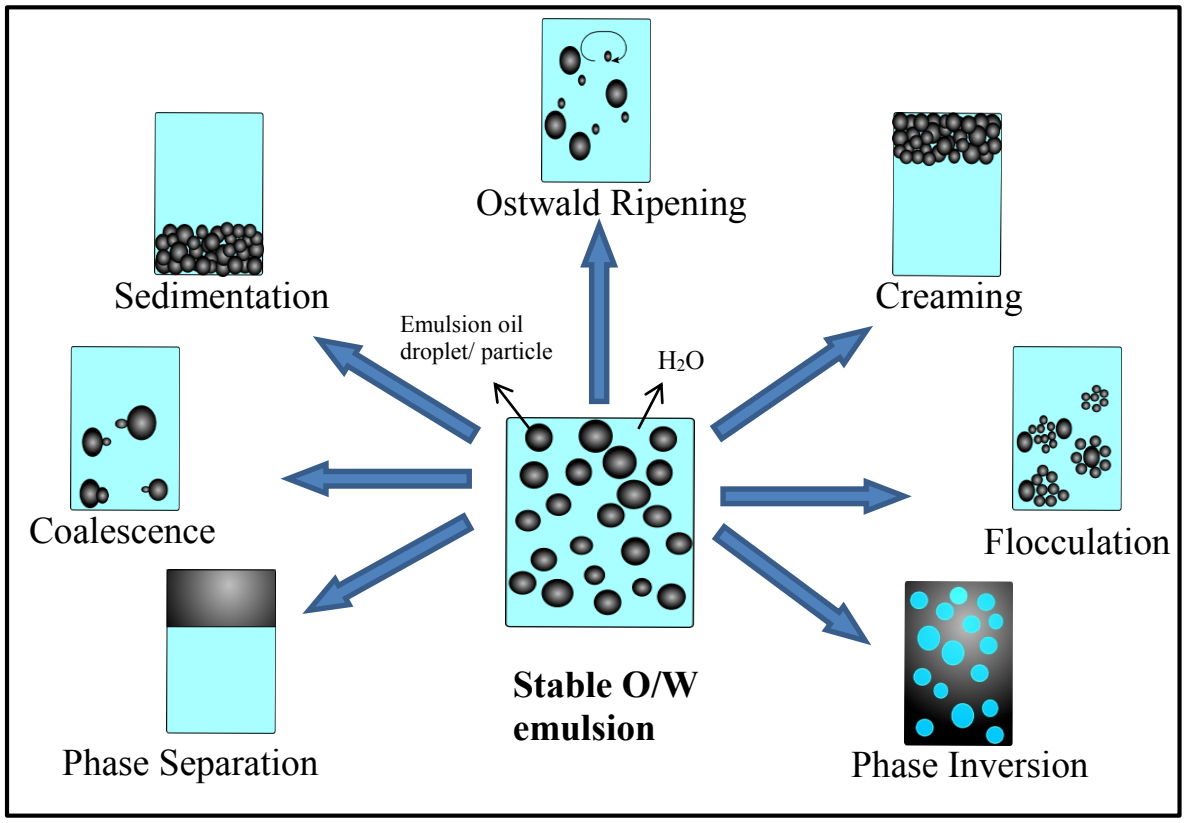

Fig.2.1 Schematic representation of the various breakdown processes in emulsions

2.1.2. Emulsification methods

Since our work is dealing with the preparation of the miniemulsion/nanoemulsion droplets by means of high and low energy methods, it is essential to briefly describe the initial preparation of the emulsions by the both methods.

2.1.2.1. High energy methods

The dispersion of a fluid into another one requires always a certain amount of energy for amplifying the boundary surface between both phases [31]. Several procedures and techniques have been used for the emulsion preparation by applying external energy to breakdown the droplets of the bulk phase into smaller ones. The applied equipment ranges from simple static mixers and general stirrers to high-speed mixers such as the Ultra-Turrax, colloid mills and high-pressure homogenizers, and ultrasound generators [32-39]. The method of preparation can be either continuous or batch-wise. The high energy required for the formation of small droplets can be understood from a consideration of the Laplace pressure Δp (the difference in pressure between inside and outside the droplet), as given by Equations 2.1 and 2.2.

$$\Delta \boldsymbol{p} = \boldsymbol{\gamma} \left(\frac{\mathbf{1}}{\boldsymbol{r1}} + \frac{\mathbf{1}}{\boldsymbol{r2}}\right) \qquad (2.1)$$

where r_1 and r_2 are the two principal radii of curvature.

For a perfectly spherical droplet $r_1 = r_2 = r$ and

$$\Delta \boldsymbol{p} = \left(\frac{\boldsymbol{2\gamma}}{\boldsymbol{r}}\right) \qquad (2.2)$$

For a hydrocarbon droplet with radius 100 nm, and γ =50mNm^{-}1, $\Delta p \sim 10^6$ Pa (10 atm).

In order to break up a drop into smaller droplets it must be strongly deformed, and this deformation increases $\boldsymbol{\Delta p}$. This is illustrated in Figure 2.2, which shows the situation when a spherical drop deforms and forms smaller droplets under the action of cavitation.

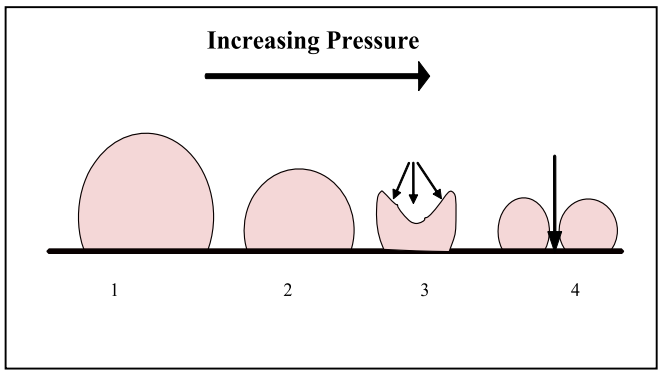

Fig.2.2 Schematic representation of the cavitation of a drop to small droplets as a result of the increase in Laplace pressure.

2.1.2.2 Low energy methods

The low energy methods achieve emulsification spontaneously as a result of the changes in the curvature of the non-ionic surfactant [21]. In 1878, Gad [40] reported for the first time observations about a spontaneous emulsification of oil droplets, containing free fatty acids, in alkaline solutions [41] without any mechanical shaking. Thereby, the emulsion formation is initiated by the stored chemical energy of the individual components and released upon contact [42]. In general the low energy approach is based mainly on phase transition of the system which could be achieved at constant composition by changing the curvature of surfactants with temperature which is well known as phase inversion temperature method, (PIT) [22, 23], or at constant temperature by varying the composition of the system and known as phase inversion composition method, (PIC) [24-26].

2.1.2.2.1 Phase Inversion Temperature approach (PIT)

This method was developed by Shinoda et al., a Japanese scientist in 1969 [22, 23]. Shinoda and co-workers found that when oil, water and nonionic surfactants are all mixed together at

room temperature, slightly stirred and then gradually heated up, the mixture undergoes a phase inversion, from oil-in-water (O/W) to water-in-oil (W/O) emulsion. This inversion happens as the surfactant solubility progressively changes from the aqueous to the oily phase. Above the phase inversion temperature the surfactant is fully solubilized in oil as described in Figure 2.3 a, b). At the PIT, the affinity of amphiphiles for each phase is similar, interfacial curvature is very low and consequently nanometric-scaled microemulsions are formed (Figure 2.3 c). Unlike nanoemulsions, microemulsions are thermodynamically stable systems [32,43], exhibiting different structures at the nanometric scale, such as spherical, tubular or disk-like micelles, lamella or sponge phases and presenting stability which only depends on thermodynamic variable change like temperature, composition and dilution. Nanoemulsions are instantly generated by performing an irreversible transformation by a rapid cooling or a sudden dilution with cold water to this system, which is maintained either at the PIT or higher than the PIT [32, 43-46] (figure 2.3 d). The generated nanoemulsions are kinetically stable for several months.

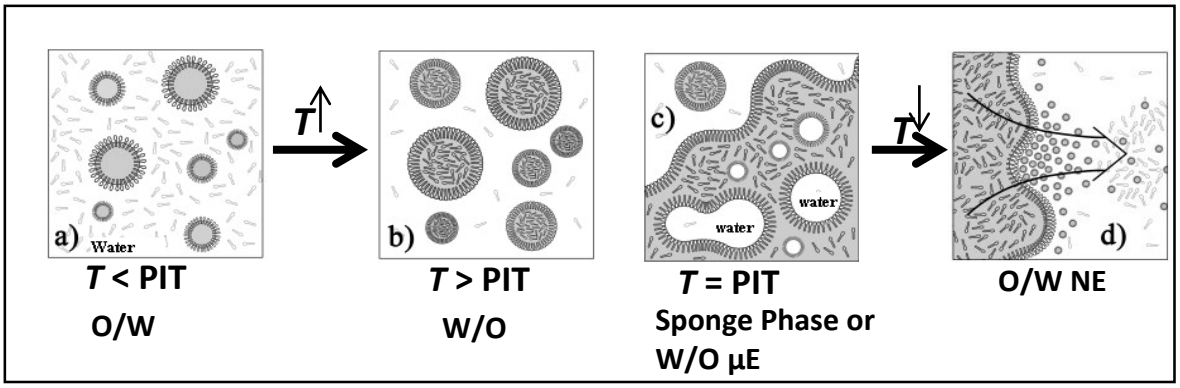

Fig.2.3 Diagram of the PIT method of water/nonionic surfactant/oil system. (a) *T* is below the PIT, an O/W macroemulsion (b) *T* > PIT, W/O macroemulsion. (c) *T* =PIT, sponge phase or µE. (d) rapid cooling induces the generation of nanoemulsions droplets [47].

2.1.2.2.2 Phase Inversion Composition (Concentration) (PIC) approach

Contrary to the PIT-method, where the phase inversion temperature (PIT) is independent of a surfactant concentration while forming emulsions [48], the phase inversion concentration method (PIC), also mentioned as phase inversion composition [46, 49, 50] or Emulsion Inversion Point (EIP) [51], is affected by a change of surfactant concentration during the emulsification pathway. Nevertheless, the nanoemulsion formation via the PIC- and PIT methods resemble each other, so that former studies of the PIT-systems by Shinoda et al. [52], Solans et al. [53], Rybinski et al. [54, 55], Salager et al. [56] and others, also help in a better understanding concerning the PIC-emulsification process. The term phase inversion

concentration (PIC) refers to the fact that simply a certain water concentration has to be added to a nanoemulsion qualified oil/surfactant composition for initializing their formation. As described in figure 2.4, emulsion systems which are finely dispersed and exhibit particle sizes in the nanoemulsion region are preferably generated close to a liquid crystalline region (lamellar [49] or cubic [25]) or bicontinuous microemulsion like phases [57]. Upon emulsification (dilution), such phases provide a spontaneous change of surfactant curvature, and hence facilitate the phase inversion [21]. This precondition, the passing of a phase with zero curvature (minimum interfacial tension), determines the suitable oil/surfactant mixtures [58]. Concerning PIT-nanoemulsions, the formation process of nanoemulsions can be traced back to the change of solubility of polyoxyethylene-type surfactants (change of Hydrophilic Lipophilic Balance (HLB) value with temperature); whereas upon PIC emulsification one presumes that, the relative quantity of surfactant present in the water phase increases with dilution and thereby modifies the composition of the amphiphilic monolayer. This then results in a reversion of the curvature of the oil/water interface due to the increasing of water solubility of surfactant. However, so far especially for the PIC method, a systematic understanding about how to choose and optimize the hydrophobic/amphiphilic systems that work efficiently still has not been achieved. This also means that both, the structural details of their formation process and the aspects relevant for their stability, are still poorly understood.

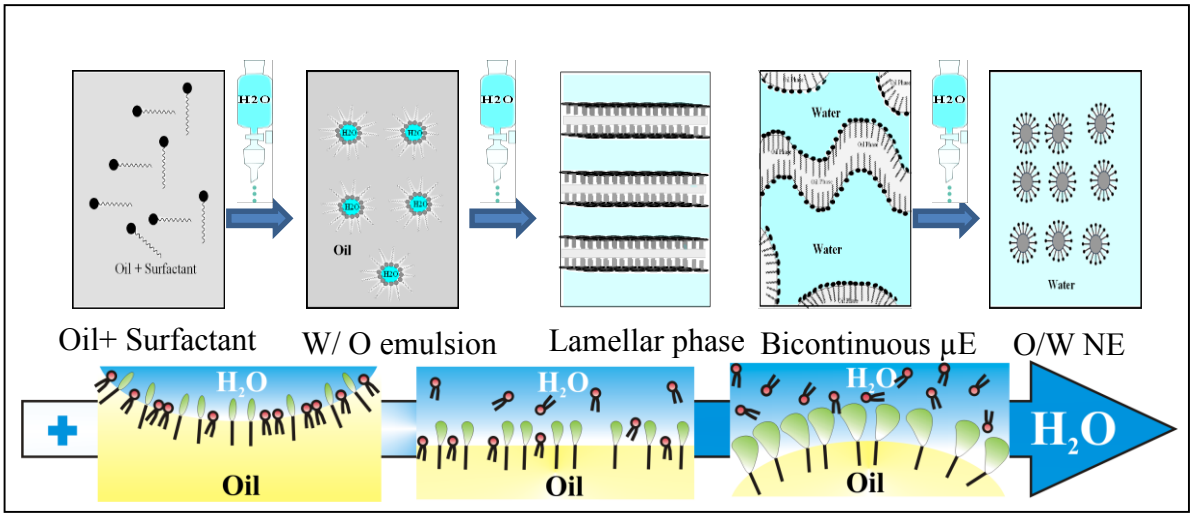

Fig.2.4 Diagram of the PIC method of a water/nonionic surfactant/oil system. Inversion of W/O emulsion to O/W nanoemulsion via passing of sponge like microemulsion phase or lamellar phase with zero curvature during stepwise water addition.

2.2. Emulsion Polymerization concept

Emulsion polymerizations are heterogeneous polymerization processes, which unlike bulk or solution polymerizations, are not uniform in composition throughout the reaction medium, but

rather contain polymerizing colloidal particles dispersed within an inert aqueous environment. Most emulsion polymerizations are free radical processes. There are several steps in the free radical polymerization mechanism: initiation [59], propagation and termination [60, 61]. In the first step, an initiator compound generates free radicals by thermal decomposition. The initiator decomposition rate is described by an Arrhenius-type equation containing a decomposition constant (kd). The free radicals initiate polymerization by reaction with a proximate monomer molecule. This event is the start of a new polymer chain. Because initiator molecules constantly decompose to form radicals, new polymer chains are also constantly formed. The initiated monomeric molecules contain an active free radical end group. During propagation, the initiated monomeric species encountered uninitiated monomer molecules and react to form dimers containing active end groups. The dimers react with monomer to become oligomers [62, 63]. The oligomeric chains grow by propagation and continue to develop in molecular weight. The rate of growth is proportional to the propagation rate constant (kp) [64], which is different for each monomer, and has an Arrhenius dependence upon temperature. The rate of growth of the polymer chains is synonymous with the polymerization rate (Rp). When the free radical end group on a growing polymer chain is deactivated, the chain stops growing, and this event is known as termination. Termination is either obtained through combination, in which two active radical end groups meet, or through disproportionation, in which the active radical is lost from a growing polymer chain by the abstraction of hydrogen from another growing chain. Chain growth may also be terminated by chain transfer [65] to another (e.g., monomeric or polymeric) species. Branching and crosslinking (gel formation) reactions may result from intermolecular chain transfer to polymer [63]. The rate of termination is proportional to the termination rate constant (kt), which also has an Arrhenius dependence upon temperature. At higher conversions of monomer to polymer, the internal viscosity of the latex particles is substantial. The rate of termination drops considerably under these conditions, and the rate of polymerization accelerates. This auto acceleration phenomenon is also known as the Trommsdorff gel effect.
Other types of free radical polymerizations have been carried out in emulsion polymerization such as the reversible addition-fragmentation transfer (RAFT) [66], atom transfer radical polymerization (ATRP) [67, 68], and stable free radical polymerization (SFRP) [69].

2.2.1 Particle nucleation mechanism in emulsion Polymerization.

Surfactants keep emulsion droplets and latex particles colloidally stable against coalescence/aggregation, but the surfactant also plays another important role in emulsion polymerization by being critically involved in the nucleation mechanism (i.e. how the particles

are formed) of the polymer latex particles [70]. The amount of surfactant used is critical in controlling the latex particle size distribution. As surfactant is added to an emulsion, some molecules remain dissolved in the aqueous phase, and some adsorb onto the surface of the emulsion droplets according to an adsorption isotherm (e.g., Langmuir, Freundlich, or Frumkin adsorption isotherms) [71].

As the free surfactant concentration in the water phase increases, it reaches a point at which no additional free surfactant is soluble. This point is known as the critical micelle concentration (CMC) [72]. Any surfactant added after the cmc has been reached will associate into aggregates called micelles [73]. The cores of the micelles are hydrophobic and attract monomer from the stabilized droplets, thereby causing a swelling of the micelles. Radicals generated by the initiator react with monomer dissolved in the water phase to form oligoradicals. Once the oligoradicals reach a critical chain length, they can either aggregate to form primary particles by homogeneous nucleation, enter monomer-swollen micelles to form primary particles by micellar nucleation, or enter monomer droplets directly to cause droplet nucleation (although the frequency of droplet nucleation is low because there are relatively few droplets present) [74]. Figure 2.5 gives an illustration of the various possible particle nucleation mechanisms. There are other nucleation mechanism theories in emulsion polymerisation, such as coagulative nucleation, that expand upon these fundamental principles.

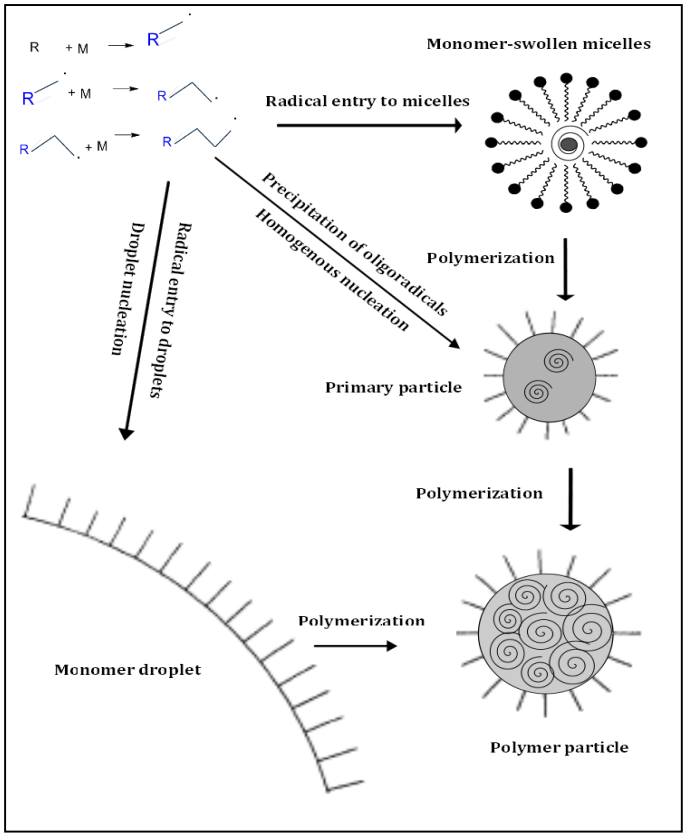

Fig.2.5 Possible particle nucleation mechanisms in emulsion polymerization processes, homogeneous, micellar, and droplet nucleation mechanisms

2.2.2 Emulsion Polymerization Processes

There are three main types of emulsion polymerizations: conventional emulsion polymerization, miniemulsion polymerization, and microemulsion polymerization. A comparison of the properties of these three systems is given in Table 2.1. However, there are some other heterogeneous polymerization processes (such as suspension and dispersion polymerization) that are not emulsion polymerizations, but which are related, and can also produce colloidal polymer particles.

2.2.2.1 Conventional Emulsion Polymerization

Most emulsion polymers are produced by conventional emulsion polymerization [75-77].

In this process, monomer droplets are dispersed in a continuous aqueous phase and are kept colloidally stable against coalescence through the use of a surfactant. The surfactant also causes polymer particles to form by homogeneous or micellar nucleation upon initiation. For conventional emulsion polymerization to be practical, the monomer must be at least slightly water-soluble, to allow the diffusion of monomer from the droplets to the site of polymerization in the growing polymer particles. Relatively low amounts (typically 1 to 3 weight percent) of

surfactant are required in emulsion polymerization, although the particle size may be controlled to an extent by the amount (and type) of surfactant present, with greater amounts of surfactant stabilizing a larger interfacial area and producing a smaller particle size. The initiator concentration and the solids content (i.e., the ratio of the monomer phase to the continuous phase) may also be adjusted to control the particle diameter. The typical size range for particles produced by conventional emulsion polymerization is > 500 nm in diameter. A broad range of monomers with relatively low water solubility has been polymerized by conventional emulsion polymerization. Acrylics, methacrylics, styrene and vinyl acetate are the most common monomers used in preparing latexes for paints, textile binders, and adhesives. Acrylic, polyester, epoxy and urethane dispersions are used in industrial coatings, where higher strength is required. Butadiene is often copolymerized with styrene in producing synthetic rubber for tire manufacture.

Table 2.1 Summary and comparison of the important properties of conventional emulsion, miniemulsion and microemulsion polymerization processes

Emulsion Type	Conventional Emulsion	Miniemulsion	Microemulsion
Droplet size range	> 1 μm	50 to 500 nm	10 to 100 nm
Duration of stability	seconds to hours	hours to months	indefinitely
Diffusional stabilization	kinetic	kinetic	thermodynamic
Nucleation mechanism	micellar, homogeneous	droplet	micellar, droplet
Emulsifier concentration	moderate	moderate	high
Costabilizer type	none	hexadecane, cetyl alcohol	hexanol, pentanol
Homogenisation method	none	mechanical or ultrasonic	none
Particle size range	50 to 500 nm	50 to 500 nm	10 to 100 nm

2.2.2.2 Miniemulsion polymerization

Miniemulsions [78] are submicron (50-200 nm average droplet diameter) dispersions of monomer that are colloidally stabilized against coalescence by a surfactant and diffusionally stabilized against Ostwald ripening using a co-stabilizer such as hexadecane [79]. Miniemulsions are formed by homogenization, through which the droplets of a coarse emulsion

are broken down into much smaller, more numerous droplets by the application of intensive shear forces and energy as shown in figure 2.6. Emulsions, which are homogenized, but contain no co-stabilizer, are called homogenized emulsions. In some miniemulsions, cetyl alcohol has been used as a co-stabilizer in preparing a gel phase that, when mixed with monomer and stirred, forms a miniemulsion. Miniemulsions are kinetically stable; in other words, they are not indefinitely stable, but are stable more than long enough for the polymerization to be performed (i.e., stability over a period of hours to months).

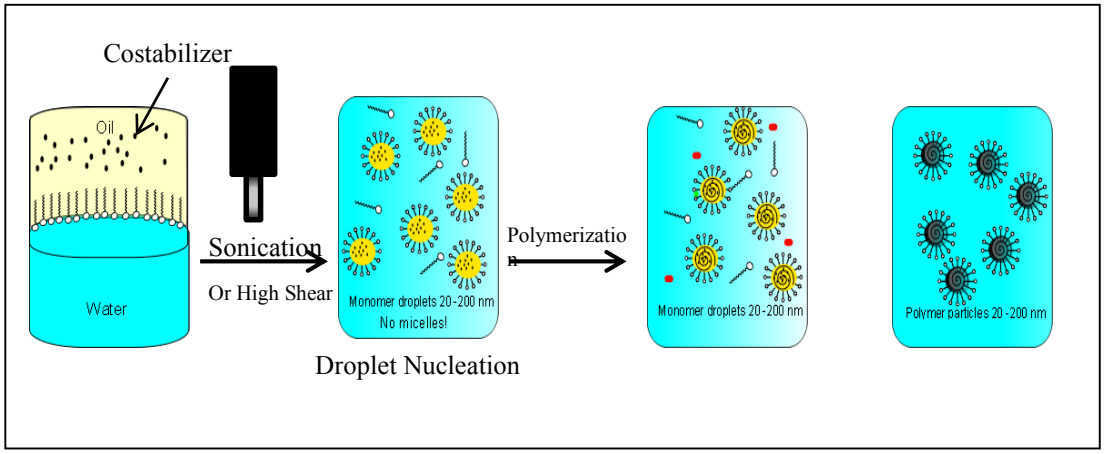

Fig.2.6 Miniemulsion polymerization principle.

The primary distinction between miniemulsion and conventional emulsion polymerisation is the nucleation mechanism. In miniemulsion polymerization [13, 80-82] radicals from the water phase enter the dispersed monomer droplets directly to initiate polymerization (i.e., the droplets act as individual reactors) as described in figure 2.7. This nucleation mechanism is referred to as droplet nucleation. Because of the small size and large surface area of the miniemulsion droplets, they are competitive for radicals relative to the homogeneous and micellar nucleation mechanisms. The monomer droplets polymerize to become polymer particles [15].

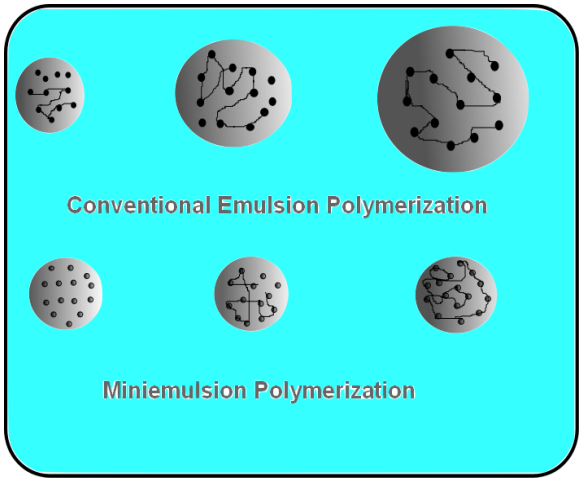

Fig.2.7 Particle growth in conventional emulsion and Miniemulsion polymerization

Miniemulsions are usually prepared with monomers of limited water solubility, such as styrene, methyl methacrylate, or butyl acrylate. In some cases, miniemulsions comprised of increasingly water-soluble monomers (such as vinyl acetate) have been prepared.

Miniemulsion polymerization offers the advantage of being able to incorporate extremely hydrophobic monomers and other water-insoluble materials, making it potentially very useful in extending the classes of materials that may be incorporated into latexes.

In miniemulsions, the copolymerization between two hydrophobic monomers is also well suited to obtain homogeneous copolymer materials; the copolymerization of hydrophobic and hydrophilic monomers leads to amphiphilic polymer particles. An overview of the numerous possibilities for radical polymerizations in miniemulsions is given in several reviews [83-85]. The strength of miniemulsion process is its ability to work with different types of polymerizations. For instance, anionic polymerization can be used to obtain polyamide in non-aqueous miniemulsions [86], and in aqueous phase, poly (butyl cyanoacrylate) nanoparticles can be synthesized by using different nucleophiles owing to the reactivity of cyanoacrylates [87]. In addition, cationic polymerization of p-methoxystyrene can be carried out in a miniemulsion [88, 89]. Catalytic polymerizations of monomer miniemulsions, in which polymerization occurs in the miniemulsion droplets to afford polymer nanoparticles, have been reported for the following reactions: the copolymerization of terminal olefins in a miniemulsion to form polyolefins [90 ,91], the copolymerization of terminal olefin miniemulsions to polyketones [92], the ring-opening metathesis polymerization of norbornene [93, 94], the homopolymerization of terminal olefins [95], the polymerization of phenylacetylene [96] and the step growth acyclic diene metathesis (ADMET) polymerization of divinylbenzene in miniemulsions to give oligo(phenylene vinylene) particles [97].

2.2.2.2.1 Encapsulation of insoluble materials by the miniemulsion polymerization

Compared to emulsion and dispersion polymerization, miniemulsion polymerization offers several advantages. In a miniemulsion, the introduction of species such as pigments into the monomer prior to miniemulsification in the water phase, followed by polymerization, leads to high encapsulation efficiencies. Encapsulation of pigments or inorganic nanoparticles with polymers using the miniemulsion polymerization technique offers the ability to control the droplet size, having the pigment particles directly dispersed in the oil phase, and to nucleate all of the monomer droplets containing the pigment particles. Using the miniemulsion approach, nanoparticles that are more hydrophobic than the monomer can be dispersed in the monomer phase without any former treatment, as recently described for the polystyrene encapsulation of organic phthalocyanine blue pigments [98] or carbon-black particles [13].

2.2.2.3 Microemulsion polymerization

Microemulsions are transparent liquid systems consisting of at least ternary mixtures of oil, water and surfactant. Sometimes a co-surfactant is needed for the formation of a thermodynamically stable microemulsion. They can exhibit water continuous and bicontinuous structures, with typical equilibrium domain sizes ranging from about 10 to 100 nm [99,100]. Over the past two decades, free radical polymerization studies have mainly been carried out in microemulsions (both O/W microemulsions and W/O microemulsions, also known as inverse microemulsions). The enormous numbers of microemulsion nano-globules are in fact potential loci for fast polymerization, producing microlatex particles less than 50 nm in diameter. High molecular weights exceeding one million can be easily obtained from these polymerization systems in spite of their small polymer particles. The most of the reported microemulsion polymerization studies have dealt with hydrophobic monomers, such as styrene (St) or methyl methacrylate (MMA), within oil cores of O/W microemulsions and with the polymerization of water-soluble monomers, such as acrylamide (AM), within aqueous cores of inverse microemulsions [101]. For both O/W and inverse microemulsion systems, the amount of monomer was usually restricted to less than 10 wt. % with respect to the total weight of microemulsion. Moreover, they require higher amounts of surfactant (10-15 wt. % based on total weight of microemulsion). For those microemulsions requiring a co-surfactant, the compatibility between the co-surfactant and the polymers formed becomes an issue and bring some limitations to this type of polymerization [102].

2.3 Textile printing applications

One goal of this thesis is to apply the prepared polymer and hybrid polymer latexes means of mini-(nano) emulsion polymerization and pigment colors encapsulation for the textile pigment and inkjet printing processes. Therefore, it is essential to briefly give an overview about the both textile printing methods.

2.3.1 Definition of textile printing

Printing produces colored designs or patterns on textile through a localized coloration process [103]. This is usually achieved by applying thickened pastes containing dyes or pigments onto a fabric surface according to a given color design. In particular, the viscosity of a print paste is critical. It determines the volume of paste transferred to the fabric and the degree to which it spreads on and into the surface yarns. The two main classical techniques used for transferring paste onto fabrics involve engraved rollers carrying paste in the recesses corresponding to the color pattern, or screens with the open mesh in the pattern areas [104].There are many classes and methods of textile printing but we will focus on the conventional pigment printing and digital inkjet printing techniques.

2.3.2 Pigment printing

Pigment printing is considered the important printing method among the textile printing methods [104]. Pigments unlike dyes have no affinity for any types of textile fabrics. Textile printing of pigments is accomplished by mechanical fixation in contrast to other methods of dyeing and printing, which are based on affinity of textile fabric to dye molecules [105]. This fixation is affected by imbedding pigment in substances, which coagulate on subsequent fixation forming insoluble films by evaporation of the solvent in which they are dissolved or dispersed, or become insoluble on high temperature condensation or polymerization. Film-forming binders are used to fix these pigments to the substrate by the fixation process at elevated temperature after printing and drying. This means that all non-volatile products, which are necessary for the print application, such as thickening agents, emulsifiers, etc. will remain on the material and will have certain influences on the finished textile material. A typical pigment print paste contains a considerable number of chemicals each of which has a specific role to play. The paste may include colored pigments, binder, thickener, flow moderator, weak acid curing catalyst, softener, defoaming agent, water absorbing chemicals or humectants such as urea or glycerol, and emulsifying agents [106].

The economic importance of pigment printing is substantial, since around 1960 these have become the largest colorant group for textile prints. More than 50% of all textile prints are

printed by this method, mainly because it is the cheapest and simplest printing method. After drying and fixation, these prints meet the requirements of the market. The washing process, carried out on classical prints to remove unfixed dye, thickening agents and auxiliaries, is not normally necessary when using the pigment printing technique. However, this technique suffers from some technological and industrial problems such as the relative high curing temperature, fabric stiffness, poor crock fastness and agglomeration of the binders and pigment particles [107, 108]. These disadvantages are related mainly to the undesirable particle size and type of binding agents and pigments which are considered the most important ingredients used in the pigment ink formulations and pastes. Thus to improve the quality of the pigment printed textile fabrics, the overall properties of the binding agents and pigment particles should be improved.

2.3.3 Inkjet (digital) pigment printing

Inkjet is a technology that enables the delivery of liquid ink to a medium whereby only the ink drops make contact with the medium. It is therefore a non-impact printing method. Inkjet technologies are typically classified in two large classes; Continuous Inkjet (CIJ) and Drop-on-Demand Inkjet (DOD). In CIJ, ink is squirted through nozzles at a constant speed by applying a constant pressure. However, in DOD inkjet, drops are ejected only when needed to form the image [109].

Inkjet printing is considered one of the most promising methods for the printing of textile fabrics. In the last 10-20 years, it has received more attentions from both academic and industrial fields. The evolving technology offers significant advantages over the conventional textile printing methods such as, the simple and fast procedures, small scale production, low pollution and low cost by reduction of the water and energy consumption [110–114]. The textile inkjet printing inks are usually classified into two categories of dye-based and pigment-based inks. Pigment-based inks show better wash and light fastness than the dye-based inks after printing. In addition, they do not require a special pretreatment on the fabrics before printing, and the final products can be achieved by simple heat curing of the printed fabrics without steaming and washing, which are needed for dye-based ink printing. Therefore, they serve to save water and energy in comparison to the dye-based inks. However, development of textile pigment inks with emulsion-based textile binders for inkjet printing is extremely challenging due to ink stability and jetting reliability (drying and nozzle clogging) issues, especially for low viscosity print heads. Moreover, the particle size and size distribution of the pigment ink and binder particles have considerable influence on the colloidal stability of inks and clogging of the nozzle and therefore the jetting reliability.

A typical pigment ink formulation for inkjet digital textile printing includes: [115]

- A pigment dispersion for color
- A polymeric binder, a solution of polymer or latex for image durability
- Water, for aqueous inkjet inks or a medium to carry other components
- A co-solvent, helping water to carry other ingredients through solubility and compatibility and enhancing the performance of other ingredients in terms of wetting and adhesion to the substrates and jetting properties
- Surfactants, for nozzle and substrate wetting and jetting reliability and also for stabilizing the key ingredients such as binder and pigment particles from coagulation
- Humectants, to prevent drying when not printing
- An antifoam agent to reduce foaming
- A viscosity control agent for damping control and droplet formation
- A penetrant to speed drying on porous media such as paper and textile
- A biocide to prevent spoilage.

2.4 References:

[1] W. R. Moser, J. Finde, S. C. Emerson, I. M. Krausz. (2001). Engineered Synthesis of Nanostructured Materials and Catalysts. J. Wei (Ed.), *Nanostructured Materials* (1st ed., pp. 2-42). San Diego, CA, USA: Academic Press.

[2] M. Montazer, E. Pakdel. (2011). Functionality of nano titanium dioxide on textiles with future aspects: Focus on wool. *J. Photochem. Photobiol. C, 12*, 293−303.

[3] M. El-Hady, A. Farouk, S. Sharaf. (2013). Flame retardancy and UV protection of cotton based fabrics using nano ZnO and polycarboxylic acids. *Carbohydr. Polym.*, *92*, 400−406.

[4] A. El-Shafei, S. Shaarawy, A. Hebeish. (2010). Application of reactive cyclodextrin poly butyl acrylate preformed polymers containing nano- ZnO to cotton fabrics and their impact on fabric performance. *Carbohydr. Polym.*, *79*, 852−857.

[5] R. Dastjerdi, M. Montazer (2010). A review on the application of inorganic nano-structured materials in the modification of textiles: Focus on anti-microbial properties. *Colloid. Surf. B, 79*, 5-18.

[6] M. Elgammal, S. Prévost, R.Schweins, R. Schneider, M. Gradzielski. (2014). Nanosized latexes for textile printing applications obtained by miniemulsion polymerization. *Colloid Polym. Sci., 292*, 1487-1500.

[7] S.Y. P. Chang, Y.C.Chao. (2011). Microemulsion Polymerization of microlatex in sublimation Ink for Cotton Fabric Inkjet Printing. *J. Appl. Polym. Sci., 122*, 1872–1881.

[8] C. Xue, M. Shi, H. Chen, G. Wu, M. Wang. (2006). Preparation and application of nanoscale microemulsion as binder for fabric inkjet printing. *Colloid Surf. A., 287*, 147-152.

[9] R. Eisenlohr, V. Giesen. (1995). Pigment printing and ecology. *Int. Dyer*, *180*, 12-18.

[10] K. Landfester. (2001). Polyreactions in miniemulsions. *Macromol. Rapid Commun.*, *22*, 896-936.

[11] M. Antonietti, K. Landfester. (2002). Polyreactions in miniemulsions. *Progress in Polymer Science, 27*, 689-757.

[12] K. Landfester. (2006). Encapsulation through (Mini) Emulsion Polymerization. S. K. Ghosh (Ed.), *Functional Coatings Functional Coatings: by Polymer*

Microencapsulation (pp. 29-66). Weinheim, FRG, Germany: Wiley-VCH Verlag GmbH & Co. KGaA.

[13] N. Bechthold, F. Tiarks, M. Willert, K. Landfester, M. Antonietti. (2000). Miniemulsionpolymerization: applications and new materials, *Macromol. Symp., 151,* 549-555.

[14] F. J. Schork,G.W. Poehlein, S. Wang, J. Reimers, J. Rodrigues, C. Samer . (1999). Miniemulsion polymerization. *Colloid Surf. A, 153*, 39-45.

[15] K. Landfester, N. Bechthold, S. Förster, M. Antonietti. (1999). Evidence for the preservation of the particle identity in miniemulsion polymerization. *Macromol. Rapid Commun.*, *20*, 81-84.

[16] V. N. Paunov, S. I. Sandler, E. W. Kaler. (2001). Critical Size and Surfactant Coverage of Styrene Miniemulsion Droplets Stabilized by Ionic Surfactants. *Langmuir*, *17*, 4126-4128.

[17] K. Landfester, N. Bechthold, F. Tiarks, M. Antonietti. (1999). Formulation and stability mechanisms of polymerizable miniemulsions. *Macromolecules*, *32*, 5222-5228.

[18] C.S. Chern, Y.C. Liou. (1999). Kinetics of styrene miniemulsion polymerization stabilized by nonionic surfactants/alkyl methacrylate. *Polymer*, *40*, 3763-3772.

[19] K. Landfester. (2003). Preparation of polymer and hybrid colloids by miniemulsion for biomedical applications. A. Elaïssari (Ed.), *Colloid Polymers: preparation and biomedical applications* (pp. 225-243). New York / Basel, USA: Dekker.

[20] K. Landfester. (2009). Miniemulsion Polymerization and the Structure of Polymer and Hybrid Nanoparticles. *Angewandte Chemie International Edition,* 49 (pp 4488-4507). Weinheim, Germany: Wiley-VCH Verlag GmbH & Co. KGaA.

[21] T. Tadros, R. Izquierdo, J. Esquena, C. Solans. (2004). Formation and stability of nanoemulsions. *Adv. Colloid Interface Sci.*, *108*, 303-318.

[22] K. Shinoda, H. Saito. (1969). The Stability of O/W type emulsions as functions of temperature and the HLB of emulsifiers: The emulsification by PIT-method. *J. Colloid Interface Sci.*, *30,* 258-263.

[23] N. Anton, H. Mojzisova, E. Porcher, J.P. Benoit, P. Saulnier. (2010). Reverse micelle-loaded lipid nano-emulsions: New technology for nano-encapsulation of hydrophilic materials. *Int. J. Pharm., 398,* 204-209.

[24] A. Forgiarini, J. Esquena, C. Gonzalez, C. Solans. (2001). Formation of nano-emulsions by low-energy emulsification methods at constant temperature. *Langmuir*, *17*, 2076-2083.

[25] I. Solè, A. Maestro, C. M. Pey, C. González, C. Solans, J. M. Gutiérrez. (2006). Nano-emulsions preparation by low energy methods in an ionic surfactant system. *Colloids Surf. A: Physicochem. Eng. Aspects, 288,* 138-143.

[26] L. Wang, K. J. Mutch, J. Eastoe, R. K. Heenan, J. Dong. (2008). Nanoemulsions Prepared by a Two-Step Low-Energy Process. *Langmuir*, *24,* 6092-6099.

[27] T. F. Tadros, B. Vincent. (1983). P. Becher (Ed.), *Encyclopedia of Emulsion Technology*; Vol. 1, Chapter 1. New York, USA: Marcel Dekker.

[28] D. N. Petsev. (1998). Interactions and Macroscopic Properties of Emulsions and Microemulsions. B. P. Binks (Ed.), *Modern Aspects of Emulsion Science*; Chapter 10, London, UK: Royal Society of Chemistry.

[29] T. F. Tadros. (2005). Applications of Surfactants in Emulsion Formation and Stabilisation, T. F. Tadros (Ed.), *Applied Surfactants: Principles and Applications* (pp.115-186). Weinheim, FRG, Germany: Wiley-VCH Verlag GmbH & Co. KGaA.

[30] H. C. Hamaker. (1937).The London-van der Waals Attraction between Spherical Particles. *Physica, 4*, 1058-1072.

[31] P. Finkle, H. D. Draper, J. H. Hildebrand. (1923). The theory of emulsification. *J. Am. Chem. Soc.*, *45*, 2780-2788.

[32] N. Anton, J. P. Benoit, P. Saulnier. (2008). Design and production of nanoparticles formulated from nano-emulsion templates - a review. *J. Controlled Release*, *128*, 185-199.

[33] M.S. El-Aasser, E.D. Sudol. (2004). Miniemulsions: Overview of research and applications. *J. Coatings Technol. Research*, *1*, 21-31.

[34] T. Forster, W. Rybinski, A. Wadle. (1995). Influence of microemulsion phases on the preparation of fine-disperse emulsions. *Adv. Colloid Interface Sci.*, *58*, 119-149.

[35] J. M. Gutierrez, C. Gonzalez, A. Maestro, I. Sole, C. M. Pey, J. Nolla. (2008). Nanoemulsions: New applications and optimization of their preparation. *Curr. Opin. Colloid Interface Sci.*, *13*, 245-251.

[36] K. Landfester, J. Eisenblatter, R. Rothe. (2004). Preparation of polymerizable miniemulsions by ultrasonication. *J .Coatings Technol. Research*, *1*, 65-68.

[37] M. Rosoff. (1998). Part A: specialized pharmaceutical emulsions. In H.A. Lieberman, M.M. Rieger, G. S. Banker (Ed.), *Pharmaceutical Dosage Forms: Disperse systems.* (pp. 1-42). New York, USA: Marcel Dekker.

[38] J.L. Salager, A. Forgiarini, L. Márquez. (2006). Nanoemulsions. *FIRP BOOKLET No. E237 A*, *Universidad de Los Andes*.

[39] P. Walstra. (1996). Emulsion stability. P. Becher (Ed.), *Encyclopedia of Emulsion Technology*, Vol.4, (pp. 1-64). New York, USA: Marcel Dekker.

[40] J. Gad. (1878). Zur Lehre von der Fettresorption. *Arch. Anat. Physiol.,* 181-192.

[41] W. D. Bancroft. (1912). The theory of emulsification I. *J. Phys. Chem.*, *16*, 177-233.

[42] R. W. Greiner, D.F. Evans. (1990). Spontaneous formation of a water-continuous emulsion from a w/o microemulsion. *Langmuir*, *6*, 1793-1796.

[43] A. Ott, W. Urbach, L. T. Lee, D. Langevin. (1991). Thermal fluctuations of surfactant films in micellar and microemulsion systems. *Langmuir, 7*, 1892-1894.

[44] D. Morales, J. M. Gutierrez, M. J. Garcia-Celma, C. Solans. (2003). A study of the relation between bicontinuous microemulsions and oil/water nano-emulsion formation. *Langmuir*, *19*, 7196-7200.

[45] P. Izquierdo, J. Esquena,T.F. Tadros, J.C. Dederen, J. Feng, M. J. García-Celma, N. Azemar, C. Solans . (2004). Phase behavior and nano-emulsion formation by the phase inversion temperature method. *Langmuir*, *20*, 6594-6598.

[46] C. Solans, P. Izquierdo, J. Nolla, N. Azemar, M. J. García-Delma. (2005). Nanoemulsions. *Curr. Opin. Colloid Interface Sci.*, *10*, 102-110.

[47] N. Anton, T. F. Vandamme. (2009). The universality of low-energy nano-emulsification. *International Journal of Pharmaceutics*, *377*, 142-147.

[48] B. P. Binks, J. Dong. (1998). Emulsions and equilibrium phase behaviour in silicone oil plus water plus nonionic surfactant mixtures. *Colloids Surf., A*, *132*, 289-301.

[49] I. Sole, C. M. Pey, A. Maestro, C. Gonzalez, M. Porras, C. Solans, J. M. Gutierrez. (2010). Nano-emulsions prepared by the phase inversion composition method: Preparation variables and scale up. *J. Colloid Interface Sci.*, *344*, 417-423.

[50] H. J. Yang, W.G. Cho, S. N. Park. (2009). Stability of oil-in-water nano-emulsions prepared using the phase inversion composition method. *J. Ind. Eng. Chem.*, *15*, 331-335.

[51] S. Gasic, B. Jovanovic, S. Jovanovic. (2002). The stability of emulsions in the presence of additives. *J. Serb. Chem. Soc.*, *67*, 31-39.

[52] K. Shinoda, H. Arai. (1964). The correlation between phase inversion temperature in emulsion and cloud point in solution of nonionic emulsifier. *J. Phys. Chem., 68,* 3485-3490.

[53] P. Izquierdo, J. Esquena,T.F. Tadros, J.C. Dederen, J. Feng, M. J. García-Delma, N. Azemar, C. Solans. (2002). Formation and stability of nano-emulsions prepared using the phase inversion temperature method. *Langmuir*, *18*, 26-30.

[54] T. Engels, T. Förster, W. von Rybinski. . (1995). The influence of coemulsifier type on the stability of oil-in-water emulsions. *Colloids Surf. A, 99*, 141-149.

[55] T. Förster, F. Schambil, W. von Rybinski. (1992). Production of fine disperse and long-term stable oil-in-water emulsions by the phase inversion temperature method. *J. Dispersion Sci. Technol.*, *13*, 183-193.

[56] J. Allouche, E. Tyrode, V. Sadtler, L. Choplin, J. L. Salager. (2004). Simultaneous conductivity and viscosity measurements as a technique to track emulsion inversion by the phase-inversion-temperature method. *Langmuir*, *20*, 2134-2140.

[57] D. Morales, J. M. Gutierrez, M. J. Garcia-Celma, and C. Solans. (2003). A study of the relation between bicontinuous microemulsions and oil/water nano-emulsion formation. *Langmuir, 19*, 7196-7200.

[58] C. M. Pey, A. Maestro, I. Sole, C. Gonzalez, C. Solans, J. M. Gutierrez. (2006). Optimization of nano-emulsions prepared by low-energy emulsification methods at constant temperature using a factorial design study. *Colloids Surf., A, 288*,144-150.

[59] R. D. Athey. (1998). Free radical initiator basics. *European Coatings Journal*, *3*, 146-149.

[60] C. S. Chern, S. Y. Lin, L. J. Chen, S. C. Wu. (1997). Emulsion polymerization of styrene stabilized by mixed anionic and nonionic surfactants. *Polymer*, *38*, 1977-1984.

[61] H. Y. Parker, D. G. Westmoreland, H. R. Chang. (1996). ESR Study of MMA Batch Emulsion Polymerization in Real Time: Effects of Particle Size. *Macromolecules*, *29*, 5119-5127.

[62] K. Tauer, K. Riedelsberger, R. Deckwer, A. Zimmermann, H. Dautzenberg, J. Thieme. (2000). A new way to control particle morphology in heterophase polymerizations. *Macromolecular Symposia*, *155*, 95-104.

[63] J. R. Ebdon, S. Rimmer. (1997). A one-pot method for the preparation of latices of telechelic oligomers, by ozonolysis of latices of polymers containing main-chain unsaturation. *Journal of Polymer Science: Part A: Polymer Chemistry*, *35*, 3255-3262.

[64] M. Jung, E. M. S. Hamersveld, T. Julien, A. M. van Herk. (2001). Pulsed-Laser Polymerization in Compartmentalized Liquids, 2a Miniemulsions. *Macromol. Rapid Commun.*, *22*, 978-982.

[65] A. Zaichenko, O. Shevchuk, S. Voronov, A. Sidorenko. (1999). Heterogeneous Catalytic Initiation by Cu^0 Colloidal Particles of Water-Dispersion Polymerization. *Macromolecules*, *32*, 5707-5711.

[66] H. Brouwer, J. G. Tsavalas, F. J. Schork, M.J. Monteiro. (2000). Living Radical Polymerization in Miniemulsion Using Reversible Addition-Fragmentation Chain Transfer. *Macromolecules*, *33, 9239*-9246.

[67] A. Heise, S. Diamanti, J. L. Hedrick, C. W. Frank, R.D. Miller. (2001). Investigation of the Initiation Behavior of a Dendritic 12-Arm Initiator in Atom Transfer Radical Polymerization. *Macromolecules*, *34*, 3798-3801.

[68] J. Qiu, S. G. Gaynor, K. Matyjaszewski. (1999). Emulsion Polymerization of n-Butyl Methacrylate by Reverse Atom Transfer Radical Polymerization. *Macromolecules*, *32,* 2872-2875.

[69] B. Keoshkerian, P.J. MacLeod, M.K. Georges. (1999). Georges. Block Copolymer Synthesis by a Miniemulsion Stable Free Radical Polymerization Process. *Macromolecules*, *32,* 3594-3599.

[70] I. Kühn, K. Tauer. (1995). Nucleation in Emulsion Polymerization: A New Experimental Study. 1. Surfactant-Free Emulsion Polymerization of Styrene. *Macromolecules*, *28,* 8122-8128.

[71] Y. H. Chang, Y. D. Lee, O. J. Karlsson. (2000). Surfactant characteristics of random block polyelectrolyte polyester emulsifier (SMTAPE) in aqueous solution and on polystyrene latex particles. *Polymer*, *41*, 6741-6747.

[72] P. Ni, F. N. Jones, S. Fu. (2000). Synthesis of amphiphilic copolymers based on acrylates by free-radical polymerization andtheir application in alkyd emulsions. *Journal of Macromolecular Science: Part A*, *37*, 1391-1406.

[73] D. O. Shah. (1998). *Micelles, Microemulsions, and Monolayers*. New York, USA: Marcel Dekker.

[74] T.J. Martin, K. Prochazka, P. Munk, S. E. Webber. (1996). pH-Dependent Micellization of Poly (2-vinylpyridine)-block-poly (ethylene oxide). *Macromolecules*, *29*, 6071-6073.

[75] F. H. Walker. (2000). Polymerization processes: III. *Journal of Coatings Technology*, *72*, 27-32.

[76] C. J. McDonald , K. J. Bouck , A. B. Chaput. (2000). Emulsion Polymerization of Voided Particles by Encapsulation of a Nonsolvent. *Macromolecules*, *33*, 1593-1605.

[77] A. Tuncel. (2000). Emulsion copolymerization of styrene and poly (ethylene glycol) ethyl ether methacrylate. *Polymer*, *41*, 1257-1267.

[78] K. Landfester, F. Tiarks, H. Hentze, M. Antonietti. (2000). Polyaddition in miniemulsions: A new route to polymer dispersions. *Macromol. Chem. Phys.*, *201*, 1-5.

[79] K. Landfester. (2002). Quantitative considerations for the formulation of miniemulsions. *Progress in Colloid and Polymer Science*, *117*, 101-103.

[80] H. Kawahara, T. Goto, K. Ohnishi, H. Ogura, H. Kage, Y. Matsuno. (2001). Preparation of epoxy resin/acrylic composite latexes by miniemulsion polymerization method. *Journal of Applied Polymer Science*, *81*,128-133.

[81] G. Baskar, K. Landfester, M. Antonietti. (2000). Comblike Polymers with Octadecyl Side Chain and Carboxyl Functional Sites: Scope for Efficient Use in Miniemulsion Polymerization. *Macromolecules*, *33*, 9228-9232.

[82] J. R. Leiza, E. D. Sudol, M. S. El-Aasser. (1997). Preparation of high solids content poly (n-butyl acrylate) latexes through miniemulsion polymerization. *Journal of Applied Polymer Science, 64*, 1797-1809.

[83] K. Landfester. (2006). Synthesis of colloidal particles in miniemulsions. *Annu. Rev. Mater. Res.,* 36, 231-279.

[84] J. M. Asua. (2002). Miniemulsion polymerization. *Prog. Polym. Sci*. *27*, 1283-1346.

[85] F. J. Schork, Y. W. Luo, W. Smulders, J. P. Russum, A. Butte, K. Fontenot. (2005). Miniemulsion Polymerization. *Adv. Polym. Sci*., *175*, 129-255.

[86] D. Crespy, K. Landfester. (2005). Anionic polymerization of ε-caprolactam in miniemulsion: synthesis and characterization of polyamide-6 nanoparticles. *Macromolecules, 38*, 6882-6887.

[87] C. K. Weiss, U. Ziener, K. Landfester. (2007). A route to nonfunctionalized and functionalized poly (n-butylcyanoacrylate) nanoparticles: preparation in miniemulsion. *Macromolecules*, 40, 928-938.

[88] S. Cauvin, F. Ganachaud. (2004). On the Preparation and Polymerization of p-Methoxystyrene Miniemulsions in the Presence of Excess Ytterbium Triflate. *Macromol. Symp*., *215*, 179-190.

[89] S. Cauvin, F. Ganachaud, M. Moreau, P. Hemery. (2005). High molar mass polymers by cationic polymerisation in emulsion and miniemulsion. *Chem. Commun*., 2713-2715.

[90] R. Soula, B. Saillard, R. Spitz, J. Claverie, M. F. Llaurro, C. Monnet. (2002). Catalytic Copolymerization of Ethylene and Polar and Nonpolar α Olefins in Emulsion, *Macromolecules*, *35*, 1513-1523.

[91] P. Wehrmann, M. Zuideveld, R. Thomann, S. Mecking. (2006). Copolymerization of ethylene with 1-butene and norbornene to higher molecular weight copolymers in aqueous emulsion. *Macromolecules*, *39*, 5995-6002.

[92] A. Held, I. Kolb, M. A. Zuideveld, R. Thomann, Stefan Mecking, M. Schmid, R. Pietruschka, E. Lindner, M. Khanfar, M. Sunjuk. (2002). Aqueous Polyketone Latices Prepared with Water-Insoluble Palladium (II) Catalysts. *Macromolecules, 35*, 3342-3347.

[93] D. Quemener, V. Heroguez, Y. Gnanou. (2005). Latex particles by miniemulsion ring-opening metathesis polymerization. *Macromolecules*, *38*, 7977-7982.

[94] D. Quemener, V. Heroguez, Y. Gnanou. (2006). Design of PEO-based ruthenium carbene for aqueous metathesis polymerization. Synthesis by the "macromonomer method" and application in the miniemulsion metathesis polymerization of norbornene. *J. Polym. Sci. Part A*, *44*, 2784-2793.

[95] P. Wehrmann, S. Mecking. (2006). Aqueous dispersions of polypropylene and poly (1-butene) with variable microstructures formed with neutral nickel (II) complexes. *Macromolecules*, 39, 5963-5964.

[96] J. Huber, S. Mecking. (2006). Aqueous Polyalkyne Dispersions. *Polym. Mater. Sci. Eng., 96*, 306-307.

[97] J. Pecher, S. Mecking. (2007). Nanoparticles from step-growth coordination polymerization. *Macromolecules, 40*, 7733-7735.

[98] S. Lelu, C. Novat, C. Graillat, A. Guyot, E. Bourgeat-Lami. (2003). Encapsulation of an organic phthalocyanine blue pigment into polystyrene latex particles using a miniemulsion polymerizationprocess. *Polym. Int*., *52*, 542-547.

[99] R. Zana, J. Lang (1987). Microemulsions: structure and dynamics. S.E. Frieberg, P. Bothorel (Ed.) Ch. 6, CRC, Boca Raton, Florida, USA.

[100] J. Biasia J, B. Clin, P. Laolanne (1987). Microemulsions: structure and dynamics. S.E. Frieberg, P. Bothorel (Ed.) Ch. 6, CRC, Boca Raton, Florida, USA.

[101] F. Candau. (1999). Handbook of microemulsion science and technology. P. Kumar, K.L. Mittal (Ed.) Ch. 22, p 679, Marcel Dekker, New York, USA.

[102] F .Candau. (1992). Polymerization in organized media. C.M. Paleos (Ed.), p 215, Gordon and Breach, New York, USA.

[103] L. W. C. Miles. (1994). *Textile Printing* (1st ed.). Bradford, UK: Society of Dyers and Colourists.

[104] C. J. Hawkyard. (2003). Screen printing. L. W. C. Miles (Ed.), *Textile Printing* (2nd ed., pp. 18-54). Bradford, UK: Society of Dyers and Colorists.

[105] H. Wigger. (1988). Modern Pigment Printing. *Textil Praxis, 44*, 45-53.

[106] M. Jassal, B. N. Acharya, P. Bajaj, R. B. Chavan. (2002). Acrylic-based thickener for pigment printing-Review. *Journal of Macromolecular Science, Part C- reviews*, *42*, 1-28.

[107] M. R. Galgali. (1994) Environmental impact of textiles, *Colourage*, *45*, 20-22.

[108] L.V. Jing, X. Min, C. Shuilin. (2003). Synthesis and characterization of non-formaldehyde releasing and low-temperature curable binder. *AATCC Rev.*, *6*, 29-32.

[109] E. M. Freire. (2006). H. Ujiie (Ed.) *Inkjet printing technology*. Cambridge, UK: Woodhead Publishing Limited and CRC Press.

[110] P. Calvert. (2001). Inkjet printing for materials and devices. *Chemistry of Materials*, *13*, 3299-3305.

[111] Y. Yang, V. Naarani. (2007).Improvement of the lightfastness of reactive inkjet printed cotton. *Dyes and Pigments*, *74*, 154-160.

[112] A. Hladnik, T. Muck. (2002). Characterization of pigments in coating formulations for high-end ink-jet papers. *Dyes and Pigments, 54*, 253-263.

[113] C.T. Kosolia, E.G. Tsatsaroni. (2010). Synthesis and characterization of hetarylazo disperse colorants: preparation and properties of conventional and microemulsified

inks for polyester ink-jet printing. *Journal of Applied Polymer Science*, *116*, 1422-1427.

[114] P. S. Choi, S. Yuen, K. A. Ku, C. W. Kwan. (2003). Ink-jet printing for textiles. *Textile Asia*, *34*, 21-24.

[115] Z. FU. (2006). Pigmented ink formulation. H. Ujiie (Ed.), *Digital printing of textiles* (pp. 218-232). Cambridge, UK: Woodhead Publishing Limited and CRC Press.

3. Materials and experimental methods

3.1 Materials

3.1.1 Monomers

The monomers used in this thesis to synthesize the corresponding polymer and copolymer latexes as well as the encapsulation of organic pigments upon subsequent polymerization are listed in table 3.1. They were purified by distillation under reduced pressure before use.

Table 3.1 List of monomers used in this study auch der Stabilisator

Monomer	Molar mass g/mole	Supplier
n-Butyl acrylate (BA) 99%	128.2	BASF
Methyl methacrylate (MMA) 99%	100.12	BASF
Styrene (St.) 99.9%	104.15	Sigma-Aldrich
Methacrylic acid (MAA) 99%	86.06	BASF
N-methylol acrylamide(NMA) 99%	101.1	Sigma-Aldrich

3.1.2 Initiators:

The radical miniemulsion or nanoemulsion polymerization was initiated using the water soluble initiator, potassium persulfate (KPS) provided by Sigma Aldrich. KPS was purified by recrystallization from water prior to use. However, the encapsulation of the organic pigments by the miniemulsion polymerization was performed with the monomer soluble initiator azobisisobutyronitrile (AIBN, 98%) supplied from Sigma Aldrich

3.1.3 Surfactants

The miniemulsion monomer templates prepared by the high energy method as well as the pigment dispersions for encapsulation were stabilized by the anionic surfactant sodium dodecyl sulfate (SDS), while the nanoemulsion monomer templates prepared by the low energy method were stabilized by the non-ionic surfactant Brij 78 is a technical grade surfactant with the chemical structure, polyoxyethylene stearyl ether, with an average of 20 mole of ethylene oxide (EO) per surfactant molecule, Table 3.2.

Table 3.2 List of surfactants used in this study

Surfactant	Chemical structure	Molar mass (g/mole)	Supplier
SDS	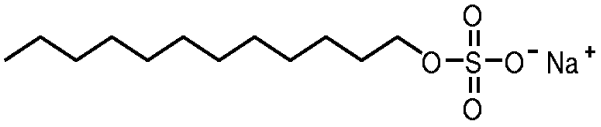	288,37	Fisher
Brij 78	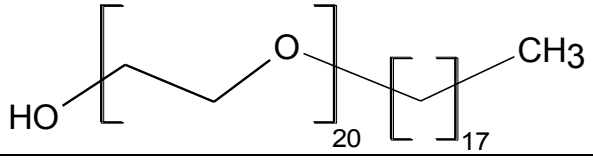	1151.57	Sigma-Aldrich

3.1.4 Solvent and other chemical materials

Water purified and deionized (reverse osmosis followed by ion exchange and filtration) by Milli-RO 5 Plus and Milli-Q Plus systems (Millipore GmbH, Germany) was used in all experiments as a continuous phase for the all water born miniemulsion/nanoemulsion polymerization or as the aqueous medium for the pigment ink dispersions. Hexadecane (HD, Sigma-Aldrich, 99%) was used as a co-stabilizer for the miniemulsion/nanoemulsion preparations, and sodium bicarbonate (BDH, 99%) was used as a buffer.

3.1.5 Textile fabrics, pigment colors and auxiliaries used for the printing pastes and ink formulations.

Textile cotton fabric (100% bleached, plain weaved, 140 g/m^2) was supplied from the ITCF institute, Denkendorf, Germany and used as substrate for the pigment printing and inkjet printing. Pigment cyan 340 EPG 4003 and pigment black 370 EPG 9006 were used as the pigment color stuffs in the conventional pigment printing. However, the synthetic polyacrylate-based thickener CHT-BEZEMA TUBIVIS DL 650, supplied from CHT R. Beitlich GmbH, was used to provide and adjust the viscosity of the pigment printing pastes.

The pigments stuffs C.I. Pigment red 112 (PR112), C.I. Pigment blue (PB. 15:3) and C.I. Pigment yellow PY.155 were provided by Clariant and used for the encapsulation study by the miniemulsion polymerization to be used in the inkjet printing. The chemical structure of the pigment colors is shown in figure 3.1. However, BYK 346 silicon surfactant and sorbitol were provided from BYK-GARDNER GmbH, Germany and used as auxiliaries additives for the inkjet printing.

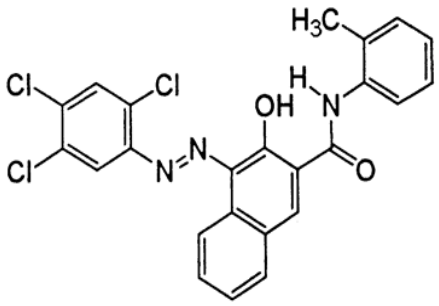

C.I. Pigment red 112

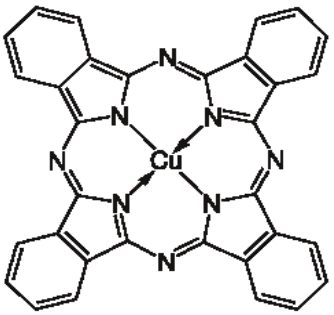

C.I. Pigment blue 15:3

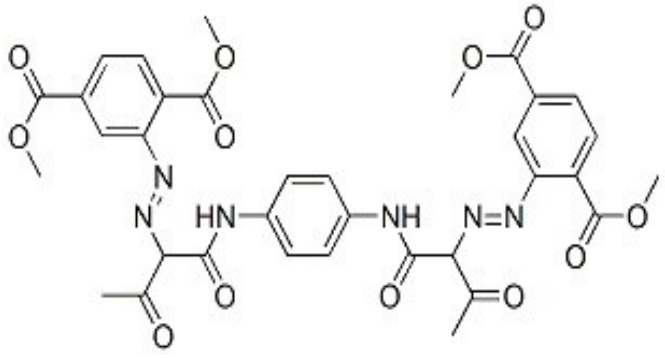

C.I. Pigment yellow 155

Fig.3.1 Chemical structure of the pigment colors used in the encapsulation study.

3. 2 Preparation procedures

3. 2.1 Miniemulsion preparation and polymerization by the high energy method

The generic miniemulsion polymerization recipe is listed in Table 3.3 for a fixed monomer solid content of 20% and SDS of 15 mM. The mixture of monomers and hexadecane were mixed and stirred for 15 minutes by magnetic stirring. Then the mixture was added to a solution of sodium dodecyl sulfate SDS and 10 mM of sodium bicarbonate and stirred for 20 minutes. Miniemulsification was carried out by sonification of the mixture by the ultrasonic processor (Branson digital model 250) for 10 minutes, at 50% amplitude. To reduce any rise in temperature that may occur during the miniemulsification process, the sonification processes were done with 5 s pulse on and 10 s pulse off cycles under ice-cooling. Miniemulsion copolymerization was done by a batch method by adding the miniemulsion to a solution of potassium persulfate and raising the temperature to 70°C. The polymerization was done under nitrogen purge. It should also be noticed that the time between miniemulsification and initiation

was minimized to 10 minutes to reduce the probability of the droplet degradation (Ostwald ripening). The reaction is usually completed after 3 h. The theoretical solid content of the latex product that was used as a binder for textile pigment printing was monitored to be approximately 20%.

Table 3.3: Generic miniemulsion recipe for nanosized copolymer latex synthesis based on 20 % monomer solid content.

Ingredients	Weight (g)	Concentration
DI Water	80	
Monomers (BA, MMA, MAA, NMA, St.)	20	20% solid contents
SDS	0.35	15 mM
HD	0.72	40 mM
Buffer ($NaHCO_3$)	0.007	10 mM
KPS	0.02	1 mM

3.2.2 Pigment encapsulation by the miniemulsion polymerization

3. 2.2.1 Dispersion of the pigment colors in aqueous medium.

The aqueous pigment ink dispersions were prepared by dispersing 10 g of the pigment color with 1.75 g SDS in 88.25 g Millipore water. The pH of dispersion was adjusted to 8 by adding sodium hydroxide (0.1 M NaOH). The pigment dispersions were stirred overnight and then sonicated by the ultrasonic processor (Branson digital model 250) for 120 minutes, at 70% amplitude. To reduce any rise in temperature that may occur during the pigment dispersion, the sonification processes were done with 5 s pulse on and 10 s pulse off cycles under ice-cooling.

3.2.2.2 Encapsulation of the pigment colors with the BA-MMA and St-BA copolymer latexes.

The miniemulsion recipe listed in table 3.4 was prepared in order to be added to the different pigment dispersions with different monomer/pigment weight ratios. The miniemulsification was performed as described in section 3.3.1, but the only exception is the addition of the oil soluble AIBN initiator to the different monomers and hexadecane. Then the encapsulation started by adding the proper amount of the miniemulsion which corresponded to the different monomer/pigment mass ratios 0.11, 0.25, 0.42, and 0.66 to 40 g of each pigment dispersion. The monomer miniemulsion/pigment dispersion was stirred for 30 minutes then pulse sonicated for 5 minutes at 70% amplitude. This process was repeated twice and the all the sonication processes were carried out under ice cooling. Finally, the polymerization was carried out by intimating the pigment- monomer miniemulsion templates at 70^{o}C overnight.

Table 3.4: miniemulsion recipe used for the encapsulation of the organic pigments

Ingredients	Weight (g)	Concentration
DI Water	80	80%
Monomers, BA, St, MMA	20	20%
SDS	0.047	2 mM
HD	0.72	40 mM
Buffer($NaHCO_3$)	0.007	10 mM
AIBN	0.2	1 wt. % of monomer

3. 2.3 Nanoemulsion formation and polymerization by the low energy method

Nanoemulsions were prepared by the phase inversion composition (concentration) method in which the stepwise addition of water to an oily phase composed of monomer /Brij 78 mixtures at 25 °C is crucial to obtain finally the O/W nanoemulsions. The oil part itself was composed of 96 wt% monomer and 4 wt% hexadecane. The region of formation of O/W nanoemulsions in the water/surfactant/ oil system was assessed visually. The water addition was carried out under mild shaking by a vibromixer. The polymerization of the oil droplets was carried out by adding the water soluble potassium persulfate (KPS) initiator or the oil soluble initiator azobisisobutyronitrile (AIBN) to the prepared monomer-nanoemulsion depending on the O/S ratios. The polymerization was performed for 5 h at 70°C in which stable polymer nanoparticles were obtained.

3. 2.3.1 Phase Diagram of the nanoemulsion system

All components were weighed, sealed in ampules, and homogenized with a vibromixer. The samples were kept at 25 °C to equilibrate. Liquid crystalline phases were determined by placing crossed polarizers on each side of the sample vial. When a liquid crystalline phase is present, light will pass through the plates, due to the birefringence of the liquid crystal. Then, the phases were further characterized using polarizing optical microscopy. Polarizing microscopy was done on a Zeiss microscope (12.5x/0.25 planchromat pol objective). Samples were placed between two cover slides and photographs were done with a Canon EOS 5D camera at ambient condition.

3.3 Characterization methods

3.3.1 Particle size and polydispersity analysis

Particle size, size distributions and morphology of the prepared latex or the hybrid pigment latex particles were determined using different techniques such as dynamic light scattering (DLS), small angle neutron scattering (SANS), Disc centrifuge (CPS) and transmission electron microscopy (TEM).

3.3.1.1 Dynamic Light Scattering

Dynamic light scattering (DLS) measurements are based on measuring the light scattered fluctuations over time [1], caused by Brownian motion of particles, as a result of thermal fluctuations of the solvent molecules [2]. The experimental set-up of the DLS is basically composed of a detector which is connected to a correlator that computes the correlation function from the intensity fluctuations as a function of time. According to the approximations in Rayleigh scattering, the intensity of the scattering light is proportional to d^6 (particle diameter) and inversely proportional to λ^4 (wavelength of incident light) [3]. Fluctuations in the scattered light frequency may be seen as a result of the Doppler Effect whether the moving particle is approaching or receding from the detector [4]. Alternatively, fluctuations can be viewed as the result of constructive and destructive interference of scattered light, as the particles move over time. An autocorrelation function is then used to analyze the intensity fluctuations over short time intervals and determine the translational diffusion coefficient D [1].

The intensity autocorrelation function is given by equation 3.1:

$$G(\tau) = \langle I(t) \bullet I(t+\tau) \rangle \qquad 3.1$$

where τ represents the correlator time. The autocorrelation function decays exponentially with time. The exponential decay time constant can be related to the diffusion coefficient D, which leads to the determination of the particle's hydrodynamic radius R_H through the Stokes-Einstein equation 3.2: [3]

$$R_H = \frac{K_B T}{6\pi\eta D} \qquad 3.2$$

where K_B is the Boltzmann constant, T is the temperature and η is viscosity of the solvent [1, 2]. Figure 3.1 represents a schematic diagram of DLS main components, illustrating their main roles and the corresponding obtained information.

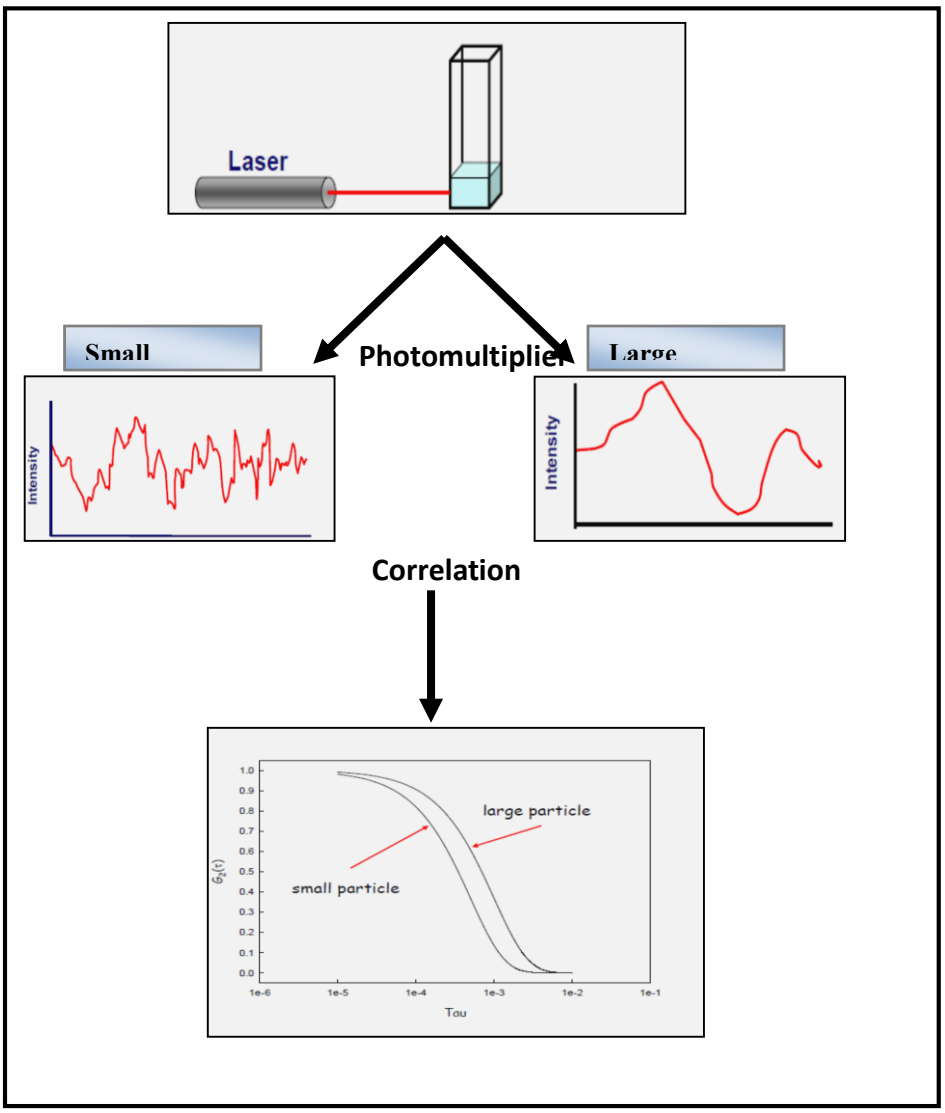

Figure 3.2 Schematic diagram of the main components of a dynamic light scattering apparatus and the obtained corresponding information.

DLS measurements were performed at 25 ^{o}C with a setup consisting of an ALV 7004 correlator, an ALV CGS-3 goniometer and a He-Ne laser with a wavelength of 632.8 nm. Cylindrical glass sample cells of 0.8 cm diameter were placed in an index-matching vat filled with toluene. The miniemulsion /nanoemulsion latex or hybrid latex pigment dispersion were diluted by ~100 times with distilled water prior to the measurements and the intensity autocorrelation functions were recorded at 90^{o} angle.

3.3.1.2 Small Angle Neutron Scattering (SANS)

Small angle neutron scattering is used as a complementary analytical method to investigate the particle size, size distribution and polydispersity of our prepared miniemulsion latexes. SANS is similar to the other scattering methods, like static light scattering and small angle x-ray scattering. The SANS experiment requires a source of neutrons. There are several types of

neutron sources depending on the mechanism to produce the neutrons, on which depend on the energy and the rate of the emitted neutrons. The specialty of neutrons is the absence of charge, where the neutrons interact with atoms via nuclear rather than electrical forces, and nuclear forces are very short-range of the order of a few fermis (1 fermi = 10^{-15} meter). Furthermore, the wavelength of neutrons is in the range of 0.1 to 1 nm and the energy is approximately 1 to 100 meV. An important feature of neutron scattering is the high incoherent scattering cross-section of hydrogen. However, hydrogen molecules appear low incoherent scattering cross section by measuring of X-ray scattering like SAXS because of the electron density [5]. SANS experiments were performed on the instrument D11 at the Institut Laue Langevin (ILL) in Grenoble, France. Two configurations were used, with a wavelength λ of 0.6 nm (FWHM 10%) and sample-to-detector distances of 8 and 34 m, the direct beam width was experimentally obtained from acquisition of the attenuated direct beam, SD=8m fwhm 3.78cm ($\sigma(\theta)=2.0\cdot10^{-3}$), SD=34m fwhm 2.46cm ($\sigma(\theta)=3.1\cdot10^{-4}$). The Q-range thus covered was 0.02 – 0.9 nm^{-1}, where Q is the magnitude of the scattering vector with θ the scattering angle (Eq.3.3),

$$Q = \frac{4\pi}{\lambda}\sin\left(\frac{\theta}{2}\right) \qquad 3.3$$

Samples were contained in quartz cuvettes of 1 mm neutron pathway. The standard deviation σ(q)/q used to account for the instrument resolution is estimated as (Eq. 3.4),

$$\left(\frac{\sigma(Q)}{Q}\right)^2 = \left(\frac{\sigma(\lambda)}{\lambda}\right)^2 + \left(\frac{\sigma(\theta)}{\theta}\right)^2 \qquad 3.4$$

The data reduction was performed with the software package Lamp [21], using the scattering by a 1 mm H_2O sample to correct for detector efficiency and solid angle variations. After correcting the data for transmission, sample thickness, detector dead-time and noise, and subtracting the scattering by the empty cell, the data presented hereafter still contain a background essentially due to the large incoherent cross-section of hydrogen. Demineralized water of 1mm thickness (and an empty cell as water background) was measured as secondary calibration standard (cross-calibrated against well-characterized h/d polymer blends). The data were put on absolute scale with the known differential scattering cross section of water, being 0.983 1/cm at 0.6 nm, as determined for D11. Scattering patterns were eventually radially averaged and data from both configurations were merged with no need for intensity correction. The data analysis was performed by fitting the spectra with the analytical normalized form factor for homogeneous spheres (Eq.3.5),

$$P_{sphere}(Q,R) = 3\left\langle \frac{\sin(QR) - QR\cos(QR)}{Q^3R^3} \right\rangle^2 \quad 3.5$$

The absolute scale scattering intensity for a system of polydisperse spheres was then calculated in the monodisperse approximation as (Eq. 3.6),

$$I(Q) = {}^1N\left\langle V^2 \right\rangle (SLD_{latex} - SLD_{solvent})^2 \int_0^\infty LogNorm(R) P_{sphere}(Q,R) \int dR \times S(Q) \quad 3.6$$

where SLD_{latex} and $SLD_{solvent}$ are the scattering length density of the particles and the solvent, $\langle V^2 \rangle$ is the average square volume, ${}^1N(R)$ is the total density number of latex particles, for which log-normal distribution was assumed (Eq. 3.7),

$$LogNorm(R > 0; R_0, s) = \frac{e^{-\frac{1}{2}\left(\frac{\ln R - \ln R_0}{s}\right)^2}}{Rs\sqrt{2\pi}} \quad 3.7$$

where s is the standard deviation and R_0 is the median.

We recall that the moments of R can be calculated as $\left\langle R^n \right\rangle = e^{n \ln R_0 + \frac{n^2 s^2}{2}}$ and the polydispersity index p is,

$$p = \sqrt{1 - \frac{\left\langle R \right\rangle^2}{\left\langle R^2 \right\rangle}} = \sqrt{1 - e^{-s^2}} \quad 3.8$$

Interactions between particles were taken into account with the structure factor for hard spheres, in the approximate solution of the Ornstein-Zernicke equation with the Percus-Yevick closure relation, that basically just has the hard sphere radius R_{HS} as relevant parameter i.e., ${}^1N$ is the same for the form and structure factor [6, 7].

$$S(Q) = \frac{1}{1 + 24\phi \frac{C(Q)}{\xi}} \quad 3.9$$

with

$$C(Q) = \alpha j_1(\xi) + \beta \frac{2\xi \sin\xi + (2-\xi^2)\cos\xi - 2}{\xi^3} + \gamma \frac{-\xi^4 \cos\xi + 4\left((3\xi^2 - 6)\cos\xi + (\xi^3 - 6\xi)\sin\xi + 6\right)}{\xi^5}$$

$$\alpha = \left[\frac{1+2\phi}{(1-\phi)^2}\right]^2, \quad \beta = -6\phi\left[\frac{1+\phi/2}{(1-\phi)^2}\right]^2, \quad \gamma = \frac{\phi}{2}\alpha, \quad \xi = 2QR_{HS}, \quad \phi = {}^1N\frac{4}{3}\pi R_{HS}{}^3 \qquad 3.10$$

3.3.1.3 Disc centrifuge (DC24000, CPS Instruments Inc.)

A disc centrifuge was used to determine the particle size and size distributions of the encapsulated pigment particles. This measurement is based on differential sedimentation according to Stokes law, which predicts the settling velocity of particles, which are exposed to acceleration in fluids as a function of their diameter. The measuring system uses the centrifugal acceleration in a hollow disc rotating at up to 24 000 rpm holding a clear fluid inside. The sample is injected through an opening in the center of the disc and spread over the surface of the fluid. Particles are subjected to centrifugal acceleration and sediment at velocities depending on their shape and size towards the outer edge of the disc. At a certain radius the extinction as a function of time is recorded utilizing a detector beam and converted according to Stokes' law into the extinction distribution $E_\lambda(d)$, where d is the diameter of the particles. In order to obtain the corresponding $q_3(d)$ mass distribution the complex refractive index is needed to perform the transformation of the extinction distribution according to the light-scattering theory of Mie (turbidity measurement). The theory of the sedimentation and detection of particles in fluids is well described in the literature [8]. To operate the measurements, a sucrose gradient with two different densities prepared using 3 % and 7 % (w/v) sucrose solutions. The gradient solution filled successively in nine steps into the disc starting with the dilution of highest density. Then the gradient solution was calibrated with a (377 nm) PVC standard and the size distributions were determined for the different pigment inks by injection of (~100 µL) onto the gradient.

3.3.1.4 Transmission Electron Microscopy (TEM)

When an electron beam strikes a specimen, several interactions result, as illustrated in Figure 3.3. Secondary and backscattered electrons are utilized in scanning electron microscopy (SEM), transmitted electrons in transmission electron microscopy (TEM), X-rays in energy dispersive x-ray analysis (EDX), diffracted electrons in diffraction patterns, both diffracted electrons and transmitted electrons are used for obtaining high resolution transmission electron microscopy images (HR-TEM) and light emitted can be used for cathodoluminescence microscopy. Except for the latter interaction, the various interactions have been employed in this work for sample characterization and would therefore be briefly explained hereunder.

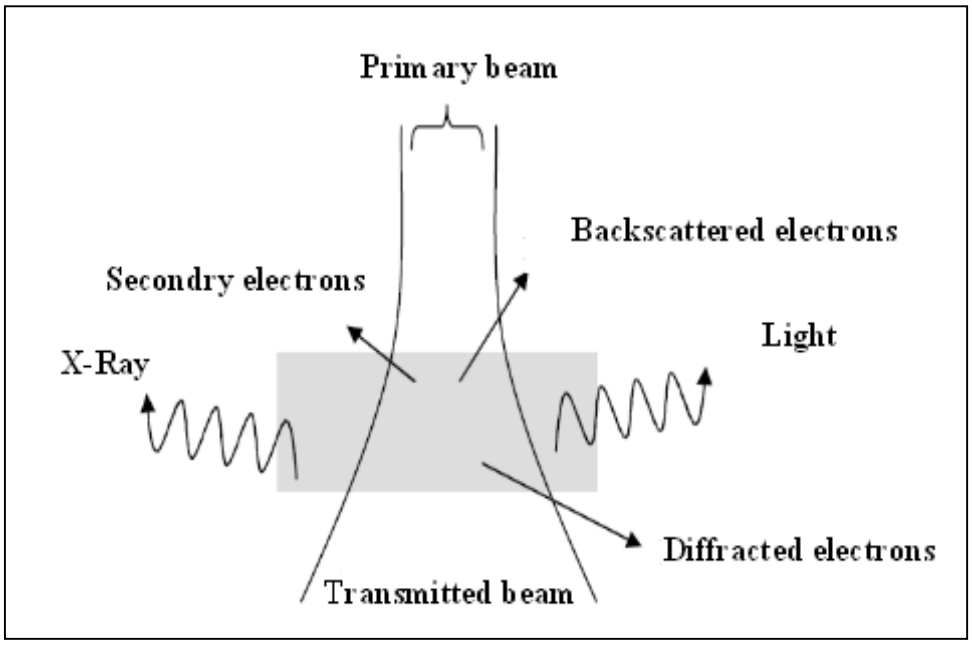

Figure 3.3 Schematic diagram of the main interactions of a primary electron beam with a specimen.

In transmission electron microscopy (TEM), electrons are emitted typically via an electron gun or a field emission gun. The emitted electrons are then accelerated down the microscope column in vacuum. Figure 3.4 shows the main components of a TEM column. The wavelength of the emitted electrons is given by: where *h* is Planck's constant, *e* is the electron charge, *me* is electron mass at rest and *c* is the speed of light. Substituting those constants in the expression leaves the wavelength as a function of *V*, the accelerating voltage [9, 10].

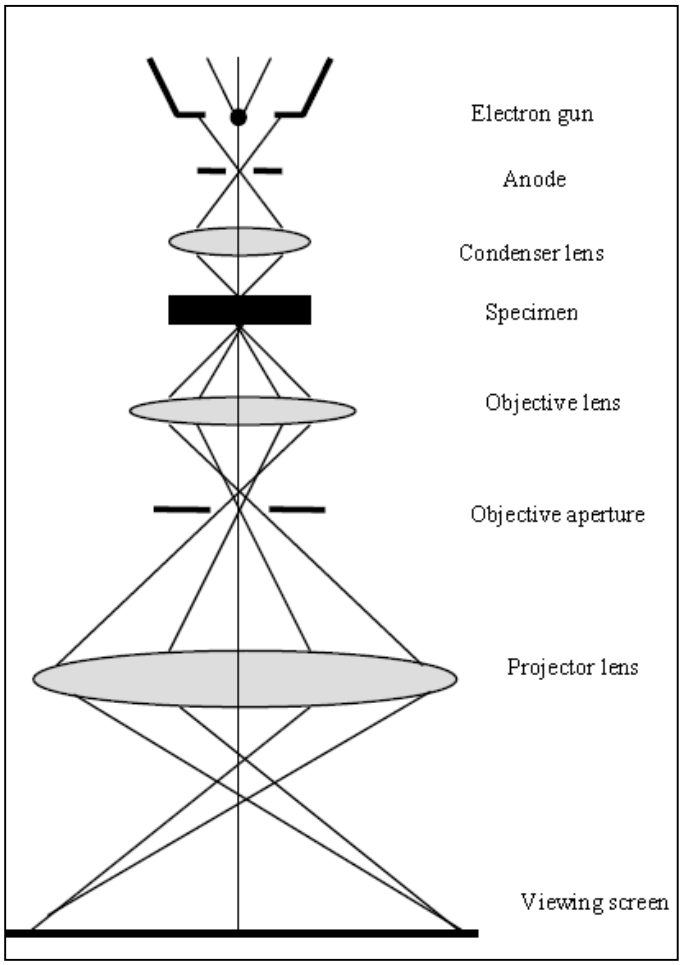

Fig.3.4 TEM ray diagram illustrating typical TEM main components [10].

In our experiments, a FEI Tecnai G² 20 S-TWIN transmission electron microscope by the Zentraleinrichtung Elektronenmikroskopie (ZELMI), Berlin Institute of Technology (TU Berlin), with an accelerating voltage of 200 kV was used to obtain further information about the morphology and particle size of the of polymer latex particles. For the sample preparation very dilute samples (~100-200 times diluted) of the latex or the hybrid latex dispersion were added to a proper amount of 2% phosphotungstic acid (PTA) solution and mixed for 10 min. A drop (1 μL) of the mixture was then placed on a copper-coated carbon grid and dried at room temperature before being placed in the electron microscope.

3.3.2 Structural characterization and molecular weight of the miniemulsion copolymer latexes.

3.3.2.1 ^{1}HNMR

The copolymer composition was determined by proton nuclear magnetic resonance (^{1}H NMR) using a n a 200 MHz Bruker AC-200 Bruker Biospin, AC200 spectrometer. The samples were prepared in deuterated chloroform. The surfactant was removed from the dried latex by dissolving the dried latex in a small aliquot of THF (~1 mL) and precipitating out the polymer with water (~10 mL). The solution was then filtered to collect the polymer, further rinsed with distilled water, and then dried. The samples were then measured to determine the copolymer composition of the miniemulsion latex.

3.3.2.2 Gel permeation Chromatography (GPC)

We determined the apparent molecular weight and weight distribution of the polymerized miniemulsion copolymer latex using THF as eluent with a flow rate of 1ml per minute. The column was a SDV-type (styrene/divinyl benzene, 100 nm porosity and 5 μm particle size, 10000 nm (5μm) and 1000000 nm (10μm)) column from PSS GmbH. Calibration of the GPC column had been done by means of polystyrene (by PSS GmbH, 0.27kD to 2570kD) standards.

3.3.3 Monomer conversion and solid content

Monomer conversion and solid content were measured by gravimetric analysis. Different samples were withdrawn from the reactor at different polymerization times during the emulsion polymerization (polymerization was stopped by adding 1% hydroquinone). A certain quantity of emulsion was cast into a Petri dish and dried in an oven at 70-80 ^{o}C, until a constant weight was reached. Solid content and final conversion were calculated by the following formulas (Eq. 3.16 and 3.17),

$$\text{Solid content (wt\%)} = \frac{W2 - Wo}{W1 - Wo} \times 100 \qquad 3.16$$

where W0 is the weight of the Petri dish and W1 and W2 are the total weight of latex and Petri dish before and after drying to a constant weight, respectively.

$$\text{Monomer conversion (wt\%)} = \frac{[W3 \times \text{Solid content} \times 100\,] - W4}{W5} \times 100 \qquad 3.17$$

where W3 is the total weight of all the materials put in a flask in each polymerization, W4 is the weight of non-volatile materials, and W5 is the total weight of monomers.

3.3.4 Surface tension

Surface tension measurements were done at 25.0 ºC using a digital tensiometer (DCAT, DataPhysics Instruments). Measurements were made using a Wilhelmy plate and data acquisition was done using the software provided by the manufacturer. The Wilhelmy Plate method (Fig. 3.5) employs a microroughened platinum iridium plate (19.90 mm in width and 0.20 mm in thickness), attached to a microbalance. The surface tension measurements were based on weight determination. As a result of test, the average value of six measurements was used [11].

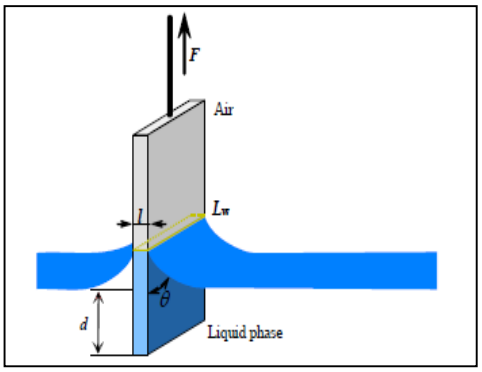

Fig.3.5 Principles of mxeasuring surface tension using Wilhelmy Plate method.

In this technique, the plate is suspended at the interface and maintained in this position by a force that balances the weight of the plate and the meniscus force of the liquid acting on the lower edge of the plate. This force is proportional to the interfacial tension as described by eq. 3.11:

$$\gamma_l = \frac{F}{p.\cos\theta} \qquad 3.11$$

where F is force measured by using a microbalance, p is perimeter of the three-phase contact line l·Lw, θ is the contact angle measured for the liquid meniscus in contact with the object surface. Repeated cycles of immersion and emersion were performed at a rate of 1 mm/s. Immersion depth of the plate was d = 10 mm.

The validity of these readings was confirmed by taking surface tension readings of pure water (71.79 ± 0.02 at 25 ºC) before each sample reading.

3.3.5 Zeta potential

Zeta potential (ζ) was used to test the long-term stability of the encapsulated pigment inks by determining the surface charge on the encapsulated pigments. The measurements were performed with a Malvern Zetasizer Nano ZS at 25.0±0.1 °C. Thereby Laser Doppler Velocimetry (LDV) measures the electrophoretic mobility of the dispersed particles of the encapsulated pigment in a spatially uniformal electrical field.

3.3.6 Thermal analysis

3.3.6.1 Differential scanning calorimetry (DSC)

Thermal analysis by DSC can give some insight into the structure and properties of the polymer by determination of the glass transition temperature (Tg), the melting temperature (Tm) and the crystallization temperature (Tc). The Tg represents an approximate measure of conformational rigidity and the transition from a frozen state to an amorphous state whereby there is sufficient thermal energy for bond torsion to occur and for the polymer to exhibit elastomeric properties [12]. In our experiments, we were interested to determine the glass transition temperature of the copolymer latex at different monomer compositions, which allows us to get initial information about the applicability of our miniemulsion latexes as binders for the textile printing. A small aliquot of the final latex solution was dissolved in THF (~1 mL), then precipitated in water (~10 mL), dried and then analyzed by a Perkin Elmer DSC 7 calorimeter for the thermal behavior analysis. The DSC scanning on the dried latex samples was performed from -100 to +200 °C at a heating rate of 10 °C/min under a nitrogen atmosphere. The T_g was taken as the intersection of the extrapolation of the base line with the extrapolation of the inflection in the DSC thermogram [13, 14].

3.3.6.2 Thermal gravimetric analysis (TGA)

TGA was used to determine the encapsulation efficiency as well as the thermal behavior of the of the encapsulated pigment particles with the polymer or the copolymer latexes. For this purpose, we performed the analysis by the thermal gravimetric analysis (TGA) (Netzsch STA 409, Germany). The experiments were performed for a powder of the hybrid-encapsulated pigments obtained after freeze-drying the hybrid pigment dispersion for 48 hours. Samples of 8-20 mg of the hybrid pigment powder were put in the gold crucible of the TGA instrument and then heated to 800 °C with heating rate 10 °C /min under nitrogen gas flow in order to observe their decomposition behavior. The experimental encapsulation efficiency of the encapsulated C.I. pigment red 112 (E_{PR112}) with the polymer latex layer was determined by incineration of

the polymer shell which estimated from the TGA data. The percentage of PR112 encapsulation efficiency was calculated as follow [15]:

$$\mathbf{E_{PR112}}\% = \frac{\text{residual weight of PR112after incineration}}{\text{theoretical weight of PR112 in samples}} \times 100 \qquad 3.12$$

where theoretical weight of PR112 is calculated as:

$$\textbf{Theoretical weight of PR112} = \text{weight of dried sample} \times \text{weight fraction of PR112 in the sample} \qquad 3.13$$

where weight fraction of PR112 is calculated as:

$$\text{Weight fraction of PR112} = \frac{\text{weight of PR112}}{\text{weight of polymer+weight of PR112}} \qquad 3.14$$

3.4 Textile printing application

The main objective of the thesis was to apply our prepared miniemulsion/nanoemulsion polymer latexes as binders for the textile pigment and inkjet printing of cotton fabrics. In addition, the encapsulated pigments with the miniemulsion copolymer latexes were applied without addition of separate binders as self-thermally curable inks in the inkjet printing of cotton fabrics. The printing methods as well as the characterizations of the printed cotton fabrics are described in this section.

3.4.1 Pigment printing method

The printing pastes of the pigment printing were prepared according to the following recipe in table 3.5 using our prepared miniemulsion/nanoemulsion or the conventional binder. The aforementioned formulated printing pastes were applied to the cotton fabrics using a conventional flat screen-printing method [16]. The fabric printing was performed with a laboratory magnetic roll-printing machine (J Zimmer, ITCF Denkendorf, Germany). After printing, the printed fabric samples were dried at 105 ^{o}C for 3 minutes followed by thermofixation in a thermostatic oven (Memmert, Switzerland) at 160 °C for 5 min.

Table 3.5 Typical pigment printing paste recipe.

Ingredients	Weight (g)	Concentration (wt %)
Pigment color	2.0	2%
Polyacrylate–based synthetic thickener (CHT-BEZEMA TUBIVIS DL 650)	1.5	1.5%
Miniemulsion binder or conventional binder	5.0	5%
DI water	91.5	

3.4.2 Inkjet printing method

The recipe of the inkjet printing is described in table 3.6. The ink formulations consist of pigment color, our prepared miniemulsion/ nanoemulsion or conventional binder, Byk 346 surfactant, water soluble humectant such as sorbitol, deionized water and other additives such as pH adjusting agents and preservatives. For the encapsulated pigments with the miniemulsion copolymer latexes, the hybrid inks were applied without addition of separate polymer binder. The obtained pigment inks were added into the cartridge of a Mimaki TX 1600 inkjet printer with the following parameters (720 dpi, 8 pass and 1 overprint), where ink droplets were produced and controlled electronically and could be directed to form the desired images on the cotton fabrics. The printed fabrics were dried at 105 ^{o}C for 3 minutes then subjected to thermofixation at 160 ^{o}C for 5 minutes.

Table 3.6 Typical ink formulation recipe for the inkjet printing

Ingredients	Weight (g)	Concentration (wt %)
Pigment color/ Encapsulated pigment color	2.0	2%
Miniemulsion/ nanoemulsion binder	5.0,10.0	5,10%
Sorbitol	5.0	5%
BYK 346	0.5	0.5%
DI water	87.5,82.5	

3.4.3 Characterization methods of the printing of cotton fabrics

3.4.3.1 Rheological data of the printing pastes and the ink formulations

The rheological properties and apparent viscosity of the printing pastes and the encapsulated pigment inks were measured using a Bohlin Gemini 200 HR Nano-Rheometer (Malvern Instrument, U.K.). For the printing pastes, the measurements were done using with cone and plate geometry with a 4 cm cone with a cone angle of 4^{o} and 0.15 mm gap at 25 ^{o}C and for

different shear rates $\dot{\gamma}$ in the range of 0 to 500 s^{-1}. The apparent viscosity η_{app} was calculated from the experimentally observed shear stress σ as,

$$\eta_{app} = \frac{\sigma}{\dot{\gamma}} \qquad 3.15$$

However, the rheological properties of the encapsulated pigment ink formulations was measured with the same plate geometry as in the printing pastes but in the presence of solvent trap to prevent evaporation, while the shear rate was varied from 0 to 750 s^{-1}.

3.4.3.2 Color strength measurements of printed fabrics

The cotton fabrics printed with pigment printing and inkjet printing techniques were individually tested for their color strength (K/S). The K/S values are a function of the spectral reflectance at a given wavelength and are defined as the ratio between light absorption (K) and scattering (S) characteristics of the sample. The color strength K/S values of the printed fabrics were instrumentally determined from reflectance measurements with the following Kubelka-Munk equation 3.18 [17, 18]:

$$\frac{K}{S} = \frac{(1-R)^2}{R^2} \qquad 3.18$$

where R is the reflectance of the colored fabric, K is the sorption coefficient, and S is the scattering coefficient of printed fabrics. The reflectance of the prints was measured on an ICS-Texicon reflectance spectrophotometer. The K/S_{max} value corresponded to the largest value of K/S over the scanned wavelength is commonly used to describe the color strength of a dye or pigment-substrate system [19]. Therefore, the increase of the K/S_{max} value can be used as a characteristic to compare our prepared miniemulsion/nanoemulsion latex binders with the conventional binders as well as the encapsulated pigment inks and non-encapsulated ones, which applied to cotton fabrics.

3.4.3.3 Color fastness of printed fabrics

Textiles are subjected to frequent washing and rubbing during their usage. Hence, color fastness of printed modified fabrics has been assessed to determine the degree of wash down. The samples were visually assessed using gray scales [20, 21]. The gray scale ranges from 5, for no shade change (or no stain on the adjacent fabric), to 1, for a severe shade change (or staining), with half points (between 4 and 5, 3 and 4, 2 and 3, 1 and 2) in between.

3.4.3.3.1 Color fastness to washing

The color fastness to washing was determined according to American Association of Textile Chemists and Colorists (AATCC) Test Method 61-2001 (AATCC, 2001). The printed samples (4x4 cm2) were sewed between two pieces of cotton and wool fabrics. The composite sample was immersed in an aqueous solution containing (5 g/l soap and 2 g/l sodium carbonate) at the liquor ratio of 50:1. The bath was thermostatically adjusted to 40 °C. The test was run for 30 minutes. The samples were then removed, rinsed twice with occasional hand squeezing, then dried. Evaluation of the wash fastness was established using the gray scale reference for color change.

3.4.3.2.2 Color fastness to rubbing

The color fastness to rubbing was determined according to AATCC Test Method 116-2001 (AATCC, 2001). This test is designated for determining the degree of color, which may be transferred from the surface of the colored fabric to another surface by rubbing. A colored test sample fastened to the base of a crockometer was rubbed with white crock test fabric under controlled conditions.

3.4.3.2.2.1 Dry rubbing test

The test sample was placed flat on the base of the crockometer. A white testing fabric was mounted. The covered finger was lowered onto the test sample and caused to slide back and forth 20 times by making ten complete turns at a rate of one turn/s. The white test sample was then removed for evaluation using the gray scale.

3.4.3.2.2.2 Wet rubbing test

The white test sample was thoroughly wetted out in deionized water to a 65 % pick up. The procedure was run as before. The white test samples were then air-dried before evaluation.

3.5 References:

[1] E. J. Folta-Stogniew. (2001). Macromolecular Interactions: Light Scattering. *Encyclopedia of Life Sciences*. New York, USA: John Wiley & Sons, Ltd.

[2] W. Schärtl. (2007). *Light scattering from polymer solutions and nanoparticle dispersions*. Heidelberg, Germany: Springer-Verlag: Berlin Heidelberg.

[3] Dynamic light scattering: an introduction in 30 minutes. *Malvern Instruments Ltd.: Worcestershire*, p 8.

[4] L. H. Sperling (2001). *Introduction to physical polymer science*. New York, USA: John Wiley & Sons, Ltd.

[5] A. Radulescu, A. Loffe. (2008). Neutron guide system for small-angle neutron scattering instruments of the julich centre for neutron science at the frm-ii. *Nuclear Instruments & Methods in Physics Research Section A-accelerators Spectrometers Detectors and Associated Equipment*, *586*, 55-58.

[6] J. K. Percus, G. Yevick. (1958). Analysis of Classical Statistical Mechanics by Means of Collective Coordinates. *J. Phys. Rev., 110*, 1-13.

[7] N.W. Ashcroft, J. Lekner. (1966). Structure and Resistivity of Liquid Metals. *J. Phys. Rev., 145*, 83-90.

[8] L. E. Oppenheimer. (1983). Interpretation of disk centrifuge data. *J. Colloid. Interf. Sci., 92*, 350-357.

[9] P.J. Goodhew, F.J. Humphreys, R. Beanland (2001). Electron diffraction. *Electron microscopy and analysis* (pp. 40-65). London, UK: Taylor & Francis.

[10] W. Zhou. (2009). Transmission Electron Microscopy. *Metal Oxide Catalysis* (pp. 443-485). Weinheim, FRG, Germany: Wiley-VCH Verlag GmbH & Co. KGaA.

[11] K. Holmberg. (2002). Vol. 1. *Handbook of Applied Surface and Colloid Chemistry* (pp. 219). New York, USA: Wiley & Sons.

[12] M. Zienkiewicz, J. Czuprynska, J. Polanski, T. Karasiewicz, W. Engelhard. (2008). Effects of electron-beam irradiation on some structural properties of granulated polymer blends. Radiation Physics and Chemistry, 77, 146-153.

[13] P. E. Cassidy. (1980). *Thermally Stable Polymers: Syntheses and Properties*. New York / Basel, USA: Marcel Dekker.

[14] J. F. Rabek. (1980). *Experimental Method in Polymer Chemistry*. New York, USA: Wiley & Sons.

[15] D. G. Yu, J. H. An, J.Y. Bae, Y.E. Lee, S.D. Ahn, S.Y. Kang, K.S. Suh. (2004). Preparation and characterization of titanium dioxide core/polymer shell hybrid

composite particles prepared by emulsion polymerization. *Journal of Applied Polymer Science, 92*, 2970-2975.

[16] L. W. C. Miles. (2003). *Textile Printing* (2nd ed.). Bradford, UK: Society of Dyers and Colourists.

[17] S. H. Amirshahi, M. T. Pailthorpe. (1994). Reduction of quenching effects of fluorescent whitening agents by blending. *Dyes and Pigments*, *26*, 121-128.

[18] J. Alvarez, B. Lipp-Symonowicz. (2003). Examination of the Absorption Properties of Various Fibers in Relation to UV Radiation. *Autex Research Journal*, *3*, 72-77.

[19] C. J. Grum. (1980). *Optical radiation measurments*. New York, USA: Academic press.

[20] Y. Q. Zhang, S. Westland, V. Cheung, S. M. Burkinshaw, R. S. Blackburn. (2009). A custom ink-jet printing system using a novel pretreatment method. *Coloration Technology, 125*, 357-365.

[21] J. H. Xin. (2006). *Total colour management in textiles*. Cambridge, UK: Woodhead Publishing in association with the Textile Institute.

4. Preparation and characterization of nanosized copolymer latexes based on butyl acrylate and methyl methacrylate by miniemulsion polymerization and their application as binders for textile pigment and inkjet printing.

4.1 Introduction

Miniemulsions are dispersions of kinetically stable oil droplets with a size of (30-200 nm) and may be prepared by shearing or sonicating a system containing oil (monomer), water, surfactant, and hydrophobe [1-5]. Miniemulsion polymerization differs from conventional emulsion polymerization in the mechanism of the particle nucleation (formation). In miniemulsion polymerization, particle nucleation takes place in the stabilized monomer droplets, while in conventional emulsion polymerization the nucleation occurs in the monomer swollen micelles [6, 7]. The application of ultrasonic or high-pressure homogenization in the initial preparation of miniemulsion is crucial to produce large numbers of small oil droplets and thus an increase in the total surface area of the monomer droplets. Consequently, they can compete effectively for the free radicals during polymerization [8-13]. The stabilization of the droplets against coalescence is due to the addition of surfactant while the addition of a highly water insoluble and low molecular weight costabilizer (hydrophobe) prevents the diffusional degradation of the droplets [14]. The costabilizer is contained inside the monomer droplets and increases the osmotic pressure inside the droplets, hence preventing the growth of the large droplets at the expense of the smaller droplets via diffusion, which is known as Ostwald ripening [15]. Typical costabilizers (or osmotic agents) that have been employed in miniemulsion systems are fatty alcohols such as cetyl alcohol and long-chain alkanes such as hexadecane or squalene as well as the polymeric hydrophobes [1-4, 16]. In miniemulsion systems, the final polymer particle size can be controlled by the initial droplet size since particle formation takes place within the monomer droplets. Some authors have claimed that droplets in miniemulsion polymerization have the same size and distribution as the final particles [17], which support the concept of a one-to-one copy from monomer droplets to polymer particles, i.e., a real templating mechanism. Although this one-to-one mechanism is not usually operative, more direct control of particle size and size distributions is possible with miniemulsion polymerization compared to conventional emulsion polymerization. Therefore, the miniemulsion polymerization method can be considered as an effective way to prepare monodisperse and well defined polymeric nanoparticles.

The main aim of the work in this chapter is to prepare monodisperse polymer latexes in diameter size range between 50-100 nm by the miniemulsion polymerization. These monodisperse latexes will then be used as '' miniemulsion binders'' as alternative way for the latex binders prepared by the conventional emulsion polymerization for the textile pigment printing, one of the most important industrial textile printing methods . Pigment fixation on textiles relies on the binding agents that require a curing process to hold the pigments on the textile fabrics [18]. During the curing process, the binder latex particles coalesce to form a polymer film covering the substrate surface while the presence of pigment particles in the film provides the final coating with color and influences other appearance properties such as opacity and gloss. The binding agents are polymers or preferably copolymers of unsaturated monomers such as ethyl acrylate, butyl acrylate, vinyl acetate, butadiene, etc. Pigment printing suffers from some technological and industrial problems such as the relative high curing temperature, fabric stiffness, poor crock fastness and agglomeration of the binders and pigment particles, which cause clogging of the nozzles and screens in both textile ink-jet and screen-printing processes [19, 20]. These disadvantages are related mainly to the undesirably large particle size for the type of binding agents and pigments, which are the most important ingredients used in the pigment ink formulations and pastes. Thus to improve the quality of the pigment printed textile fabrics, the overall properties of the binding agents should be improved by going to smaller and well-defined particles.

In this regard we prepared monodisperse aqueous dispersions of copolymer latexes by the miniemulsion polymerization method to be applied as alternative binding agents for the textile printing, as with respect to their smaller size they are very promising candidates for improved textile printing. The copolymer miniemulsion latex chains were based mainly on a high content of the soft monomer butyl acrylate and low content of the hard monomer methyl methacrylate. In some of our miniemulsion recipes, methacrylic acid and N-methylol acrylamide were added to perform functionality, which enhances the crosslinking reaction of the polymer chains during the curing process. The size and polydispersity of the latex particles were investigated by DLS, SANS and TEM. The application of the miniemulsion latex as a binder for the pigment printing and inkjet printing of cotton fabrics was examined and compared to the conventional processes. The aim of our work then was to correlate the structure and composition of the nanolatexes with their performance in the textile printing application.

4.2 Results and discussion

The main features of the miniemulsion preparations are the application of high shear using an ultrasonic processor or a high-shear mechanical homogenizer to create small size monomer droplets, and a surfactant/costabilzer system to maintain and stabilize the miniemulsion monomer droplets against diffusional degradation and coalescence. Therefore, the mechanism of the particle nucleation in the polymerization of miniemulsions is supposed to proceed through the droplet nucleation in which the particles grow up from the monomer droplets rather than the micelles [21]. Therefore, polymerization in the miniemulsion droplets leads to the synthesis of monodisperse latex particles. Figure 4.1 shows TEM images of butyl acrylate-co-methyl methacrylate latex particles prepared by the miniemulsion and conventional emulsion polymerization. One can observe clearly from the TEM pictures that the miniemulsion polymerization generated latex particles with relative monodispersity and narrow size distributions while the prepared latex particles by conventional emulsion polymerization have obviously higher polydispersity values. Using the concept of the miniemulsion polymerization, we synthesized miniemulsion copolymer latexes, which are composed mainly of a high content butyl acrylate (BA) and a low content methyl methacrylate (MMA) monomers.We selected this copolymer composition to be suited for the application as binder for textile cotton printing. In order to reach optimum conditions at which we could obtain the desired miniemulsion latex particles, we have studied the different parameters, which have major influence on the formation of the initial miniemulsion monomer droplets and their subsequent miniemulsion latex particles after polymerization. These parameters include the influence of the sonication time, variation of the amount of surfactant, variation of the monomer solid contents and functionalization of the miniemulsion latexes by addition of cross-linking agents to the copolymer structure to improve their film properties for the textile printing application.

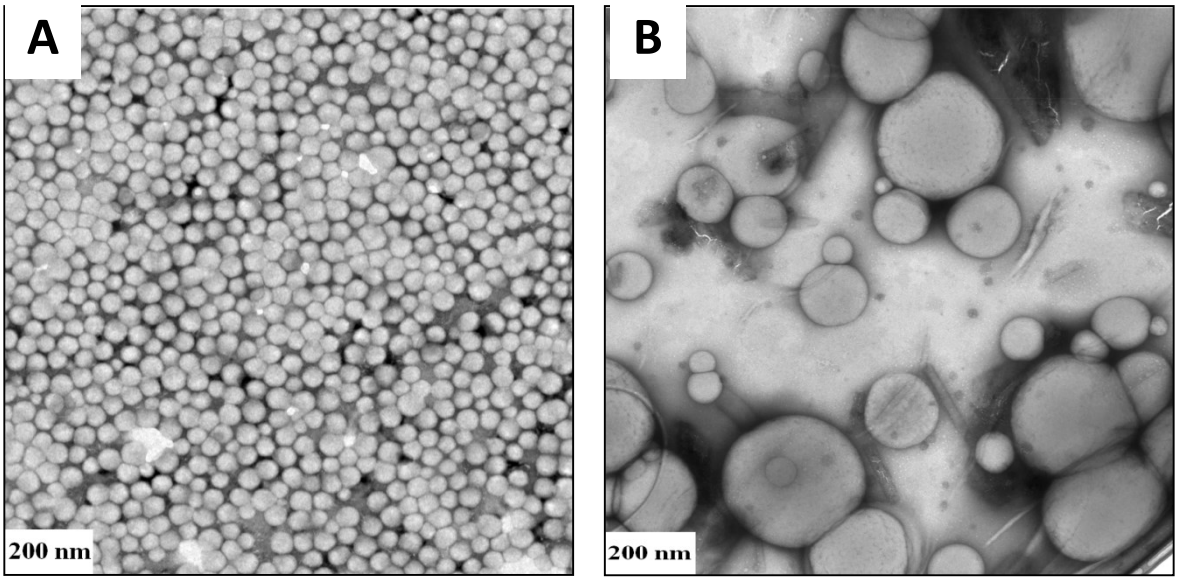

Fig.4.1 TEM images of A) BA-MMA(85:15 wt %) based copolymer latex prepared by the miniemulsion polymerization using 20 % solid content, SDS 7.5 mM, hexadecane 4 wt% (based on monomer) and sonication time 10 min.; B) BA-MMA based copolymer latexes prepared by the conventional emulsion polymerization using 20 % solid content and SDS 7.5 mM (without high shear and hexadecane).

4.2.1 Influence of the sonication time on the particle size and polydispersity of the miniemulsion droplets and the latex particles.

The influence of the sonication time during the initial preparation of the miniemulsions on the size and polydispersity of the droplets and particles before and after polymerization was studied. Table 4.1 describes the hydrodynamic radius and polydispersity of the droplets and particles of the BA-co-MMA based miniemulsion as determined from DLS at different sonication times from 60 seconds to 20 minutes. It should be noted that the monomer solid content was adjusted to a concentration of 5 wt% in order to measure the size and polydispersity of the monomer droplets before polymerization by DLS without dilution and correlate them with the polymerized latex particles. The results show that the hydrodynamic size and polydispersity of the miniemulsion droplets and particles depend mainly on the sonication dose during the miniemulsification process. The hydrodynamic radius and polydispersity decrease steadily when the sonication dose increased by varying the sonication time from 1 to 5 minutes.

Table 4.1 Hydrodynamic radius (Rh) and polydispersity index (PDI) determined by DLS for the miniemulsion droplets and particles prepared at different sonication times, solid content 5 %, SDS 15mM, HD 4 wt% (based on monomer), KPS 1 wt% (based on total weight).

Sonication time (min.)	**Miniemulsion droplets**		**Miniemulsion particles**	
	R_h	**PDI**	**R_h**	**PDI**
1	123	0.42	79	0.28
3	59	0.29	41	0.11
5	44	0.16	39	0.09
7.5	45	0.13	38	0.05
10	46	0.12	37	0.05
15	43	0.1	36	0.05
20	44	0.1	37	0.04

The decrease in the Rh and PDI of the droplets with increasing the intensity of the sonication dose caused by the cavitations of the miniemulsion droplets which breaks up the larger monomer droplets into smaller droplets during the miniemulsification process. However, one cannot see a pronounced change in the Rh and PDI for the sonication time range between 10 and 20 minutes for the miniemulsion droplets and latex particles. Apparently, here one reaches a limiting lower size. Therefore, we adjusted the sonication time at 10 minutes for all miniemulsification experiments.

Similarly, as described in figure 4.2, we observed that the Rh and PDI of the polymerized BA-MMA copolymer latexes with a monomer solid content of 20% decrease as the sonication dose increases. It should be noticed that we could not compare these results with the miniemulsion droplets before polymerization as the dilution of the miniemulsion changes the particle size and polydispersity of the monomer droplets.

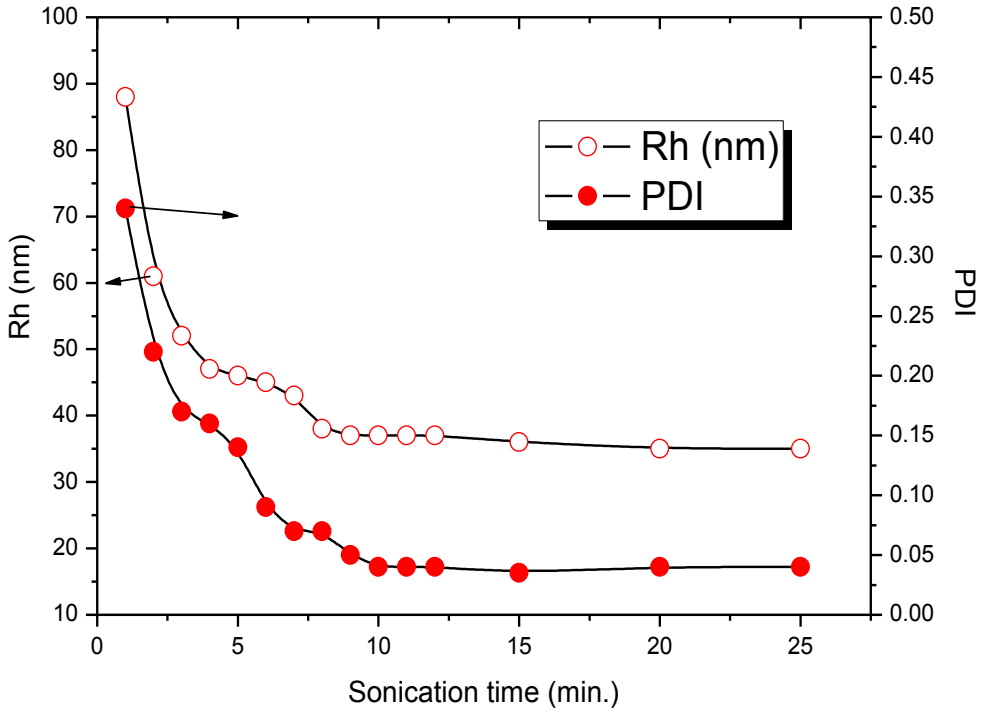

Fig.4.2 Hydrodynamic radii R_h and polydispersity of the miniemulsion BA- co-MMA latexes obtained by DLS at different sonication times , solid content 20 %, SDS 15mM, HD 4 wt% (based on monomer), KPS 1 wt% (based on total weight). Each sample diluted to 0.2% solid content before measurements.

4.2.2 Monomer conversion of the miniemulsion copolymer with different solid contents.

In order to find the optimum conditions (with respect to structural definedness) of the desired latex solid contents in the miniemulsion polymerization, we have investigated the effect of the variation of the monomer concentrations (solid contents) on the overall fractional monomer conversion. Different monomer concentrations based on BA/MMA (with fixed monomer composition of 85:15 BA: MMA) were studied at constant SDS, HD and KPS concentrations of 15 mM, 4 wt%, and 1 wt%, respectively. Figure 4.3 shows the fractional conversion of BA/MMA monomers as a function of time. It was observed that fast polymerization rates were obtained at higher monomer concentrations and reached to about 90% after 45 minutes of initiation while the lower monomer concentration miniemulsion recipes reached only about 70% conversion after 60 minutes. After 3 hours of initiation, we obtained approximately 98% conversion for the 20% monomer solid contents recipes and about 88% conversion for the 5% solid content. This difference in monomer conversion and polymerization rate values between the high and low monomer solid contents may be attributed to reactivity ratio difference between BA and MMA (r_{MMA}=2.55, r_{BA}=0.36) [22]. A pseudo first-order kinetics plot of our experimental data is shown in Fig. 4.3. Plotting the data of

-ln (1- x), where x is the fractional conversion; versus polymerization time resulted in a straight line with a slope, from which we derived the rate constant of each miniemulsion polymerization of the different monomer solid contents.

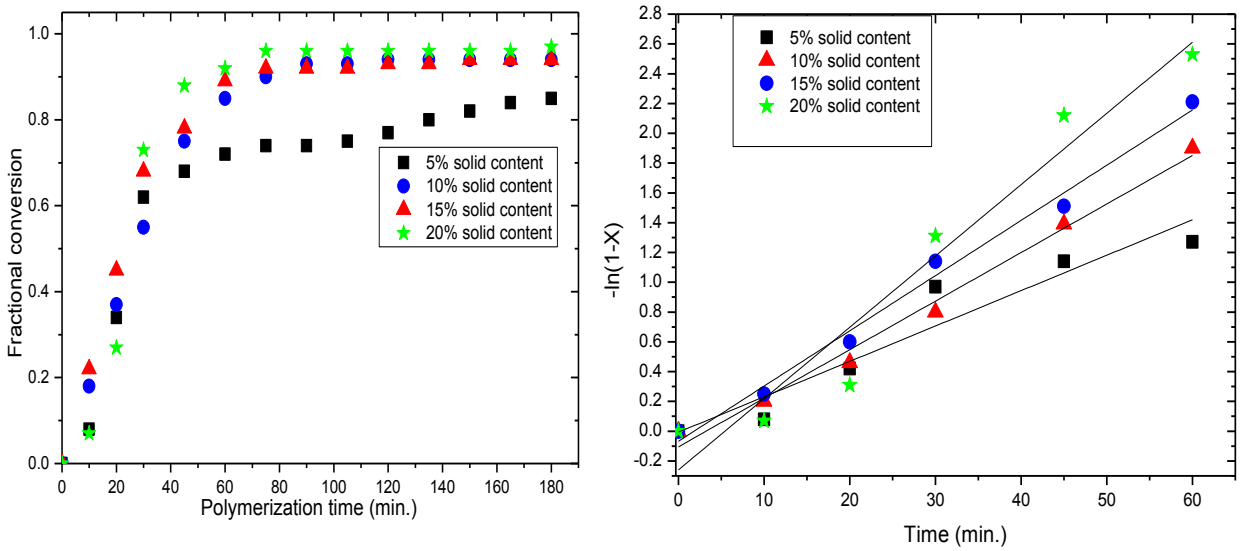

Fig.4.3 The overall fractional conversion by gravimetry as a function of polymerization time and pseudo-first-order kinetics data treatment (x is the fractional conversion of the monomer) as a function of polymerization time for different monomer solid contents in miniemulsion polymerization of BA/ MMA (85:15 wt %), SDS 15 mM, HD 4 wt % [a], KPS 1 wt% [b] and polymerization temperature 70 °C for 3 hours. a) based on the weight of monomer, b) based on the total weight. *K (rate constant) 5% solid content =0.024 min^{-1}, 10% solid content =0.033 min^{-1}, 15% solid content=0.037 min^{-1}, 20% solid content=0.048 min^{-1}.*

The increase of the propagation rate constant values with increasing monomer solid contents as determined in figure 4.3 may be attributed to the increase of MMA monomer content, which has higher solubility value than BA in continuous phase. Hence, the water soluble KPS has the ability to initiate higher contents of MMA monomer at reaction loci and consequently the propagation rate constant increases with increasing the whole monomer content. After approximately one hour of reaction and due to the decrease of the monomer concentration at the reaction loci; we observed that the rate of miniemulsion polymerization decreases for the different solid contents throughout reaction as shown in figure 4.3.

4.2.3 Structural characterization of the miniemulsion copolymer latex.

4.2.3.1 ^{1}HNMR

Figure 4.4 shows a typical ^{1}H NMR spectrum of the prepared miniemulsion butyl acrylate-co-methyl methacrylate copolymer latex with a BA: MMA monomer ratio of (85:15). The relative intensity of the resonances at δ 3.6 and δ 4.04 ppm represent the protons (-OCH3) of MMA and (-OCH2) of BA substitutes respectively. It should be noted that the integration of peaks showed that the monomer ratio of the BA to MMA in the copolymer composition is approximately in order of 85:15, which agrees with the initial monomer ratios. The details of the other proton signals of PBA and PMMA are described in the ^{1}HNMR spectrum in Fig. 4.4, the α-CH, β-CH2 and ^{4}CH3-protons of the PBA appear at (δ 2.2-2.4) ppm, (δ 1.8-2.0 ppm and δ 0.88-0.97 ppm respectively. In case of PMMA, one can see the resonance signals of the protons as follow, the -OCH3 is around δ 3.6 ppm, the β –CH2- protons was observed around δ 2.0 ppm and the α –CH3 protons are between δ 1.0 and δ 1.6 ppm [23].

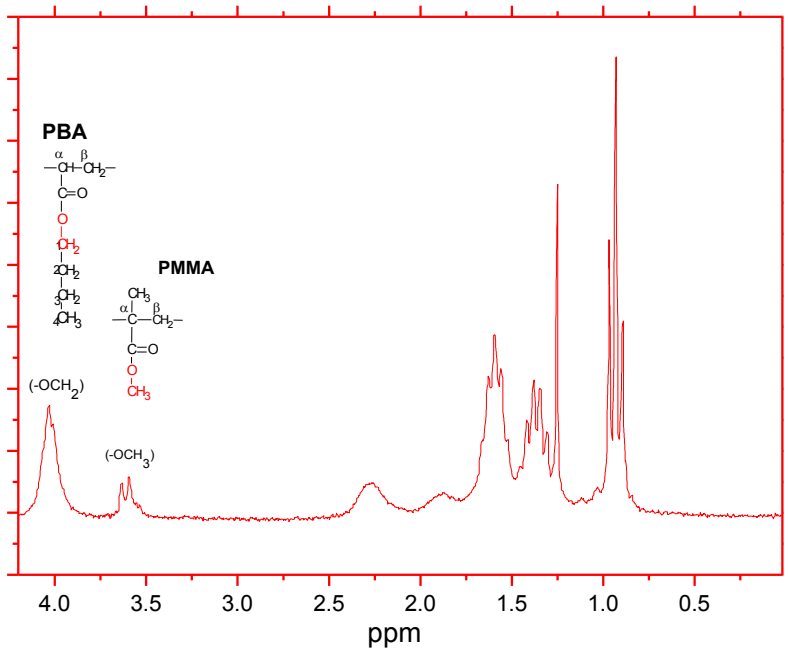

Fig.4.4 ^{1}HNMR spectrum of the Poly butyl acrylate-co-methyl methacrylate (PBA-co-PMMA) latex.

4.2.3.2 GPC

The molecular weight and molecular weight distribution of the miniemulsion BA-MMA copolymer latex with fixed monomer composition of (BA: MMA 85:15) is shown in figure 4.5 as determined from Gel Permeation Chromatography (GPC). The molecular weight of the copolymer BA-MMA latex is around (1.06×10^6 g/mole) and the polydispersity is 1.22 which indicates that the miniemulsion copolymerization generates latex with relatively high molecular weight. In addition, the chromatographic record showed only one peak, which indicates that the polymer latex is very likely composed of copolymer chains of butyl acrylate BA, and methyl methacrylate MMA rather than homopolymer of each polymer chain of BA and MMA.

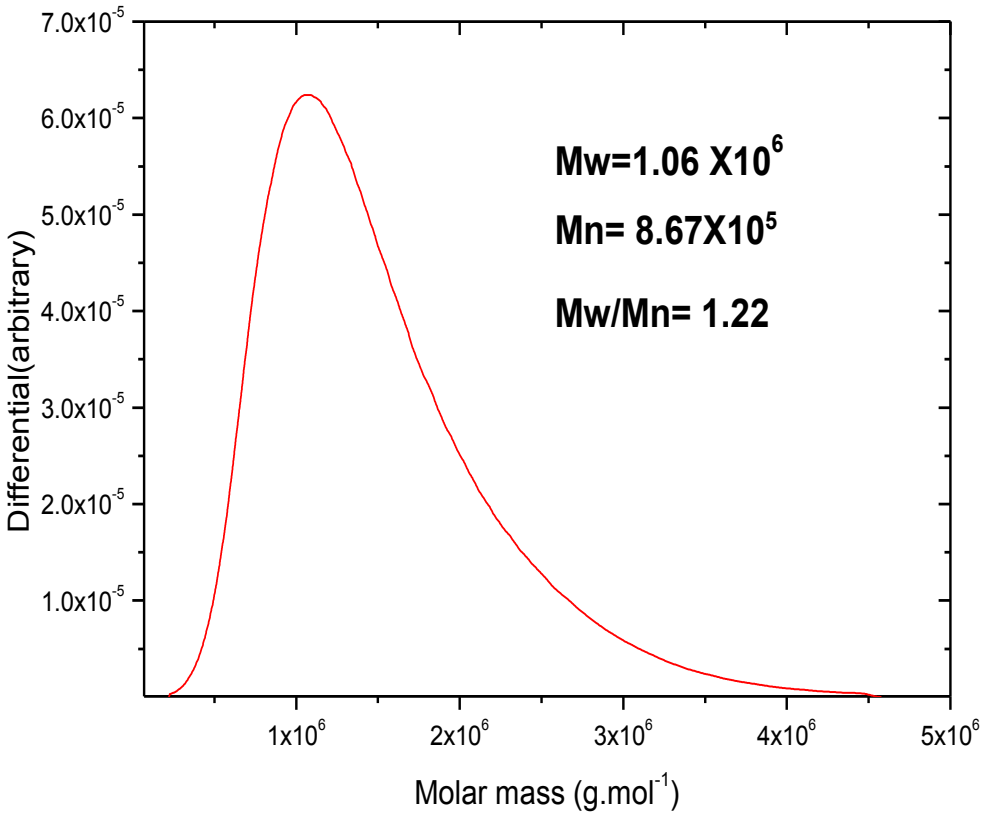

Fig.4.5 Molecular weight distributions of the miniemulsion poly (BA-co-MMA) latex obtained from GPC using THF as eluent with a flow rate of 1 ml per minute.

4.2.4 Particle size and polydispersity analysis of the miniemulsion copolymer latex by DLS, TEM and SANS - variation of SDS surfactant content.

The main goal of this work is to obtain miniemulsion copolymer latex particles based mainly on butyl acrylate (BA) and methyl methacrylate (MMA) with well-defined size distributions to improve their applicability as binder for ink formulations and printing pastes. In miniemulsion systems, the stability and the size of the droplets after mimiemulsification depend directly on the surfactant concentration [24]. Therefore, we studied the influence of variation of the anionic SDS surfactant concentrations on the particle size and polydispersity of the polymerized miniemulsion BA-co-MMA latexes by different analytical methods such as DLS, TEM and SANS.

4.2.4.1 Dynamic Light Scattering and surface tension measurements.

Table 4.2 shows the hydrodynamic radius and polydispersity of obtained from DLS as well as surface tension measurements of the miniemulsion droplets and latexes before and after polymerization at different SDS concentrations. It should be noticed that the miniemulsion recipes were carried out at fixed monomer concentration of 20% and all particle size and polydispersity data were measured after polymerization as the size of the polymer particles does not change upon dilution .The results showed that the variation of the SDS from lower concentration of 1 mM to higher concentration of 60 mM caused a considerable decrease in the particle size of the BA-MMA latex particles. The radii of the BA-MMA copolymer latexes ranged between 213 to 28 nm, while the surface tension of the miniemulsion droplets and particles decreases by increasing in the amount of SDS. The polydispersity of the latex particles slightly increases with decreasing particle size as a result of increasing the amount of SDS; however it still quit low for the all miniemulsion recipes. This slight change in the polydispersity at higher SDS concentrations may be attributed to the probability of the formation of free micelles. Therefore, the mechanism of the particle nucleation may be performed partially through micellar or homogeneous nucleation. Accordingly, the particles will be nucleated outside the droplets, which might lead to an increase in the polydispersity. In general, by increasing SDS concentration, the interfacial tension of the miniemulsion decreases and the size of the miniemulsion droplets decreases which upon subsequent polymerization, latex particles having roughly the same size of its initial droplets were obtained.

Table 4.2 Hydrodynamic radius (R_h) and polydispersity index (PDI) determined by DLS and interfacial tension for different miniemulsion latexes prepared with different SDS concentrations, γ of free SDS[60 mM] solution =34.41 mN .m^{-1}.

SDS concentration [mM]	Rh (nm)	P.D.I	Surface tension γ (mN .m^{-1})	
			Miniemulsion droplets	Miniemulsion Particles
1	213	0.035	56.63	55.04
2	70	0.06	52.44	51.47
5	62	0.05	51.58	50.27
7.5	46	0.04	50.03	48.78
10	43	0.04	49.63	47.89
15	38	0.05	48.13	46.23
25	34	0.07	47.09	43.33
35	33	0.06	44.32	40.61
60	28	0.09	38.92	35.04

The distributions of hydrodynamic radii of the miniemulsion latexes obtained from DLS are given in figure 4.6. At higher SDS amounts, the size distributions become slightly broader. The slight change in the polydispersity and size distributions at higher SDS concentrations may be attributed to the probability of the formation of free micelles. Therefore, the mechanism of the particle nucleation may be performed through micellar or homogeneous nucleation. Accordingly, the polymerization followed the principle of the conventional emulsion, which leads to latexes with relatively wide size distributions. Although the miniemulsion latexes that contain 60 mM SDS have smaller particle size (R_h = 28 nm), in addition to its translucent and bluish appearance, we assume that the latexes were nucleated by a conventional emulsion polymerization rather than a miniemulsion polymerization.

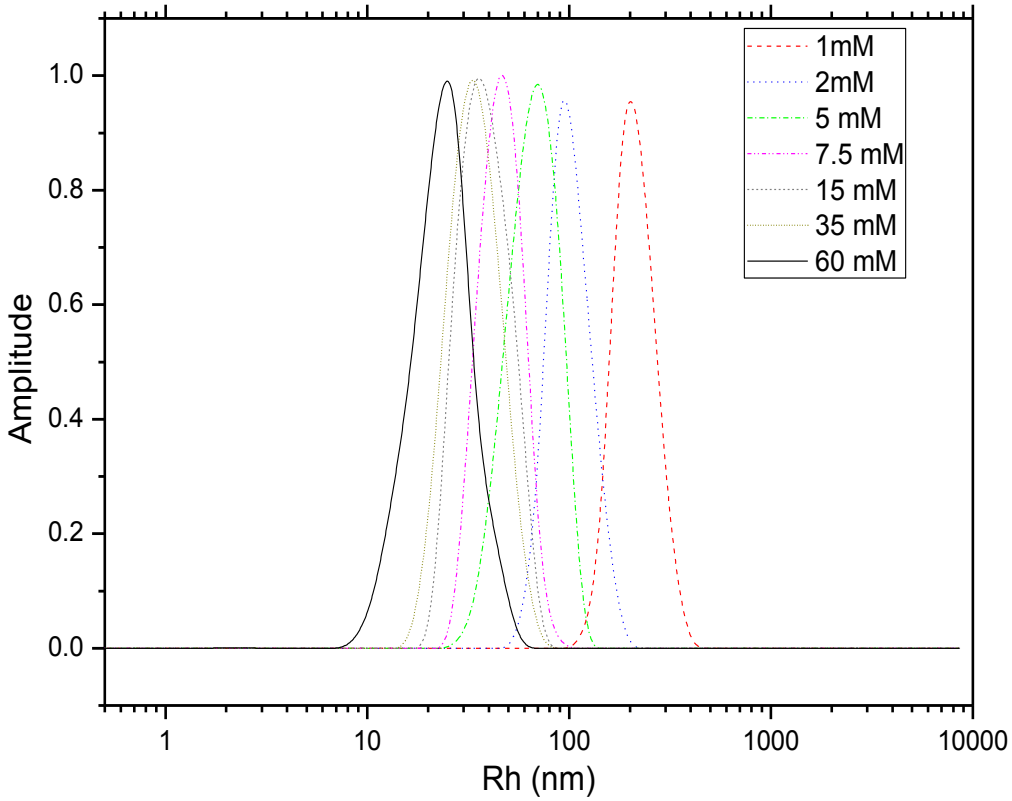

Fig.4.6 Hydrodynamic radius R_h distributions by DLS for different miniemulsion latexes prepared with different SDS concentrations with fixed 20% monomer solid content and BA/MMA ratio of 85:15, HD 4 wt%, KPS 1 wt% and polymerization temperature 70 ^oC for 3 hours.

4.2.4.2 Transmission Electron Microscopy (TEM).

The particle size of the miniemulsion latexes prepared with different SDS concentrations was corroborated by the transmission electron microscopy as shown in the images in Figure 4.6. The TEM images of the different miniemulsion recipes show that the latex particles are spherical and regular in shape with relative monodispersity, while the particle size diameters ranging between 50 to 420 nm depending on the SDS concentration. In general, the results obtained from TEM agree very well with the particle size measurements obtained from DLS.

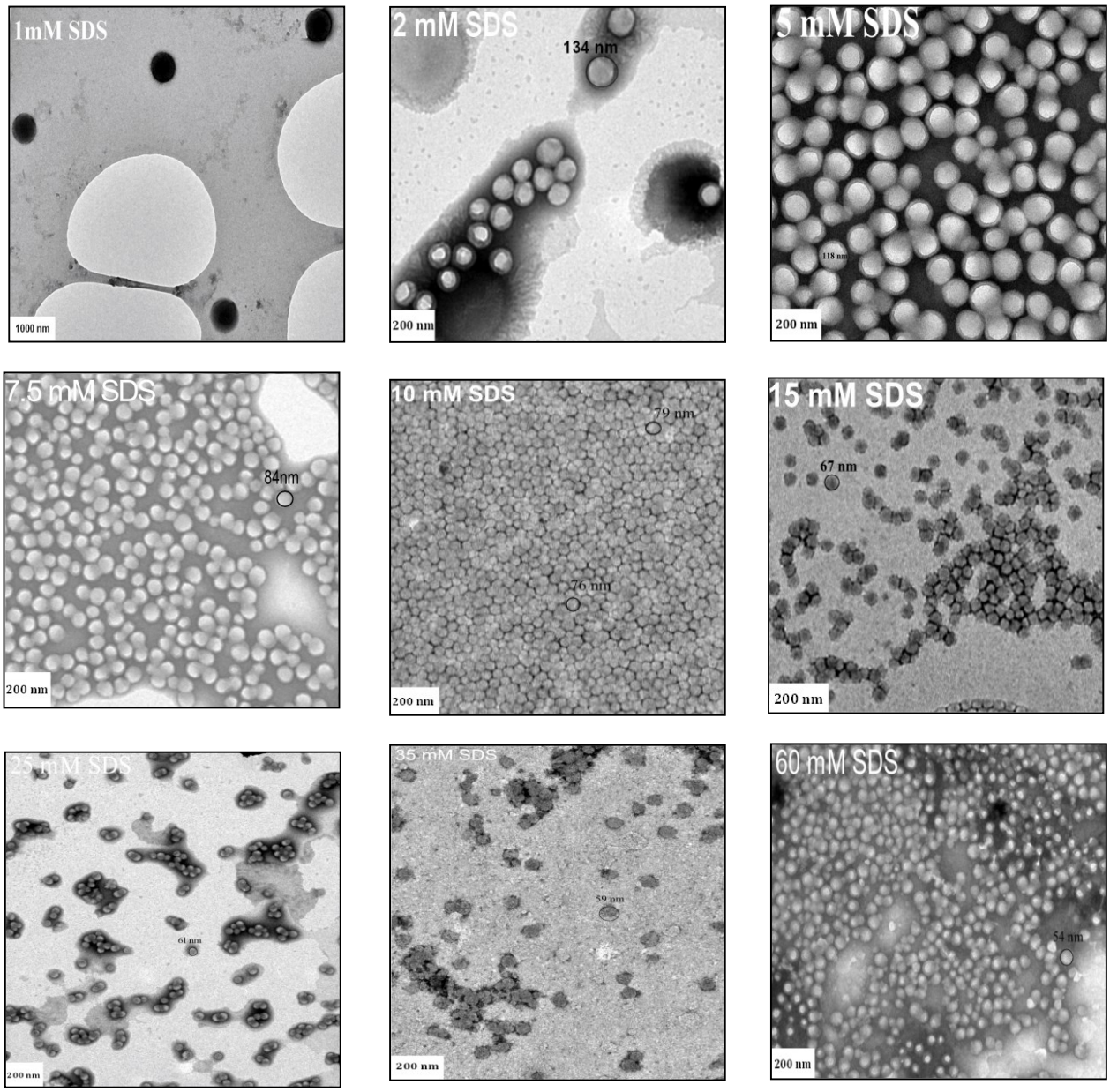

Fig.4.7 TEM images for the different miniemulsion latexes prepared with different SDS concentration.

4.2.4.3 Small angle neutron scattering (SANS).

In order to make further validations regarding the particle size and size distributions of the latexes, we performed SANS experiments with varying the SDS concentrations. SANS is probing spatial fluctuations in the so-called "scattering length density" (SLD), which depends on the atomic composition of domains and their apparent densities. SLDs of H_2O, SDS and latex are -0.56 10^{-4}, -0.37 10^{-4} (for the micellar core), and 0.69 10^{-4} nm^{-2}, respectively. This means that the SANS

"contrast", i.e., the difference in SLD, is extremely small for SDS versus water, and 8 times larger for latex. Hence to a good approximation only the latex particles will contribute to the scattering intensity, and we can consider SDS micelles as transparent. This even more so as the latex particles typically have a volume more than 1000 times larger than the micelles and therefore a correspondingly higher scattering power.

Figure 4.8 shows the obtained I (q) versus q scattering curves of the miniemulsion latex with different SDS concentrations. Generally, the increase of SDS concentration is accompanied by systematic changes in the scattering curves. One observes that at high *q*, a constant scattering background (mostly due to the H contained in the samples) characterizes the scattering curves of the latex particles and oscillations with minima in the q-range of 0.11-0.2 nm^{-1} are observed. The oscillations are due to the particle form factor and their pronouncedness indicates the extent of monodispersity of the samples, which apparently is rather high here. From the location one can conclude that the radius of the particles is 30-55 nm (as the minimum for a solid sphere appears at 4.47/R). The oscillation becomes less pronounced with increasing SDS content thereby indicating a corresponding increase in polydispersity, which is in agreement with our DLS observations (table 4.2). At still lower q one observes a correlation peak that arises from the inter-particle interactions; it is well visible as the particles are rather concentrated and in addition repel each other due to electrostatics. In addition, the difference between experimental and theoretical fitted data at low q may be attributed to the attractive interaction between particles or might be due to the presence of some large particles. The experimental data were now described in a quantitative way by assuming the presence of homogeneous spheres that interact repulsively (Eq. 3.6). The fitting results of the measured scattering curves with this model (solid lines in figure 4.8) show that the particle size radius of the miniemulsion latexes stabilized by 7.5 mM SDS is around 40 nm with PDI of 0.11. By increasing the SDS concentration to 15 mM the size decreases to 33 nm with PDI of 0.12. At higher SDS concentration (35 mM and 60 mM) the particle size decreases to 30 and 25 nm with PDI of 0.12 and 0.14, respectively. In general, one observes very good agreement between the particle sizes obtained from DLS and SANS, especially when one considers that our SANS analysis yields a number averaged size and

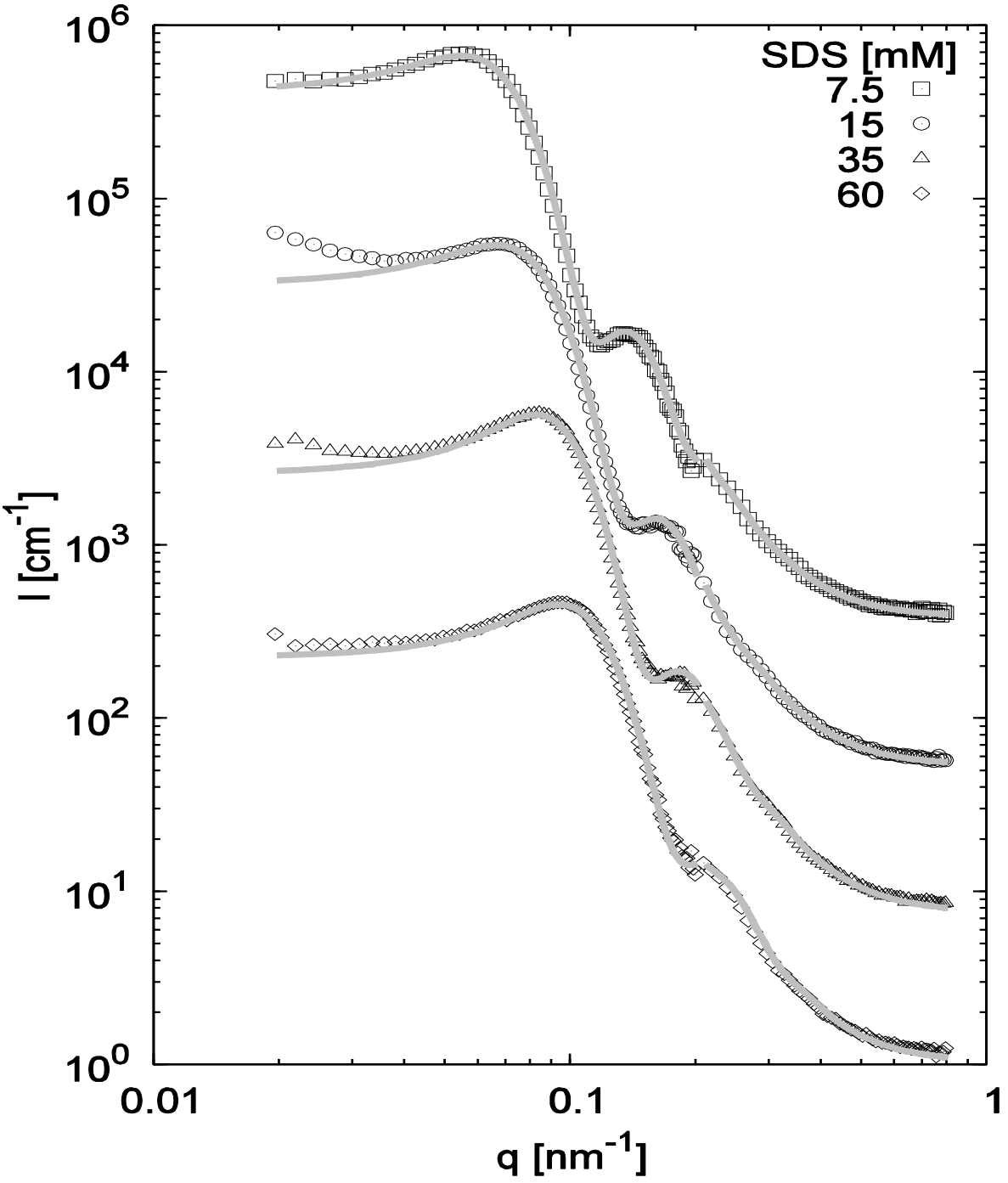

Fig.4.8 SANS data of different miniemulsion latexes prepared with different SDS concentrations at constant 20% monomer solid content with fixed BA/MMA ratio of 85:15, HD 4 wt%, and KPS1 wt% and polymerization temperature 70 ^{o}C for 3 hours. Fitted curves are given as solid lines. Data are incrementally shifted by a factor 7 for readability; data for [SDS] =60 mM are at absolute scale.

DLS a z-average. Therefore the SANS distribution was converted to the corresponding z-average (R_z) using the description given in [25] and this value (also given in Table 4.3) then always coincides within less than 10% with the DLS value. The latter is always larger which can be explained by the fact that first one does not see here the SDS shell (which should have a thickness of about 1.8 nm) and in addition in DLS the hydration shell of the particle (typically in the range of 0.3-0.5 nm) is seen. Taking into account these two points one has an almost perfect agreement between the two measurements. The theoretical radius R_{th} of the miniemulsion droplets/ particles can be calculated if we simply assume the spherical droplets or particles (that contain the oil and the hydrophobic part of the surfactant) to be covered by all of the surfactant. Simple geometry then yields:

$$R_{th} = 3\left(\frac{v_s}{a_h} + \frac{N_{oil}v_{oil}}{N_s a_h}\right) \approx \frac{3\phi_{oil}}{N_{Av} a_h c_s} \qquad (4.1)$$

where v_s and v_{oil} are the molecular volumes of the hydrophobic part of the surfactant and of the oil molecules, respectively, a_h the head group area of the surfactant (taken as 0.66 nm^2 as found for the water/1-hexene interface [26]), N_{oil} and N_s the number of oil and surfactant molecules, respectively, ϕ_{oil} the volume fraction of the oil/monomer or particles, N_{Av} the Avogadro constant, and c_s the surfactant concentration. The values obtained by this simple theoretical model are also contained in table 4 and compared to the experimental data.

The polymerization in miniemulsions with high SDS values (35, 60 mM) results in particles whose radii agree reasonably with the calculated theoretical radii, while for lower SDS values the particles are smaller than the predicted theoretical radii by a factor of 3 to 5. Apparently, at high SDS content the size is determined in a direct way by the SDS concentration, while at lower SDS content the size is mainly due to the mechanical energy input and only to a lesser degree by the surfactant concentration. The results indicated in table 4.3 summarize the particle size measurements of the miniemulsion latexes obtained from the different methods. Generally, there is good agreement between the three methods in which the particle size decreases and the polydispersity increases with increasing SDS concentration. The slight increase in PDI and the smaller particle size at higher SDS concentration observed in the SANS experiments supports the assumption that here micelles are present and the particle nucleation may be proceeded by the conventional emulsion rather than the miniemulsion polymerization.

Table 4.3 Particle size radii and polydispersity indexes determined by DLS, SANS, TEM and theoretically for different miniemulsion latexes prepared with different SDS concentrations with fixed 20%monomer solid content and BA/MMA ratio of 85:15.

SDS concentration [mM]	DLS		SANS		TEM	R_{th} (nm) (eq. 4.1)
	Rh (nm)	P.D.I	$R(R_z)$ (nm)	P.D.I	R (nm)	
7.5	46	0.04	40 (42.5)	0.11	42	186
15	38	0.05	33 (35.4)	0.12	36	96
35	33	0.06	30 (32.2)	0.12	31	42
60	29	0.08	25 (27.5)	0.14	26	28

4.2.4.4 Particle size measurements during miniemulsion polymerization.

The particle size of the miniemulsion droplets before initiation and during the growth process of the latexes was followed by DLS as a function of time for various monomer concentrations. The results given in figure 4.9 show that there is no considerable change in the particle size during the formation process of the nanolatexes, i. e., the initially present size of droplets becomes successfully templated. However, there is some moderate increase of the particle size with time, which indicates that monomer from not nucleated droplets diffuses to particles where growth is taking place. In agreement, one also observes a slight increase in size with increasing total content of monomer.

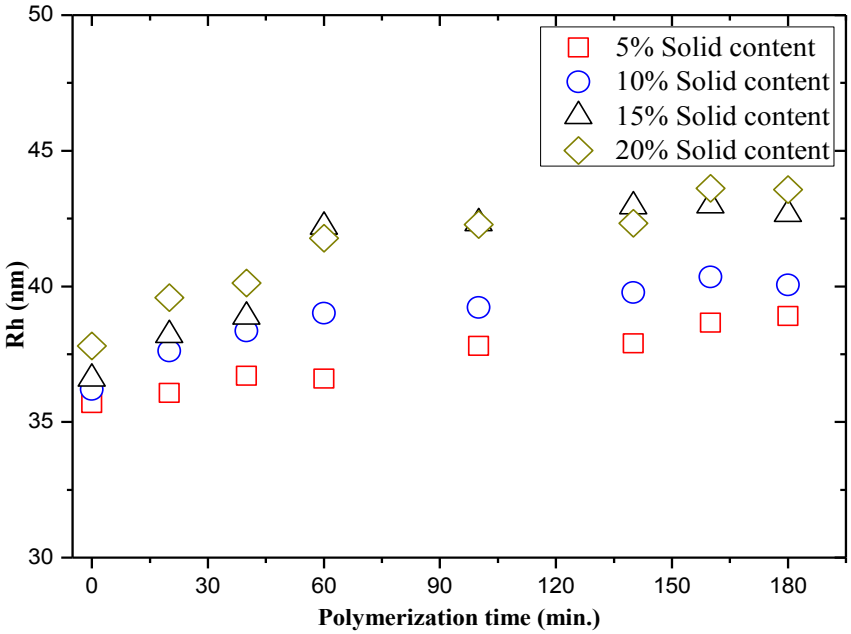

Fig. 4.9 Hydrodynamic radii R_h obtained by DLS as a function of polymerization time for different monomer solid contents in miniemulsion polymerization of BA/ MMA (85/15 wt %), SDS 15mM, HD 4 wt%(based on the weight of monomer), KPS 1 wt% (based on the total weight) and polymerization temperature 70 °C for 3hours.

4.2.5 Functionalization of the miniemulsion latexes.

The incorporation of hydrophilic or hydrophobic functional monomers was done in order to vary the properties of the nanolatexes, thereby providing reactive sites for crosslinking to the latex as well as providing colloidal stability and improving the mechanical properties of the film obtained from these latex miniemulsions in textile printing applications [27]. For that purpose, we employed the hydrophilic monomer methacrylic acid (MAA) and methylol acrylamide (NMA) to the original BA/MMA copolymer latex in order to modify the BA/MMA chains correspondingly. The addition of such reactive sites has been shown to improve the applicability of the miniemulsion latex as a binder for the textile pigment coloration [28]. For this variation of particle composition, the particle size and polydispersity as well as the glass transition temperatures of the different miniemulsion latex compositions have been investigated after and before the addition of MAA and NMA. As shown in Table 5 the hydrodynamic radii of the latex particles, as measured by DLS, are little affected by the addition of the hydrophilic MAA and NMA monomers to the basic hydrophobic MMA-BA miniemulsions while the polydispersity indices in general are somewhat larger. As an

example, the DLS size distributions of samples 1 and 4 are compared in Fig. 4.10, showing that both samples have narrow size distributions but the one of sample 4 is slightly wider than that of sample 1.

Table 4.4 Hydrodynamic radius (R_h) and polydispersity index (PDI) obtained from DLS and the glass transition temperature T_g and its theoretical estimate (according to eq. 4.2) for different miniemulsions latexes prepared with different monomer compositions with fixed SDS 7.5 mM and 4 wt% HD.

Sample	Monomer Composition	Rh (nm)	PDI	Theort. Tg ^{O}C	Measured Tg ^{O}C
1	BA,MMA (8.5,1.5)	46	0.05	-34.4	-32.7
2	BA,MMA,NMA (8.5,1.25,0.25)	44	0.2	-33.9	-31.1
3	BA,MMA,MAA (8.5,1.25,0.25)	51	0.15	-33.4	-32.1
4	BA,MMA,MAA,NMA (8.5,1.25,0.125,0.125)	41	0.08	-33.4	-33.9
5	BA,MMA,MAA,NMA (8,1,0.5,0.5)	45	0.10	-25.0	-24.2
6	BA,MMA,MAA,NMA (7.5,2,0.25,0.25)	43	0.08	-21.5	-23.6
7	BA,MMA,MAA,NMA (7.5,1.5,0.5,0.5)	49	0.12	-19.3	-19.3
8	BA,MMA,MAA,NMA (7,2.5,0.25,0.25)	45	0.11	-15.6	-20.8
9	BA,MMA,MAA,NMA (7,2,0.5,0.5)	46	0.09	-13.3	-14.4

The structural picture of the different latex miniemulsions was corroborated by TEM investigations. TEM images of samples 4, 5, 7 and 9 shown in figure 4.11 exhibit regular and relatively monodisperse spherical latex particles with particle size diameters ranging from 70 to 85 nm with little coagulum which corresponds well to the results obtained from DLS.

DSC curves of different copolymer latexes are shown in figure 4.12 and the corresponding theoretical and measured glass transition temperatures are presented in Table 5. The Flory-Fox equation (Eq. 14) has been used to determine the theoretical glass transition temperature of the different copolymer latexes [29].

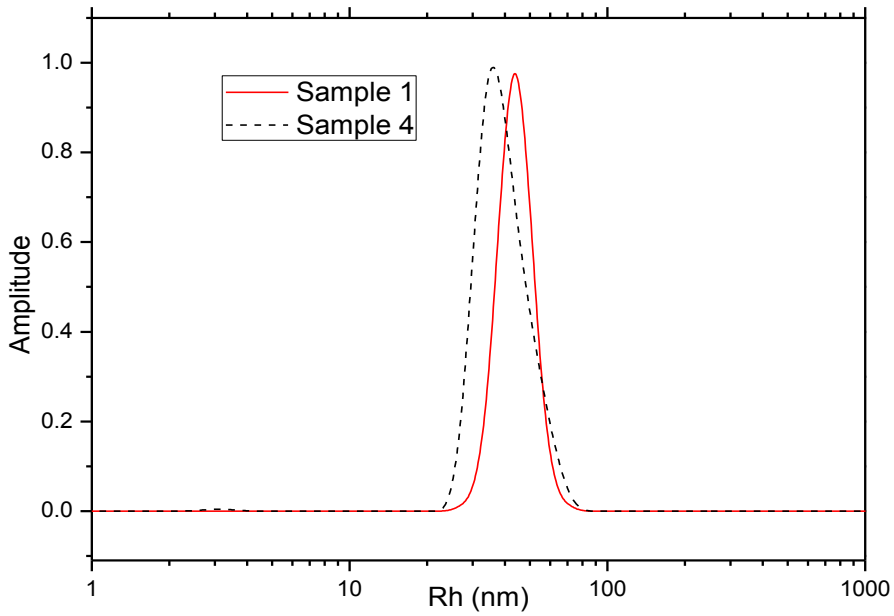

Fig.4.10 Hydrodynamic radius (R_h) size distributions by DLS of sample 1 (BA: MMA 8.5:1.5) and sample 4 (BA: MMA: MAA: NMA (8.5:1.25:0.125:0.125).

$$\frac{1}{T_g} = \frac{W_1}{T_{g1}} + \frac{W_2}{Tg2} \qquad (4.2)$$

Here W_1 and W_2 are the weight fractions of components 1 and 2, respectively, and T_{g1} and T_{g2} are the glass transition temperatures of monomers 1 and 2, respectively. The theoretical and measured T_g values listed in the Table 5 indicate that the variation of the ratio between the soft (BA, T_g = -52 ^{O}C) and hard (MMA, MAA, NMA) is well described by the Flory-Fox model and the T_g's increase by decreasing the content of the soft segment (BA) in the copolymer. The first heating DSC curves of the miniemulsion latex from sample 1 which does not contain MMA or NMA and the other latexes with the different monomer compositions is also given in figure 4.12. It has only one endothermic slope indicating that the T_g of the miniemulsion latex is -33 ^{o}C, whereas for the other curves (like sample 4), it has one endothermic slope due to the T_g (-34 ^{o}C) and one exothermic peak indicating that here the curing reaction takes place in a temperature range between 150 to 160 ^{o}C. In general, the T_g's increase by increasing the content of the MMA, MAA, and NMA in the copolymer latexes.

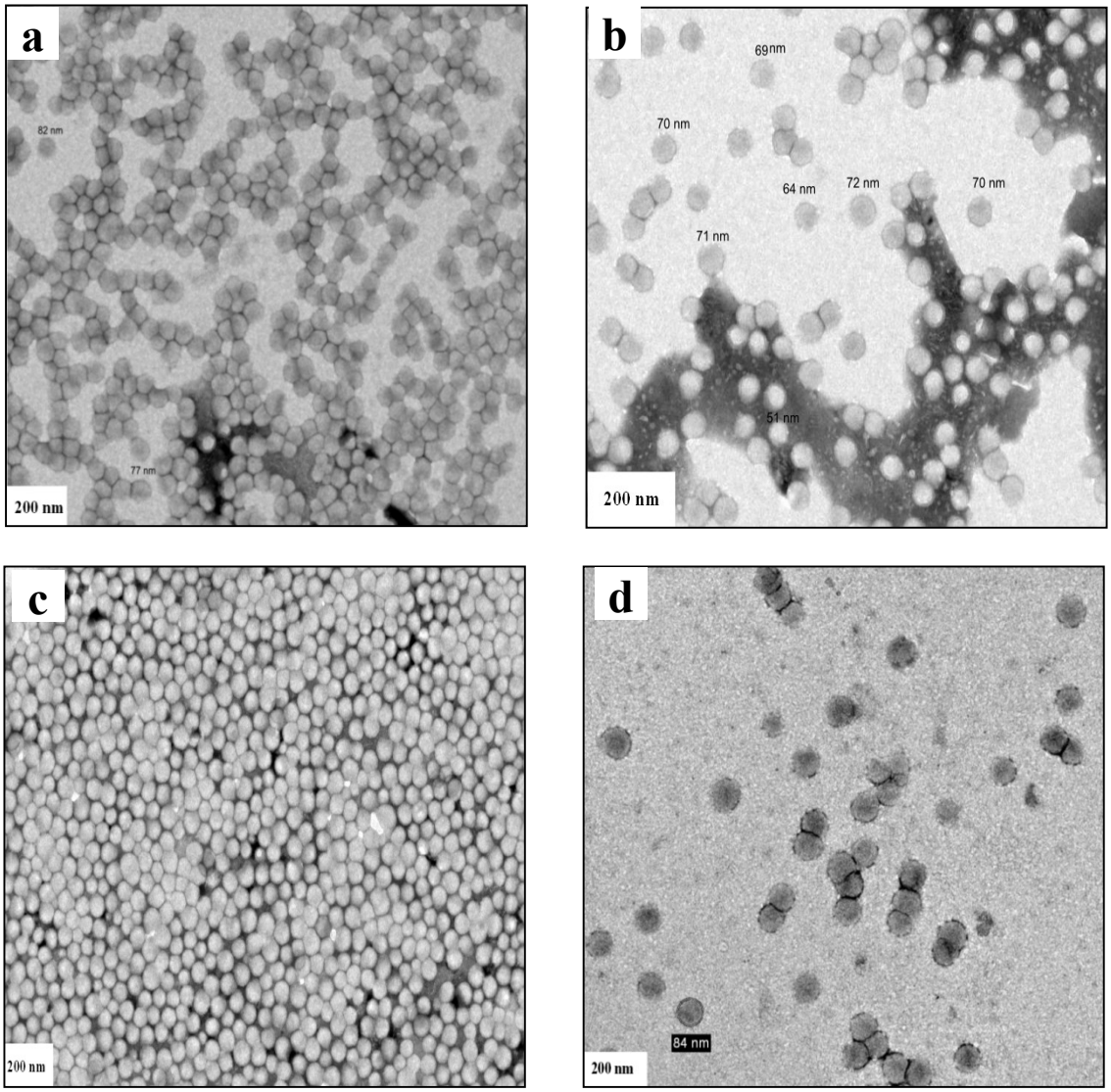

Fig. 4.11 TEM images for the different miniemulsion latexes a) sample 4, b) sample 5, c) sample 7, d) sample 9.

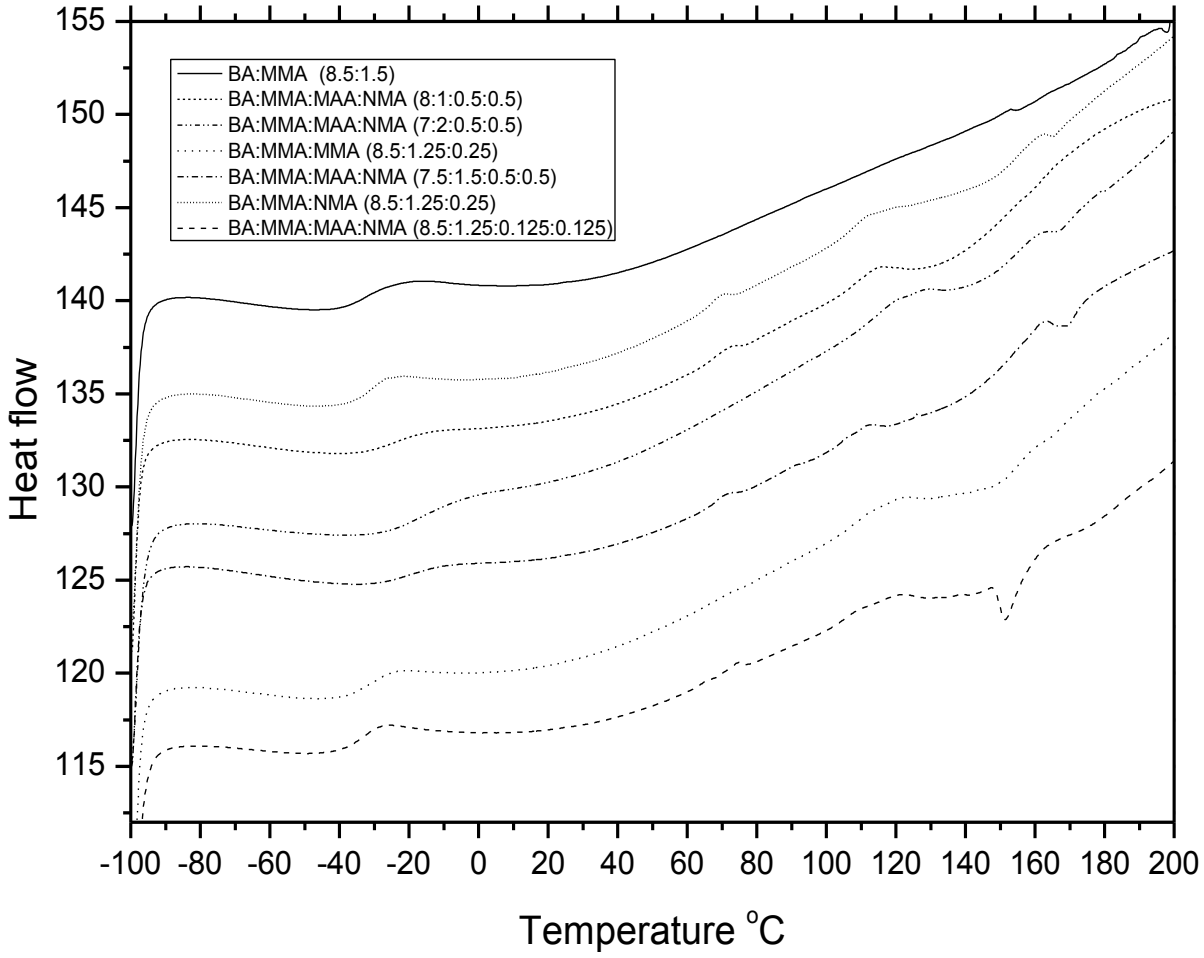

Fig. 4.12 DSC curves of the miniemulsion latexes prepared with different monomer compositions.

4.2.6 Application of the miniemulsion latexes as binders for cotton pigment and inkjet printing application.

The functionalized miniemulsion copolymer latexes with their smaller particle size and well-defined size distributions were applied successfully for the conventional pigment printing as well as the inkjet printing of cotton fabrics. The mechanism of the binder film formation on the surface of the textile fabric is shown in figure 4.13. The cross-linking reaction of the polymer chains is supposed to be formed in the curing process at 160 ^{o}C through the loss of water to form the ester or methylene ether bridges or by the loss of formaldehyde to form the methylene bridge through the polymer chains [30].

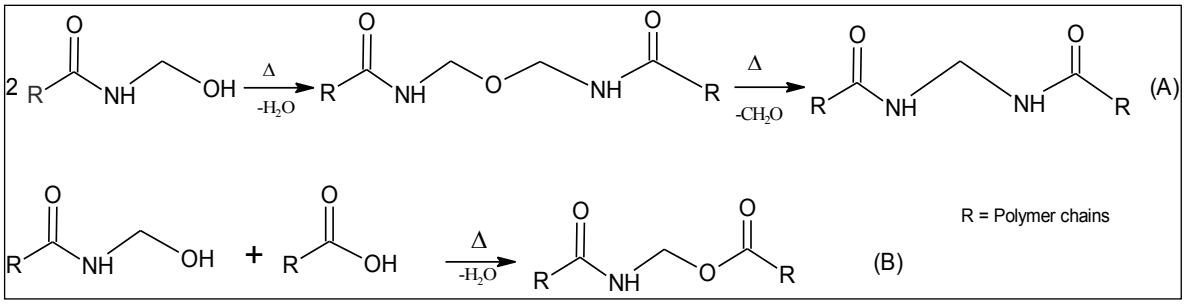

Fig. 4.13 Mechanism of the crosslinking reaction of the polymer chains (R) attached with the N-methylol acrylamide.

4.2.6.1 Pigment printing of cotton fabrics with the miniemulsion binders.

The samples from 1 to 9 which are presented in table 4.4 were applied successfully as binders in the pigment printing of cotton fabrics with pigment blue color. In general, the poor rubbing fastness and stiffness of the printed fabrics are the most severe drawbacks of applying binders in this method. Consequently, we focused on testing the rubbing fastness and stiffness of the treated cotton fabrics with the different miniemulsion latex binders in order to correlate them with the physico-chemical parameters of the miniemulsion latexes. It is shown in table 6 that the addition of the MAA and NMA to the basic BA and MMA recipe improves the rubbing fastness of the printed fabrics while the softness of the printed fabrics changes by varying the monomer compositions of the miniemulsion binder and depends mainly on the glass transition temperature of the different miniemulsions. In general, it should be noted that the fabric softness, which is a very important property in textile application, increases substantially with the content of MMA, MAA, and NMA (table 4.5). This may be explained that the addition of MMA and NMA to the BA and MMA copolymer introduces functionality to the chains which during the thermal curing, they crosslink and increase the sturdiness of the latex film and make the handle of the textile fabrics a bit stiffer and more robust and thereby accordingly improve the rubbing fastness.

Table 4.5: Rubbing and softness of the printed fabrics using different miniemulsions latex binders prepared with different monomer compositions with fixed monomer solid content 20%, SDS 7.5 mM and 4 wt% HD.

sample	Monomer Composition	Rubbing Fastness *		Fabric softness ($mNcm^2$)
		Dry	Wet	
1	BA:MMA (8.5:1.5)	2-3	2-3	4.8
2	BA:MMA:NMA (8.5:1.25:0.25)	3	2-3	5.9
3	BA:MMA:MAA (8.5:1.25:0.25)	3-4	2-3	5.5
4	BA:MMA:MAA:NMA(8.5:1.25:0.125:0.125)	4	2-3	5.1
5	BA:MMA:MAA:NMA (8:1:0.5:0.5)	4	3	6.2
6	BA:MMA:MAA:NMA (7.5:2:0.25:0.25)	3-4	2-3	6.3
7	BA:MMA:MAA:NMA (7.5:1.5:0.5:0.5)	4-5	3	6.5
8	BA:MMA:MAA:NMA (7:2.5:0.25:0.25)	4	2-3	7.6
9	BA:MMA:MAA:NMA (7:2:0.5:0.5)	4-5	2	7.6

***Rubbing fastness values of fabrics are divided into five levels according to the AATCC testing methods. The highest one is the fifth level, the higher the better.**

4.2.6.1.1 Rheological properties of the pigment printing pastes.

The rheological properties of the printing paste is of great importance for the handling in printing and to control the dye or pigment penetration, depth of shade, sharpness of the print and levelness on the textile fabrics. Therefore, we investigated the rheological properties of the printing paste containing our prepared miniemulsion binder (sample 4) in order to study its influence on the rheology of the printing paste in comparison to a conventional binder and the printing paste without binder. Figure 4.14 shows the shear stress as a function of the shear rate and the apparent viscosities (eq. 3.) of the pigment printing pastes which were prepared as described in table 2 including 5% of the miniemulsion and the conventional lefasol binders. The results indicated that the rheological behavior of the all-printing pastes is non-Newtonian pseudoplastic in which all the pastes exhibit pronounced shear thinning and resist flow until a yield stress is reached (~ 125 Pa with binder, ~ 175 Pa without binder). This behavior is typical for the industrial textile printing pastes [31, 32]. It should be noted that the addition of the miniemulsion and conventional binders to the printing

pastes decrease the viscosity somewhat, however the viscosity of the miniemulsion binder printing paste is slightly higher than the conventional binder paste.

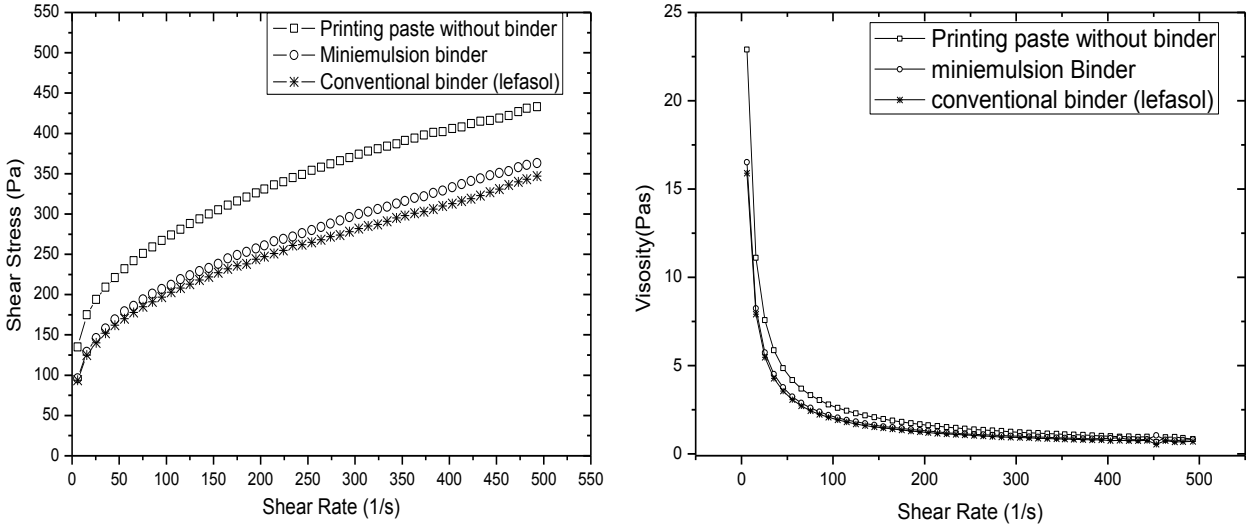

Fig.4.14 Rheological properties and apparent viscosities of the different pigment printing pastes with and without the miniemulsion and conventional lefasol binders.

4.2.6.1.2 Evaluation of the pigment printed cotton fabrics with the miniemulsion binder.

Miniemulsion latex binder with different solid contents were formulated in the pigment printing pastes and applied for the screen pigment printing of cotton fabrics. The miniemulsion binder composed of BA, MMA, MAA and NMA in ratio of (8.5:1.25:0.125:0.125), which provided the best results in term of fabric softness as well as resistance to rubbing in comparison to other compositions of the miniemulsion binders is presented in table 4.6. It is known that the rubbing fastness and soft handle of the pigment printing are the most significant disadvantages of this printing method [19, 20]. The color strength of the printed cotton fabrics with the pigment blue and pigment black using miniemulsion binder with different solid contents is shown in figure 4.15. The printing pastes were prepared according to the recipe in table 3.3 in chapter 3 with a fixed miniemulsion binder concentration of 5%. It is clear that the color strength of the printed fabrics with both pigment colors increases with increasing the binder solid content. This may be explained as the degree of the crosslinking of the film formation incorporating the pigment color during the

curing process depends on copolymer solid content of the binder and increases with increasing copolymer solid content.

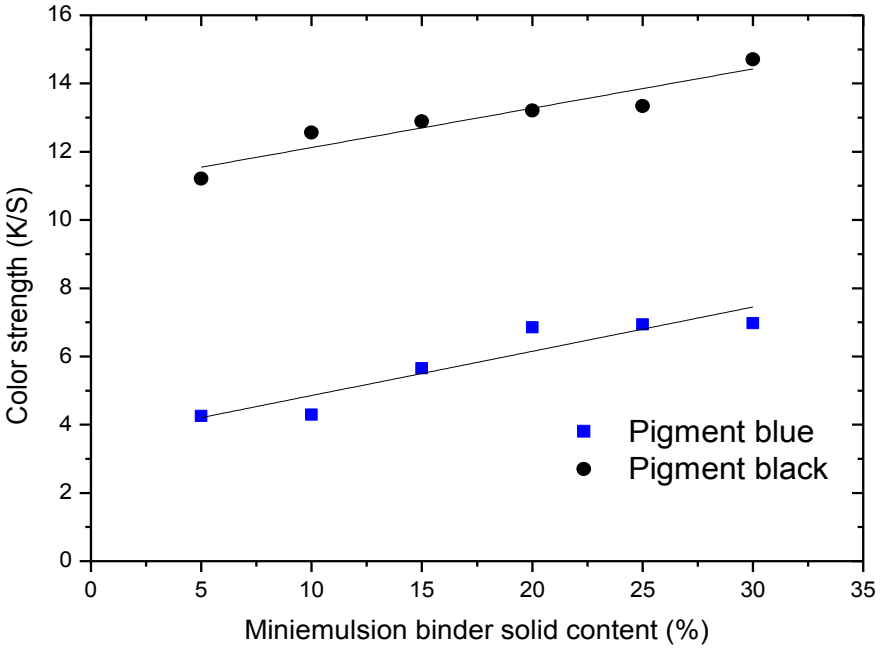

Fig. 4.15 Color strength of the printed cotton fabrics with the pigment blue and black colors using different solid contents of the miniemulsion binder.

The fastness properties towards rubbing and washing as well as the fabric softness of the printed fabrics using different solid contents of the miniemulsion binder are presented in table 4.6. Similarly, it can be observed that the dry and wet rubbing fastness of the printed fabrics with the both pigment blue and black colors improved by increasing the miniemulsion binder solid content in the printing recipes. The rubbing fastness of the printed fabrics depends mainly on the variation of the binder solid content and concentration in the printing paste recipes. The improvement of the rubbing fastness is related mainly to the formation of rigid networks after the crosslinking reaction which is proportional to the corresponding solid contents of the binder. However, as the rubbing fastness improved by increasing the binder solid content, the soft handle of the printed cotton fabrics becomes relatively stiff which is an undesirable property for the printed fabrics. It should be noted that the variation of the miniemulsion binder solid content did not bring remarkable change in the washing, which has a particle size diameter of about 73 nm with relative monodispersity, produced printed fabrics with satisfactory properties, particularly the soft handle and good fastness to rubbing. Therefore it was chosen as an optimized miniemulsion binder and compared to the properties of the printed fabrics with a conventional binder.

Table 4.6 Rubbing and washing fastness and fabric softness values of the printed cotton fabrics with pigment color cyan and black using different solid contents of the prepared miniemulsion binder.

Miniemulsion binder solid content % - BA:MMA:MAA:NMA (8.5:1.25:0.125:0.125)	Pigment color	Rubbing fastness				Washing fastness		Fabric softness ($mNcm^2$)
		Warp Dry	Warp Wet	Weft Dry	Weft Wet	Color change	Staining on wool	
5	Pigment blue	2	1	1-2	1	3-4	4	3.9
	Pigment black	3	1	3	1	3	4	4.1
10	Pigment blue	2-3	1-2	2	2	4	4	4.3
	Pigment black	3	1-2	3	1	4	4	5.2
15	Pigment blue	2-3	2-3	2-3	2-3	4-5	4-5	4.6
	Pigment black	3-4	1	3	1-2	4-5	4-5	5.3
20	Pigment blue	4-5	4	4	3-4	4-5	4-5	5.1
	Pigment black	4	1-2	4	1-2	4-5	4-5	5.4
25	Pigment blue	4-5	3-4	3	3	4-5	4-5	6.2
	Pigment black	4	2	4	1-2	4-5	4-5	5.7
30	Pigment blue	5	4	4-5	5	4-5	4-5	6.5
	Pigment black	4-5	2	4-5	2	4-5	4-5	5.8

The color strength as well as the rubbing and washing fastness properties and softness of the blue and black pigment printed cotton fabrics with the miniemulsion and conventional binders are described in figure 4.16 and table 4.7. It can be seen that the color strength of the printed cotton fabrics with the miniemulsion latex binder yielded slightly higher values for the blue and black pigments.

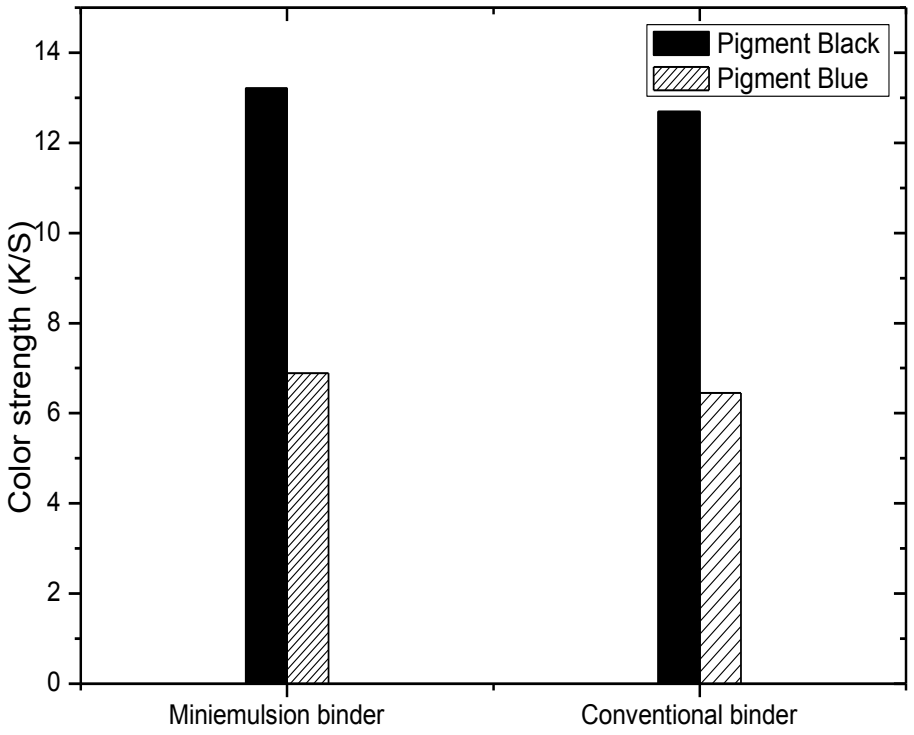

Fig.4.16 Color strength of the printed cotton fabrics with pigment cyan and black using miniemulsion and lefasol commercial binders

A photograph of the printed samples with the two types of binder is showed in figure 4.17. From this photograph, one can see clearly the difference in color shade between the printed fabrics with the miniemulsion and conventional binders, particularly the printed fabrics with the pigment blue color. In addition, as presented in table 4.7, the dry and wet rubbing fastness properties of the printed fabrics with the miniemulsion binder using pigment blue color showed improved values in comparison to the conventional binder, while the rubbing fastness of the printed fabrics with the black pigment color showed similar results regardless of the type of binder used.

Table 4.7 Comparison between the rubbing and washing fastness and fabric softness values of the printed cotton fabrics with the miniemulsion binder and conventional binder lefasol 206.

Pigment color	Binder	Rubbing fastness [a]				Washing fastness [a]		Fabric softness ($mNcm^2$)
		Warp Dry	Warp Wet	Weft Dry	Weft Wet	Color change	Staining on wool	
Pigment cyan	Miniemulsion binder	4-5	4	4	3-4	4-5	4-5	5.1
	Conventional binder	4	2-3	4	2-3	4-5	4-5	6.4
Pigment black	Miniemulsion binder	4	2	4	2	4-5	4-5	5.3
	Conventional binder	4	2	4	2-3	4-5	4-5	5.4

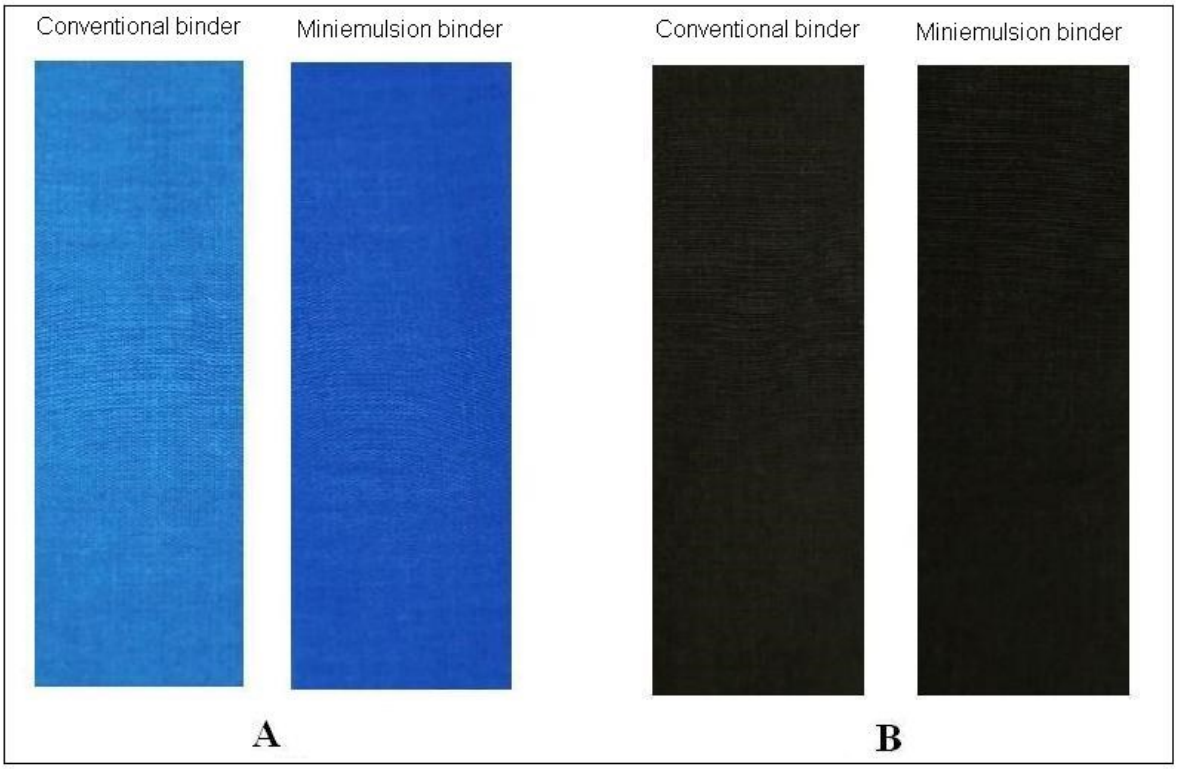

Fig.4.17 Printed cotton fabrics with A) pigment cyan and B) pigment black using miniemulsion and lefasol commercial binders.

In combination with the satisfied rubbing fastness, the miniemulsion binder offered printed fabric with better soft handle properties for both pigment colors in comparison to the commercial binder. In addition, we have obtained the same values from the washing fastness of the printed fabrics with the two colors using the two different binders. In general, the miniemulsion latex binders with their uniform shape and smaller size in addition to their structural composition offered advantages over the conventional processes, particularly the rubbing fastness and softness of the printed fabrics.

4.2.6.2 Inkjet pigment printing of cotton fabrics with the miniemulsion binder.

4.2.6.2.1 Influence of the particle size of the miniemulsion binder on the inkjet printing.

The optimized miniemulsion latex from the conventional pigment printing was also successfully applied for the ink-jet printing of cotton fabrics. Here the quality of the latex in addition to the latex particle size is of crucial importance as the main problem in inkjet pigment printing is typically the clogging of the nozzles. Consequently, we have prepared the optimized miniemulsion with three different size diameters 52, 73 and 118 nm with low polydispersity values by controlling the miniemulsion polymerization. The miniemulsion binders with the different particle size were formulated in the four pigment ink color dispersions (cyan, magenta, yellow and black), while the inks then were printed on the textile cotton fabrics by the digital inkjet printing method. It should be noted that the prepared four ink dispersions with the different miniemulsion binders were filtered easily and showed excellent printing behavior, as they did not cause any nozzle-blocking problem to the printer machine, which is different to many conventional systems. The fastness properties of the inkjet printed cotton fabrics towards rubbing and washing with the three different sizes of the miniemulsion binder as well as the values color strength are presented in table 4.8 and compared to the digital printed fabrics with conventional binder. The results indicated that there was no remarkable change in the rubbing fastness values of the three miniemulsion binders while the washing fastness values were identical. Similarly, the variation of the particle size of the miniemulsion binder did not cause considerable change in the color strength values of the printed fabrics. However, these values were comparable with the printed fabrics with the conventional binder. In general, inkjet printing with the miniemulsion binder with particle size diameter range between 50 to120 nm offered printed cotton fabrics with similar and comparable fastness properties and color strength which met the criteria of the standard tests, particularly the rubbing fastness.

Table 4.8. Fastness properties towards rubbing and washing values and color strength of the inkjet printed cotton fabrics with the different inks using different particle size of 5 % miniemulsion binder and 2% pigment concentration and comparison to the conventional binder lefasol 206.

Pigment ink	Miniemulsion binder diameter size (nm)	Rubbing fastness		Washing fastness		Color strength K/S
		dry	wet	Color change	Staining on wool	
Pigment cyan	52 nm	2-3	1-2	5	5	3.8
	73 nm	2	1-2	5	5	3.9
	118 nm	2	1-2	5	5	3.9
	Conventional binder	2-3	1-2	4-5	5	4.1
Pigment yellow	52 nm	3	3	5	5	3.6
	73 nm	3	3	5	5	3.5
	118 nm	3	2-3	5	5	3.7
	Conventional binder	3	2-3	5	5	3.5
Pigment magneta	52 nm	2-3	2	5	5	3.1
	73 nm	3	2-3	5	5	3.0
	118 nm	3	2	5	5	2.9
	Conventional binder	2-3	2-3	5	5	3.2
Pigment black	52 nm	2-3	1-2	5	5	5.9
	73 nm	3	1-2	5	5	5.8
	118 nm	3	1-2	5	5	5.9
	Conventional binder	3-4	2	4-5	4-5	6.1

4.2.6.2.2 Influence of the miniemulsion binder concentration on the inkjet printed cotton fabrics.

The miniemulsion binders with two concentrations were formulated in the four-ink dispersion in order to study the influence of the binder concentration on the properties of the inkjet printed cotton fabrics. The color strength of the printed cotton fabrics with the four pigment inks using 5 and 10 % of the miniemulsion binder is shown in figure 4.18. The color strength of the printed fabrics with 10 % binder showed slightly higher values for the pigment cyan, yellow and magenta while the pigment black showed a lower value in comparison to the 5% binder concentration.

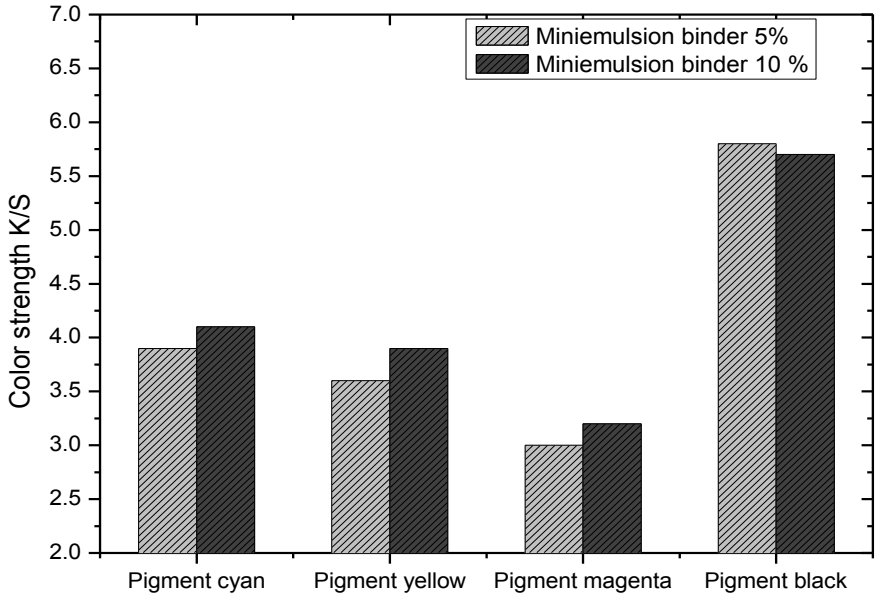

Fig.4.18 Color strength of the inkjet printed cotton fabrics with the four inks using different concentrations of the miniemulsion binder.

The results in table 4.9 describe the rubbing and washing fastness of the inkjet printed fabrics with the different inks using the two concentrations of the miniemulsion binder. It can be observed that the 10% binder concentration showed better rubbing properties than that of 5% binder concentration. This can be attributed to the relation between the degree of the crosslinking network of the binder polymer chains and its corresponding concentration in the ink formulation, while the washing fastness and the color strength of the printed fabrics showed similar and comparable results. Generally, the fastness toward rubbing and washing and color strength of the fabrics after printing with both binder concentrations agree well with the standard tests of the inkjet printing of cotton fabrics.

Table 4.9 Fastness properties towards rubbing and washing values of the inkjet printed cotton fabrics with the different inks using two concentrations of the prepared miniemulsion binder.

Pigment ink	Miniemulsion binder concentration wt.%	Rubbing fastness		Washing fastness	
		dry	wet	Color change	Staining on wool
Pigment cyan	5%	2-3	1-2	5	5
	10%	2-3	3	5	5
Pigment yellow	5%	3	3	5	5
	10%	3	3	5	5
Pigment magneta	5%	2-3	2	5	5
	10%	3	2-3	5	5
Pigment black	5%	2-3	1-2	5	5
	10%	4	2-3	5	5

4.3 Conclusion

In this chapter, the miniemulsion polymerization was successfully employed to prepare latex particles based on the soft butyl acrylate and hard methyl methacrylate monomers. Miniemulsification was prepared by the ultrasonic processor. The influence of sonication time on the miniemulsion particle size was studied. The sonication time was adjusted to 10 minutes for all miniemulsification preparations. The structural composition of the miniemulsion copolymer latex was confirmed by ^{1}H-NMR. The molecular weight and molecular weight distribution of the copolymer latexes was found to be around (1.06×10^{6} g/mol) and the polydispersity is 1.22 as determined by GPC. The particle size and polydispersity analysis obtained from DLS, SANS and TEM showed that the particle diameter ranged between 50-400 nm with relatively narrow size distributions and is controlled by the ratio (monomer+oil) to surfactant. While the addition of functional monomers such as methacrylic acid and N-methylol acrylamide to the original miniemulsions imparted functionality to the polymer chains, it did not affect the particle size and the polydispersity of the miniemulsion latex, where in particular the smaller size reduces the risk of clogging in inkjet printing. The miniemulsion latexes were applied as binders for the pigment and inkjet printing of cotton fabrics as an alternative system able to overcome some of the drawbacks of conventional systems. They were formulated successfully in the printing pastes and ink formulations without agglomeration and they allowed for an easy printing process with some advantages over the conventional systems. This is the case as the miniemulsion binders succeeded to overcome some of the technological problems of the pigment and inkjet printing processes such as clogging of the nozzles and screening of the printing machines. Moreover, the printed fabrics with the miniemulsion binder showed better soft handle due to the low glass transition temperature (T_g: -34 ^{o}C) of the latex, while the color strength and fastness properties toward washing and rubbing of the printed fabrics were slightly improved in comparison to the conventional processes. In summary, this investigation opens up a promising new pathway for textile printing applications by employing tailor-made nanosized latexes obtained by miniemulsion polymerization.

4.4 References

[1] J. Ugelstad, M. S. El-Aasser, J. W. Vanderhoff. (1973). Emulsion polymerization: Initiation of polymerization in monomer droplets. *J. Polym. Sci. Polym. Lett. Ed., 11*, 503-513.

[2] Y. T. Choi, M. S. El-Aasser, E. D. Sudol, J. W. Vanderhoff. (1985). Polymerization of styrene miniemulsions. *J. Polym. Sci. Polym. Chem. Ed.23*, 2973-2987.

[3] J. Delgado, M. S. El-Aasser, J. W. Vanderhoff. (1986). Miniemulsion copolymerization of vinyl acetate and butyl acrylate. I. Differences between the miniemulsion copolymerization and the emulsion copolymerization process. *J. Polym. Sci. Polym. Chem*. *Ed*., *24*, 861-874.

[4] P. L. Tang, E. D. Sudol, C. A. Silebi, M. S. El-Aasser. (1991). Miniemulsion polymerization- a comparative study of preparative variables *J. Appl. Polym. Sci., 43,* 1059-1066.

[5] C. M. Miller, E. D. Sudol, C. A. Silebi, M. S. El-Aasser. (1995). Polymerization of Miniemulsions Prepared from Polystyrene in Styrene Solutions. 1. Benchmarks and Limits *Macromolecules*, *28,* 2754-2764.

[6] F. K. Hansen, J. Ugelstad. (1979). Particle nucleation in emulsion polymerization. IV. Nucleation in monomer droplets. *J. Polym. Sci. Polym. Chem. Ed., 17*, 3069-3082.

[7] B. J. Chamberlain, D. H. Napper, RG. Gilbert. (1982). Polymerization within styrene emulsion droplets. *J. Chem. Soc. Faraday Trans.1, 78,* 591-606.

[8] F. J. Schork, G.W. Poehlein, S. Wang, J. Reimers, J. Rodrigues, C. Samer. (1999). Miniemulsion polymerization. *Colloids and Surfaces A, Physiochemical and Engineering Aspects*, 153, 39-45.

[9] K. Landfester. (2001). The Generation of Nanoparticles in Miniemulsions. *Adv. Mater.*, *13*, 765-768.

[10] K. Ouzineb, C. Lord, N. Lesauze, C. Graillat, P. A. Tanguy, T. Mckenna (2006). Homogenisation devices for the production of miniemulsions. *Chem. Eng. Sci.*, *61*, 2994-3000.

[11] K. Landfester. (2000). Recent developments in miniemulsions-formation and stability mechanisms. *Macromol. Symp*., *150*, 171-178.

[12] K. Fontenot, F. J. Schork. (1993). Batch polymerization of methyl methacrylate in mini/macroemulsions. *J. Appl. Polym. Sci.*, *49*, 633-655.

[13] M. Stang, H. Karbstein, H. Schubert. (1994). Adsorption kinetics of emulsifiers at oil-water interfaces and their effect on mechanical emulsification. *Chem. Eng. Process*, *33*, 307-311.

[14] M. Antonietti, K. Landfester. (2002). Polyreactions in miniemulsions. *Prog. Polym. Sci.*, *27*, 689-757.

[15] W.Z. Ostwald. (1897). Studies on the formation and transformation of solid bodies. *Z Phys. Chem., 22*, 289-330.

[16] J. L. Reimers, A. H. P. Skelland, F. J. Schork. (1995). Monomer droplet stability in emulsion-polymerized latexes. *Polym. React. Eng., 3*, 235-240.

[17] V. S.Rodriguez, J. Delgado, C. A. Silebi, M. S. El-Aasser. (1989). Interparticle monomertransport in miniemulsions. *Ind. Eng. Chem. Res.*, *28*, 65-74.

[18] R. Eisenlohr, V. Giesen. (1995) Pigment printing and ecology. *Int. Dyer, 180*, 12-18.

[19] M. R. Galgali. (1998). Environmental impact of textiles. *Colourage*, *45*, 20-22.

[20] L.V. Jing, X.Min, C.Shuilin. (2003). Synthesis and characterization of nonformaldehyde releasing and low-temperature curable binder. *AATCC Rev*., 6, 29-32.

[21] K. Landfester, N. Bechthold, S. Förster, M. Antonietti. (1999). Evidence for the preservation of the particle identity in miniemulsion polymerization. *Macromol. Rapid Commun*., *20*, 81-84.

[22] M. Buback, A. Feldermann, C. Barner-Kowollik, I. Lacik. (2001). Propagation Rate Coefficients of Acrylate-Methacrylate Free-Radical Bulk Copolymerizations. *Macromolecules, 34*, 5439-5448.

[23] S. Roy, S. Devi. (1997). High solids content semicontinuous microemulsion copolymerization of methyl methacrylate and butyl acrylate. *Polymer*, *38*, 3325-3331.

[24] K. Landfester, N. Bechthold, F. Tiarks, M. Antonietti. (1999). Formulation and stability mechanisms of polymerizable miniemulsions. *Macromolecules*, *32*, 5222-5228.

[25] S. J. Rehfeld. (1967). Adsorption of sodium dodecyl sulfate at various hydrocarbon-water interfaces. *J. Phys. Chem.*, *71*, 738-745.

[26] J. C. Thomas. (1987). The determination of log normal particle size distributions by dynamic light scattering. *J. Colloid Interface Sci.*, *117*,187-192.

[27] C. Pichot. (1990). Recent developments in the functionalization of latex particles. *Makromol. Chem. Macromol. Symp*., *35/36*, 327-348.

[28] S. Fourdrin, M. Rochery, M. Lewandowski, M. Ferreira, S. Bourbigot. (2006). Rheological and thermogravimetric studies of the crosslinking process of functionalized acrylic latexes. *J. Appl. Polym. Sci., 99*, 1117-1123.

[29] J. G. Tsavalas, C. D. Sundberg. (2010). Hydroplasticization of Polymers: Model Predictions and Application to Emulsion Polymers. *Langmuir*, 26, 6960-6966.

[30] S. Krishnan, A. Klein, M.S. El-Aasser, E.D. Sudol. (2003). Influence of Chain Transfer Agent on the Cross-Linking of Poly (n-butyl methacrylate-co-N-methylol acrylamide) Latex Particles and Films. *Macromolecules*, 36, 3511-3518.

[31] R. L. Derry, R. S. Higginbotham. (1953). The Flow Properties of Textile Printing Pastes. *J. Soc. Dyers Colour., 69*, 569-575.

[32] B. F. Dowds. (1970). Variables in Textile Screen Printing. *J. Soc. Dyers Colour., 86,* 512-519.

5. Encapsulation of pigment colors by miniemulsion polymerization and their application as self-curable hybrid inks in textile inkjet printing.

5.1 Introduction

Inkjet printing is considered one of the most promising methods for the printing of textile fabrics and therefore has received intense attention from both academic and industrial research. This evolving technology offers significant advantages over conventional textile printing methods such as, the simple and fast procedures, options for small scale and customized production, low pollution and low cost by reduction of the water and energy consumption [1–5]. Inks for fabric printing are usually classified into two categories, dye-based and pigment-based inks. The pigment-based inks type has become more popular because of its ability to give fuller and brighter shades without the need for any pretreatments as well as the better washing and light fastness and the applicability to all types of textile fabric substrates [6]. The pigment and binder are the principle ingredients in the pigment-based ink formulations of the textile inkjet printing. The pigments are typically manufactured with particle sizes below 500 nm in order to deliver optimum color conditions and other appearance properties such as opacity and gloss [7]. However, the pigment particles tend to agglomerate in aqueous and non-aqueous dispersions due to their high surface area and the pronounced attractive van der Waals forces between particles. This in turn can lead to serious problems during jetting of inks such as clogging the nozzles of the inkjet printer. In addition, the agglomeration reduces the pigment efficiency and the smoothness of the printed fabrics by the appearance of aggregates on the film surface, resulting finally in a lower quality product.

Therefore, it is crucial to develop pigment ink dispersions methods to prevent the association and agglomeration of the pigment particles and hence control the particle size and enhance the stability of the pigment ink dispersions. In this regard, the encapsulation of the pigment particles with a polymer layer is an alternative way to minimize the risk of particle agglomeration, thereby improving the dispersibility and stability of pigment inks. Moreover, the pigment encapsulation protects the pigment particles from the effect of the UV radiation or the pH variation. Recently, several methods have been reported for the encapsulation of pigment particles such as dispersion, emulsion and miniemulsion polymerization [8]. Conventional emulsion polymerization was used to encapsulate inorganic particles such as colloidal silica, [9] titanium dioxide pigments, [10] silver particles, [11], and organic pigments [12]. However,

emulsion polymerization generated insufficient encapsulation efficiencies, due to the complexity of the nucleation mechanism in this process. In the last 10 years, some work has described the encapsulation of organic and inorganic pigments by miniemulsion polymerization [13-15]. Miniemulsion polymerization differs from conventional emulsion polymerization in the mechanism of the particle nucleation which takes place in the stabilized monomer droplets [16, 17]. Accordingly, the introduction of the pigment particles to the stabilized droplets by miniemulsification leads to high encapsulation efficiencies upon subsequent polymerization.

In this work, we aimed at preparing water based hybrid dispersions of polymer encapsulated organic pigment inks in order to enhance the stability and dispersibility of the ink formulations by reducing the pigment particle–particle interactions and thereby lowering the risk of the agglomeration of the pigment particles. In addition, the encapsulated pigments were applied successfully as inks for the cotton fabrics without adding separate polymer or copolymer binders to the inkjet printing formulations which allows the hybrid ink to have dual property, creating a polymer film during curing on substrate beside the basic role of inks as color delivery. We have achieved the encapsulation with different pigment colors but we focused our study on the C.I. Pigment Red 112, an azo-naphthalene based pigment color stuff widely used for textile coloration. The miniemulsion polymerization method using the co-sonication technique with butyl acrylate-co-methyl methacrylate (BA-co-MMA) and styrene-co-butyl acrylate (St-co-BA) copolymer latexes performed the encapsulation. The anionic SDS surfactant was used to stabilize the pigment dispersions, miniemulsions, and hexadecane used as co-stabilizer for the miniemulsion preparations. The pigment-polymer weight ratio has been varied in order to study its influence on the encapsulation efficiencies as well as the physical properties and the printing behavior of the ink formulations and finally reach optimum hybrid ink recipes. The particle size, morphology, encapsulation efficiency, thermal analysis, stability, rheology and other physical properties of the encapsulated pigments were studied. Of course, a key aspect here is confirming and quantifying the encapsulation efficiency, which is not an obvious task. Finally, the properties of the printed cotton fabrics with the encapsulated hybrid-pigments were compared to conventional inks. The general aim of these investigations was to optimize by a miniemulsion-based polymerization in a systematic way the conditions for preparing latex encapsulated pigments with long-time stability and low tendency of clogging of printing nozzles, which are essential prerequisites for their successful application in inkjet printing.

5.2. Result and discussion:

5.2.1 Encapsulation methodology of the C.I. Pigment red 112 by the miniemulsion polymerization.

In order to achieve efficient encapsulation with high pigment contents in the ink dispersion and enabling different ratios between pigment and latex, we used the miniemulsification method by cosonication [18, 19]. In this method, the pigment and miniemulsion components were dispersed and sonicated separately in an aqueous medium and then they were mixed and sonicated together in different ratios to form a pigment- monomer hybrid template from which upon subsequent polymerization, hybrid polymer-pigment particles were obtained as described in Fig. 5.1. We studied the encapsulation of the C.I. pigment 112 with butyl acrylate-co-methyl

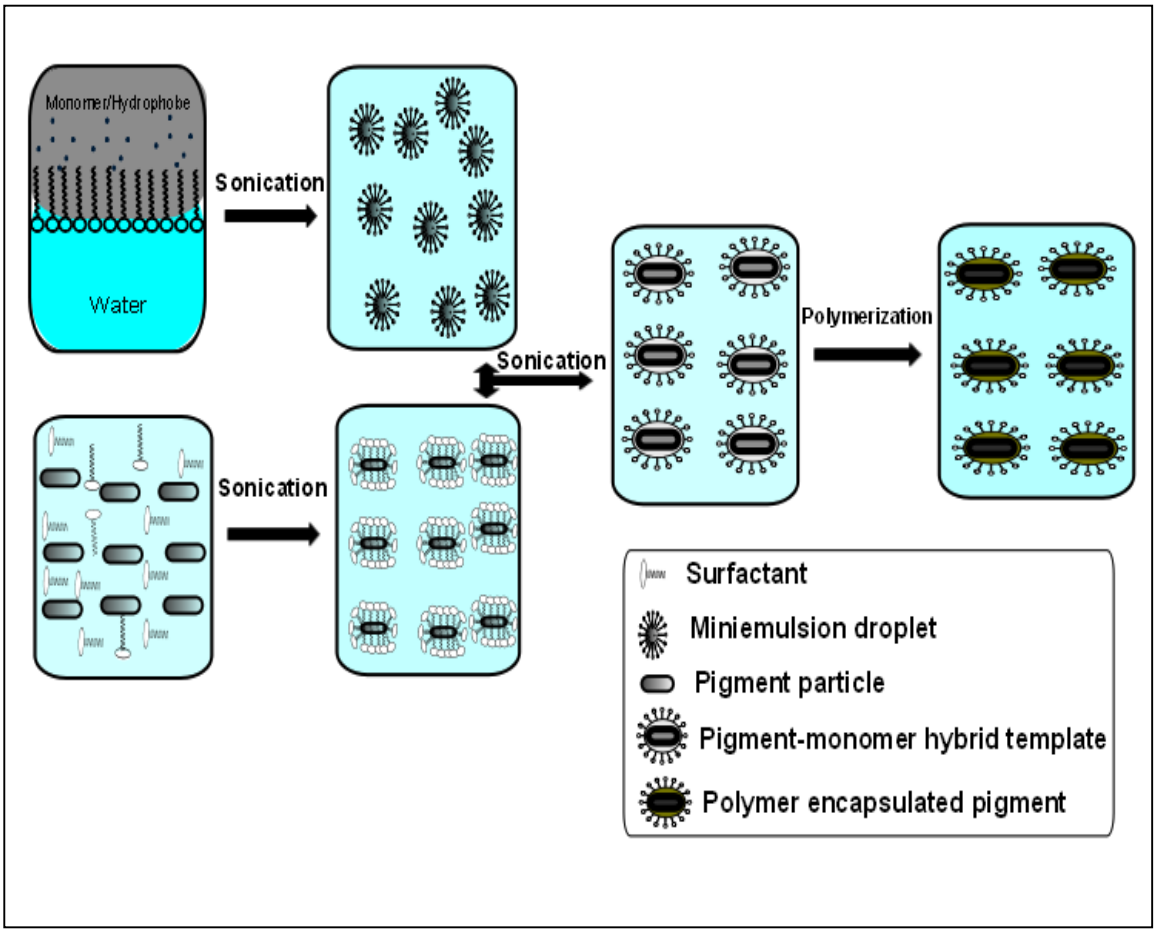

Fig. 5.1 Miniemulsion polymerization (cosonication) method concept for the encapsulation of pigment particles.

methacrylate (BA-MMA) and styrene- co-butyl acrylate (St-BA) copolymer latexes. Miniemulsion polymerization was carried out using the oil-soluble initiator AIBN, while butyl acrylate was chosen in both copolymer structures due to its low glass transition temperature to

produce soft handle polymer films in the application of the hybrid pigment-polymer particles in the inkjet printing of textile fabrics. The pigment red 112 was dispersed in aqueous solution with the anionic surfactant SDS and sonicated for 120 minutes. The particle size and polydispersity of the pigment particles before encapsulation was followed by DLS at different sonication time and the corresponding data are given in table 5.1. The pigment particle size diameter decreases from approximately 400 nm to 170 nm after 120 min. sonication. The morphology and particle size of the pigment particles after 120 minutes sonication was also investigated by TEM as described in figure 5.2. It is clear that the pigment particles tend to agglomerate and the size of pigment particles is between 150 to 200 nm, and exhibiting quite irregular shape.

Table 5.1: Particle size and polydispersity of the PR112 dispersion at different sonication times.

Sonication time (min.)	Particle size diameter (nm)	PDI
0	398	0.48
15	236	0.40
30	222	0.37
45	214	0.35
60	204	0.36
75	198	0.33
90	186	0.28
120	170	0.29

5.2.2 Particle size analysis and size distributions of the encapsulated PR112 by DLS and CPS DC.

The pigment-latex ratio was varied for two copolymer latex compositions (PBA-co-PMMA and PSt-co-PBA). Particle size and polydispersity after encapsulation were followed by DLS and CPS DC and correlated to the theoretical particle size diameter of the encapsulated pigment inks as described in table 5.2. It should be noted that the specific monomer compositions of the two-copolymer structures were selected in order to suit the inkjet printing application, especially the soft handle of the final polymer film formation on textile substrate (see 4.2.6).

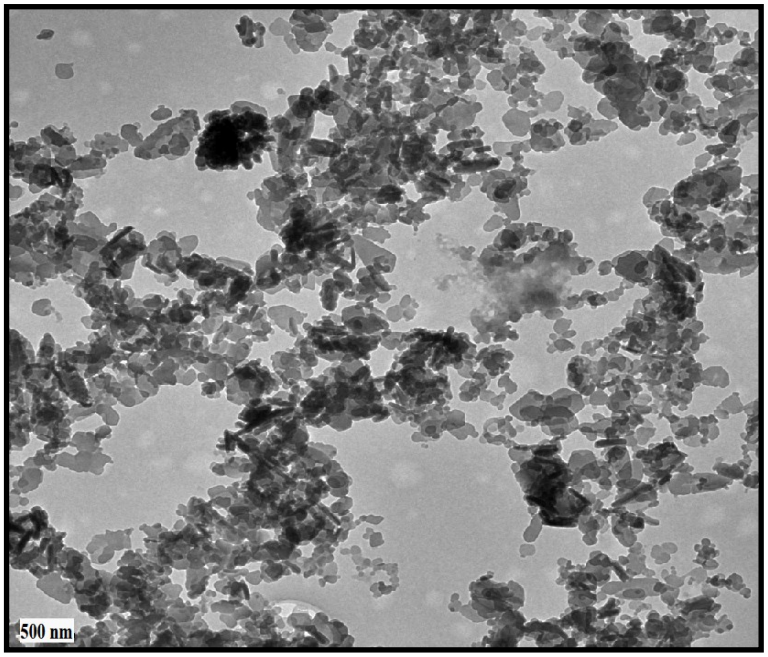

Fig. 5.2 TEM picture of C.I Pigment red 112 before encapsulation.

The particle size diameter of the PR112 before encapsulation was estimated to correspond to 170 and 167 nm as determined from DLS and CPS DC, respectively. Based on that, the theoretical particle size diameters of the encapsulated pigments with the different copolymer latex–pigment ratios were calculated, if we assume that the spherical pigment particles have diameter of 170 nm (as calculated from DLS) and becomes coated with the polymer latex shell layer at different latex /pigment volume fractions as described in Eq.6.1:

$$\frac{\emptyset_{Latex}}{\emptyset_{Pigment}} = \frac{V_{Latex}+V_{Pigment}}{V_{Pigment}} = \frac{{}^{4}/_{3}\pi\,(R+t)^{3} - {}^{4}/_{3}\pi R^{3}}{{}^{4}/_{3}\pi R^{3}} \qquad \text{Eq. 6.1}$$

where the ∅ is the volume fraction, R is the radius of the pigment core and t is the thickness of the polymer shell.

As shown in table 5.2 the experimental particle size diameter of the encapsulated PR112 as seen by DLS and CPS DC increased after encapsulation in all recipes. This may be attributed to the coating of the pigment particles with a polymer latex layer or shell. Also we noticed that the particle size of the encapsulated PR112 depends on the latex-pigment ratios and increases by increasing the latex content which agrees well with the calculated theoretical particle size diameter values. For instance, the particle diameter of the encapsulated PR112 with the PBA-co-PMMA (latex composition 80:20) increased from 172 to 184 nm and from 178 to 205 nm by varying the latex-pigment ratios from 0.11 to 0.66 as determined from DLS and CPS DC,

respectively, while the theoretical particle size diameter after encapsulation was increased from 179 to 214 nm by varying the same latex-pigment ratio. The increase in the particle size of the encapsulated pigment particles by varying the latex-pigment ratios can be attributed to an increasingly thick copolymer coating layer, which indicates successful encapsulation.

The particle size distributions of the pigment particles before and after encapsulation with PBA-co-PMMA (BA: MMA monomer composition 80:20) copolymer latex with different latex-pigment ratios were further analyzed by the CPS DC particle size analyzer and DLS. As described in figure 5.3 one can see that the size distributions of the PR112 after encapsulation are shifted to higher values with the variation of the latex-pigment ratios. The observed small peaks of the DLS size distributions at diameters size range between 20-50 nm may be attributed to some free latex polymer particles that did not polymerize on the surface of pigment particles or some aggregations of the SDS surfactant.

Fig. 5.3: Size distributions obtained from of the original PR112 and the encapsulated PR112 with PBA-co-PMMA (80:20) copolymer latex with different latex- pigment ratios a) Disc Centrifuge particle size analyzer b) DLS.

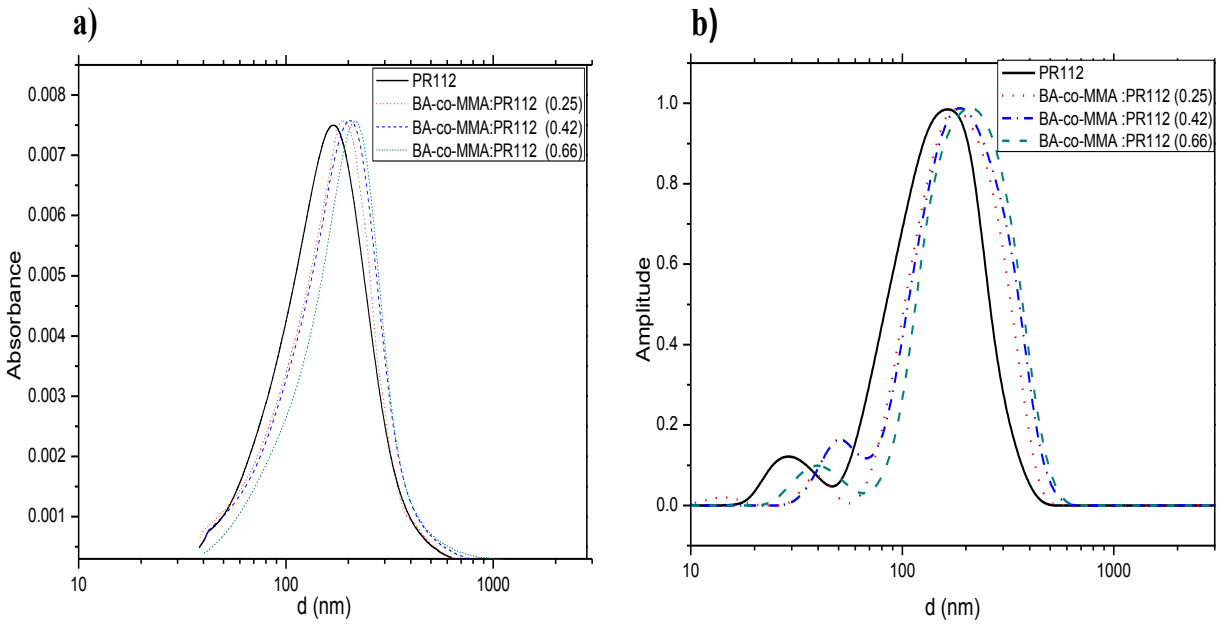

In general, the experimental particle size diameters and size distributions of the encapsulated pigment particles were found to be in good agreement with the calculated theoretical size diameters after encapsulation

Table 5.2: Particle size and polydispersity as determined from DLS CPS disc centrifuge (DC) of the encapsulated PR112 with different Latex – pigment ratios of two latex compositions of PBA-co-PMMA and PSt-co-PBA using different PR112 contents stabilized with 15 wt% (total) SDS. PR112 size diameter and PDI before encapsulation 170 nm and 0.29, as determined from DLS and 167 nm as determined from CPS (DC).

Copolymer latex	*Monomer composition* (mass ratio)	*Latex-PR112 ratio (wt.)*	*PR112 content wt.%*	*DLS*		*CPS* (DC) d(nm)	*Theo. d(nm)*
				d (nm)	*PDI*		
PBA-co-PMMA	80:20	0.11	11.8	**172**	**0.27**	**178**	**179**
		0.25	11.1	**177**	**0.31**	**187**	**189**
		0.42	10.3	**179**	**0.25**	**198**	**201**
		0.66	9.4	**184**	**0.29**	**205**	**214**
	60:40	0.11	11.8	**176**	**0.32**	**183**	**179**
		0.25	11.1	**178**	**0.33**	**183**	**189**
		0.42	10.3	**181**	**0.26**	**187**	**201**
		0.66	9.4	**182**	**0.24**	**203**	**214**
PSt-co-PBA	80:20	0.11	11.8	**176**	**0.27**	**187**	**182**
		0.25	11.1	**182**	**0.31**	**193**	**193**
		0.42	10.3	**191**	**0.22**	**202**	**205**
		0.66	9.4	**196**	**0.24**	**207**	**218**
	60:40	0.11	11.8	**174**	**0.31**	**-**	**182**
		0.25	11.1	**180**	**0.24**	**-**	**193**
		0.42	10.3	**182**	**0.23**	**-**	**205**
		0.66	9.4	**187**	**0.21**	**-**	**218**

5.2.3 Estimate of the polymer encapsulation efficiency and thermal properties of the hybrid PR112 polymer latex.

In order to estimate the encapsulation efficiency and to get an idea about the thermal properties of the encapsulated PR112, we performed thermogravmetric analysis (TGA) and differential scanning calorimetry (DSC). Figure 5.4 shows typical TGA thermograms for the encapsulated PR112 with BA-MMA copolymer latex (latex pigment ratio 0.42), the blank PR112 and the reference BA-MMA copolymer latex (polymerized without pigment). It can be observed that the encapsulated PR112 with BA-MMA copolymer latex showed three degradation temperatures. The first one lies between 168°C and 245°C with weight loss of 17%, which may be attributed to the evaporation of residual water, remaining hexadecane and the decomposition of the surfactant molecules. The second decomposition temperature occurred between 280°C and 340°C with 23% weight loss, which correspond, to the decomposition of the azo-naphthalene of the PR112 molecule [20]. The last degradation temperature was observed between 379°C and 411°C with a weight loss of 27% indicating the removal of the BA-MMA copolymer latex. However, the thermogram of the blank PR112 showed only two degradation temperatures, the first one between 167°C and 233°C representing the decomposition of the residual water, while the second weight loss occurred between 287°C and 324°C corresponding to the decomposition of the azo-naphthalene of the pigment molecule. Finally, the thermogram of the BA-MMA copolymer latex showed two decomposition temperatures, one due to evaporation of water between 106°C and 188°C and the other attributed to the decomposition of the copolymer latex between 332°C and 396°C. From the three different TGA thermograms, we can conclude that the encapsulated PR112 shows better thermal stability in comparison to the blank PR112 as a result of the shift of the onset temperature of decomposition of the BA-MMA copolymer latex from 332°C to 379°C.

The results of the thermal analysis by means of TGA and DSC of the encapsulated PR112 with PBA-co-PMMA and PSt-co-PBA latexes using different latex pigment ratios are summarized in table 5.3, where by DSC the glass transition temperature Tg was determined, as well as the encapsulation efficiency values, obtained from TGA and calculated according to eq. 3.12. Obviously, the onset temperatures of the thermal decomposition of the encapsulated PR112 with the copolymer latexes are shifted to higher temperature in comparison to the latex free pigment reference, quantifying the improvement of the thermal stability of the encapsulated pigment, regardless of the type of copolymer or the variation of the latex / pigment ratios. It should be also noted that the onset temperature of the encapsulated PR112 slightly increases as their polymer content increases as a result of the variation of the latex / pigment ratios.

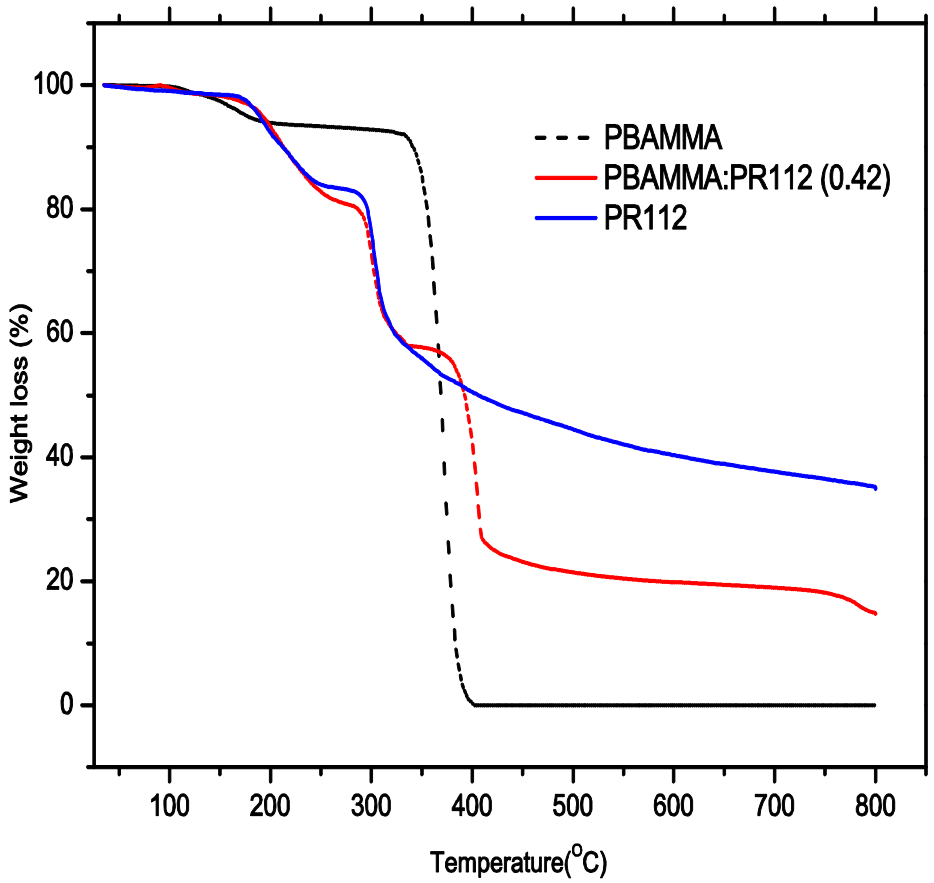

Fig. 5.4 TGA thermogram of the PR112 hybrid PBA-co-MMA, PR112free latex and the PBA-co MMA latex.

The glass transition temperature (Tg) of the hybrid pigment/polymer latex is an important property for the inkjet printing application as it is related to the degree of the film softness on substrates. Therefore, we have investigated the Tg of the encapsulated PR112 with the BA-MMA and St-BA copolymer latexes using different latex/pigment ratios. The Tg values of the encapsulated PR112 with the BA-MMA copolymer latexes range between -26 °C and -31 °C, by varying the latex /pigment ratios, while for the St-BA copolymer latexes Tg's lie between 49 °C and 56 °C, predicting that the encapsulated PR112 inks with BA-MMA copolymer binder will form softer films on the substrates after printing application in comparison to the encapsulated PR112 with St- BA copolymer latexes. The higher Tg of the St-BA can simply be attributed to the presence of styrene, as polystyrene is known to have a high glass transition temperature of 95°C [21]. The encapsulation efficiency of the PR112, as determined from TGA, increases when increasing the polymer content. By variation of the latex/pigment ratio from 0.11 to 0.66 using BA-MMA as a copolymer latex, the encapsulation efficiency increases from

20% to 37%, while the it increases from 26% to 51% using St-BA copolymer latex by increasing the same latex/pigment ratio. In general, the encapsulation efficiencies of the PR112 particles with the St-BA copolymer show higher values than the encapsulated ones with the BA-MMA copolymer. This observation may be attributed to the lower polarity and higher hydrophobicity of the St-BA co-latexes in comparison to the BA-MMA co-latexes. Therefore, we assume that the pigment particles will diffuse more easily in the more hydrophobic St-BA latex droplets and lead to housing the pigment particles inside the droplets, which produces higher encapsulation efficiency values after polymerization.

Table 5.3: TGA data, glass transition temperature Tg (DSC) and encapsulation efficiency of the encapsulated PR112 with PBA-co-PMMA and PSt-co-PBA latexes.

Copoly. latex	Latex-pigment ratio	Weight (mg)		Decomp. onset temp. of latex free PR112 (°C)	Decomp. onset temp. encapsul. PR112 (°C)	Tg (DSC)	Encapsul. eff. % (polymer content)
		Initial	Final				
PBA-co-PMMA (80:20)	0.11	8.8	1.59	332	371	-29	20.08
	0.25	9.46	2.36	-	369	-26	28.04
	0.42	19.31	3.91	-	379	-31	27.91
	0.66	10.58	2.37	-	378	-27	37.33
PSt-co-PBA (80:20)	0.11	9.6	2.28	386	409	49	26.39
	0.25	11.13	2.78	-	416	51	31.17
	0.42	12.9	4.83	-	411	56	41.6
	0.66	11.42	4.02	-	422	53	51.08

5.2.4 Transmission Electron microscopy (TEM)

For further insights into the effectiveness of copolymer encapsulation of the PR112 particles, we analyzed the hybrid particles by transmission electron microscopy (TEM) from which we could further validate whether the pigment particles are encapsulated in the polymer latex or not. Additionally, the morphology and particle size of the encapsulated PR112 particles can be

determined. However, by TEM it is rather difficult to estimate quantitatively the encapsulation efficiencies, i.e., the exact polymer coating layer, due to the lack of the crystalline structure of pigment particles, which renders it rather difficult to distinguish them from the amorphous polymer layer as well as the possibility of particle agglomeration after drying pigment dispersion drop on the TEM grid. Therefore, we used TEM only as a qualitative tool in combination with the data obtained from DLS, DC, and TGA. TEM images were obtained for PR112 encapsulated with BA-MMA copolymer latex and compared to images of PR112 without latex, BA-MMA copolymer latex and a proper physical mixture of the copolymer latex and the PR112 particles in ratio of (0.25) as shown in figures 5.5. The TEM picture of the blank PR112 (before encapsulation) (figure 5.5 A) shows pigment particles which are often highly agglomerated due to the strongly attractive pigment-pigment particle interactions. The pigment free BA-MMA copolymer latex particles shown in (figure 5.5 B), are spherical with regular shape and have approximately a diameter of 150 nm. The spherical latex particles can be seen clearly and separately beside the PR112 particles in (figure 5.5 C), which represent a physical mixture of pigment particles and BA-MMA copolymer latex in a mixing ratio for latex /pigment of 0.25. The encapsulated PR112 particles with the different BA-MMA copolymer latex contents with latex pigment ratios of 0.11, 0.25 and 0.66 are shown in (figures 5.5 C, D, and F). Here, one can observe clearly the absence of the regular shape of the spherical copolymer latex particles, while the pigment particles are probably covered with a polymer layer shell, which might indicate the successful encapsulation. However, it is difficult to determine accurately the thickness of the polymer shell layer due to the indefinite structure of the pigment particles in the TEM observations. The TEM images of the encapsulated PR112 with St-BA copolymer latex in figure 5.6 indicate an increasingly thick copolymer shell. The pigment particles were encapsulated with a layer of the St-BA copolymer latex and the thickness of the polymer shell increases with increasing latex pigment ratio. The hybrid structure of the encapsulated PR112 is especially well visible in (figure 5.6 B), in which the pigment particles are the core and a thin layer of the St-BA copolymer latex is the shell. However, also for higher latex/pigment ratios (figures 5.6 C and D) one can see the core-shell structure in various particles but also that the particles are bigger and more polydisperse. In general, by correlation of the results obtained from TEM with the TGA data, we have found that the TEM observations to be in good agreement with the derived encapsulation efficiency values presented in table 5.3.

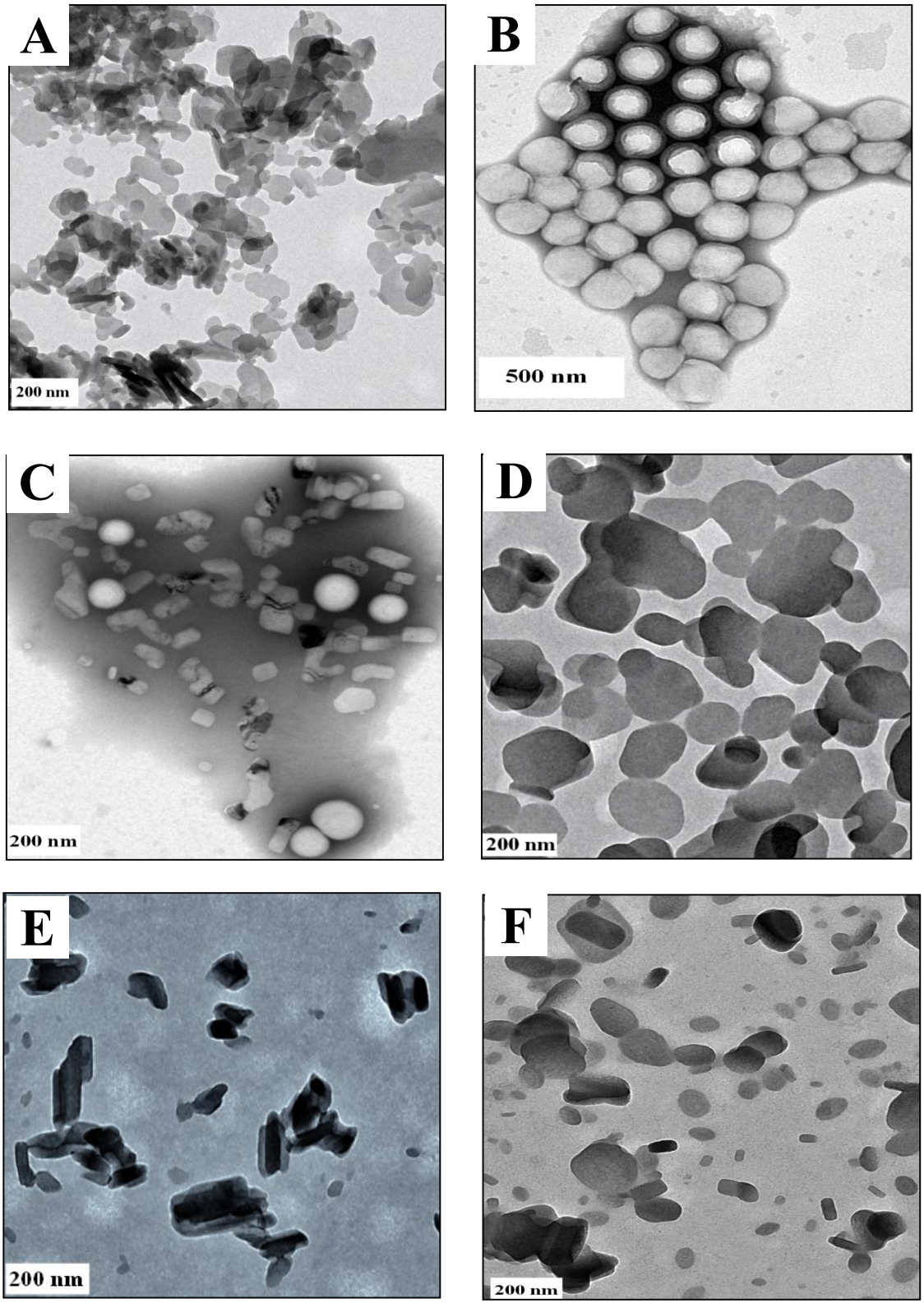

Fig. 5.5:TEM pictures of A) PR112 free latex, B) BA-MMA copolymer latex, C) physical mixture of PR112 and BA-MMA copolymer latex particles, D) encapsulated PR112 with BA-MMA copolymer (latex/pigment ratio 0.11), E) encapsulated PR112 with BA-MMA copolymer (latex/pigment ratio 0.25), F) encapsulated PR112 with BA-MMA copolymer (latex/pigment ratio 0.66).

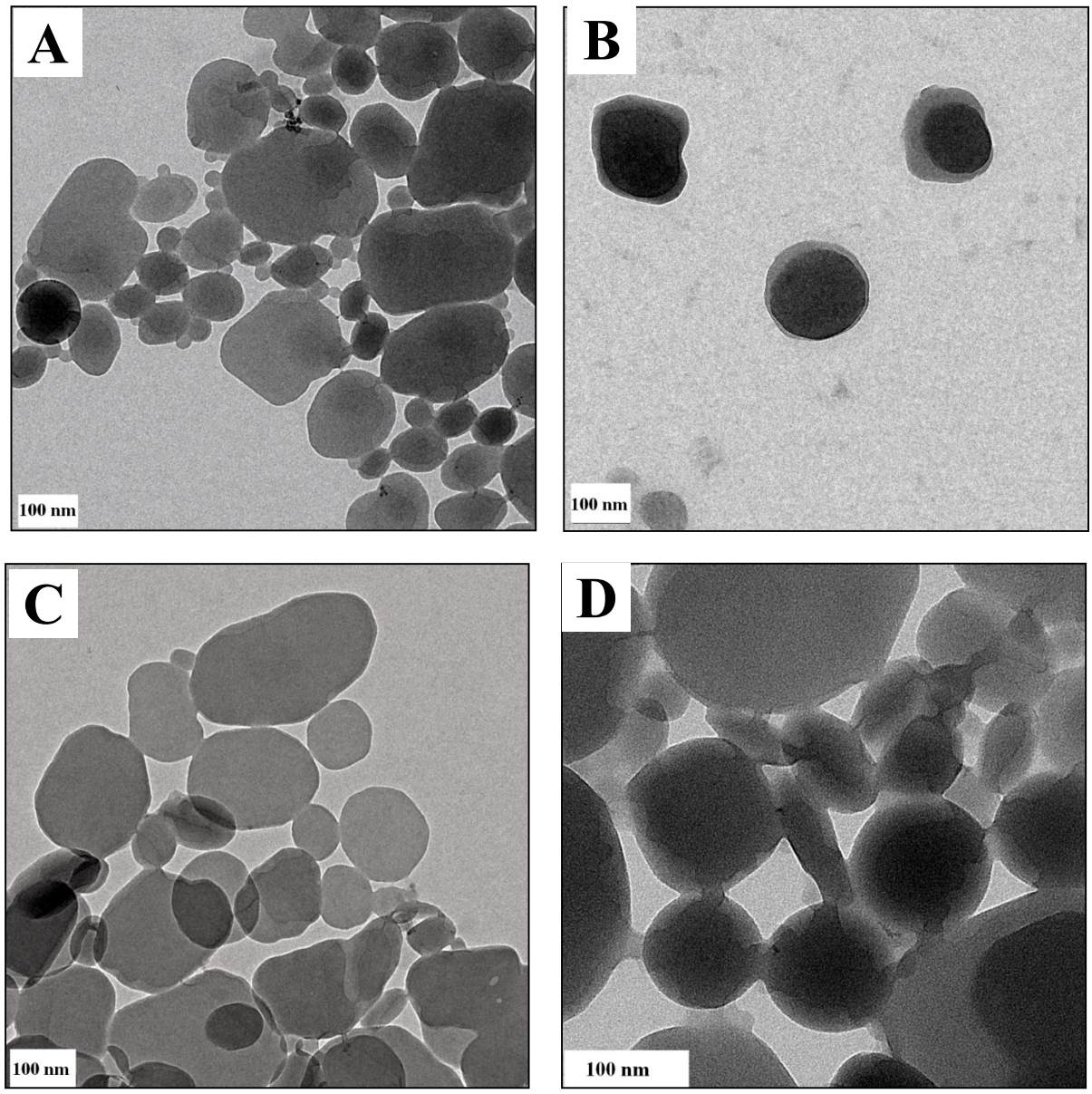

Fig. 5.6: TEM pictures of A) encapsulated PR112 with St-BA copolymer (latex/pigment ratio 0.11), B) encapsulated PR112 with St-BA copolymer (latex/pigment ratio 0.25), C) encapsulated PR112 with St-BA copolymer (latex/pigment ratio 0.42), D) encapsulated PR112 with St-BA copolymer (latex/pigment ratio 0.66).

5.2.5 Stability and aging of the encapsulated PR112 inks.

The stability of the pigment ink dispersions with respect to a variety of formulation ingredients, solvents, surfactants and polymeric binders is very important because if the ink is not stable, the other properties become meaningless. The particle size and size distribution of the pigment particles, on the one hand, affect the image quality, especially color density, in terms of ink holdout and the effective use of each pigment particle for light absorption [22]. Therefore, we followed the aging of the particle size of the encapsulated PR112 hybrid dispersions with the two copolymer latexes as function of the storing time for 6 months by DLS. As shown in figure 5.7 the hydrodynamic radius (R_h) of the encapsulated hybrid PR112 with the BA–MMA copolymer latex increases slightly during six months for all the encapsulated PR112 dispersions with the different latex/ pigment ratios. In contrast, no change of R_h was observed for the PR112 encapsulated with the St-BA copolymer latex, i. e., they are colloidally fully stable. Apparently, the long-time stability of the encapsulated pigments depends on the type of copolymer coating.

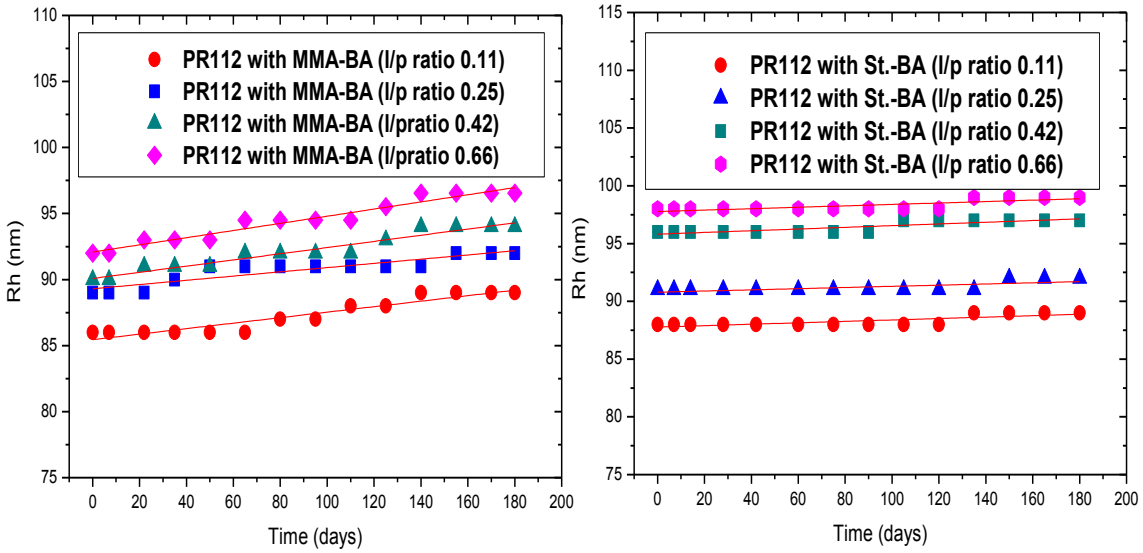

Fig. 5.7: Hydrodynamic radius Rh of the encapsulated PR112 with the BA-MMA and St-BA copolymer latexes for different latex/pigment (l/p) ratios as a function of time storing in days.

The long-term stability of the encapsulated PR112 was confirmed by zeta potential (ζ) measurements. In dispersions where ζ is smaller than 25 mV, particles tend to agglomerate, while for ζ >30 mV, particles in dispersions tend to repel each other sufficiently strongly to not agglomerate [23, 24]. The determined values of zeta potential of the encapsulated PR112 with the BA-MMA and St-BA copolymer latexes are given in table 5.4 and range between -39 and

-43 mV. This negative surface charge arises from the adsorption of the SDS surfactant on the surface of the encapsulated pigment particles. In general, the stability of the particle size can be attributed to this electrostatic stabilization. However, apparently the stabilization is not purely determined by the ζ-potential, as the dispersions of the encapsulated PR112 particles with the St-BA copolymer latexes are more stable than the ones with BA-MMA. Despite having similar ζ-potential values, the relative stability arises from the effective encapsulation of St.-BA copolymer in comparison to BA-MMA copolymer.

Table 5.4: ζ-potential values of the encapsulated PR112 inks with the BA-MMA and St-BA copolymer latexes prepared with different latex pigment ratios at fixed pH 8 and [62.5 mM].

Latex / Pigment wt. ratio	*ζ-potential [mV] for PR112 encapsulated with BA-MMA*	*ζ-potential [mV] for PR112 encapsulated with St-BA*
0.11	-41	-43
0.25	-41	-41
0.42	-42	-42
0.66	-40	-39

5.2.6 Inkjet printing of the encapsulated pigments on textile cotton fabrics.

5.2.6.1 Physical properties of the polymer encapsulated PR112 inks.

The physical properties of the pigment ink dispersions in the inkjet printing process have a major influence on the jetting of the inks over substrates, which determines finally the overall print performance. There are many physical properties to be determined and adjusted before jetting inks but the most important properties are ink viscosity, surface tension, pH, particle size, total solid content, and ink mass density. In general, pigment ink dispersions with low viscosity and high surface tension are more preferable in order to eject ink droplets correctly and to get enough color density. If the ink viscosity exceeds the range of the optimum values, the ink becomes too viscous to flow through the nozzle or pass through the orifice, resulting in a clogging problem during drop ejection. If the surface tension is too high, the ink droplets will be too small and they may not spread enough and thus affect the quality of the printed image. Oppositely, if the surface tension is too low, the ink droplets become too large, which causes them to spread too much, causing bleeding and overbanding. The typical properties of a water-based ink suitable for printing on a textile fabric should have a viscosity between (1-5 mPas), surface tension values between (25 – 60 mNm^{-1}); a pigment color weight between (2-5%) and particle diameters below 500 nm [25, 26]. Table 5.5 summarizes the values of the ink viscosity,

particle diameter, and surface tension of the encapsulated PR112 with the BA-MMA and St-BA copolymer latexes at different pigment latex ratios, mixed dispersions of BA-MMA and St-BA copolymer latex and PR112 (polymer / PR112 ratio : 0.66), and the PR112 free copolymer latex. The viscosity of the encapsulated PR112 with the BA-MMA and St-BA copolymer latexes increases as the copolymer latex content increases markedly by changing the latex /pigment ratio from 0.11 to 0.66. However, one observes that the viscosity values of the encapsulated PR112 inks with the BA-MMA and St-BA copolymers are always lower than the mixed dispersions of latex and PR112 with the latex free PR112. This rheological data reveal that all PR112 ink viscosities are rather independent from the shear rate, as typically observed for not too concentrated particle dispersions. This means that all PR112 inks exhibited a Newtonian behavior, which is the typical flow behavior of inks in the inkjet printing of textile fabrics.

Table 5.5: Shear viscosity, particle size and surface tension measurements of the encapsulated hybrid PR112 inks, physical mixture of non-encapsulated PR112 and latex binder and the PR112 without latex binder. PR112 concentration 4 wt. %, SDS [25 mM] and pH adjusted to 8.

Type of pigment ink	Latex/ pigment ratio	Particle size (d) (nm), (DLS)	Shear Viscosity (m Pas) at shear rates (1/sec) of			Surface tension (mNm^{-1})
			50	250	750	
Encapsulated PR112 with BA-MMA copolymer latex	0.11	172	1.77	1.71	1.59	43
	0.25	177	2.33	2.13	2.16	41
	0.66	184	3.43	3.27	3.12	37
Encapsulated PR112 with St-BA copolymer latex	0.11	176	1.82	1.66	1.79	41
	0.25	182	2.11	2.19	2.22	38
	0.66	196	3.46	3.39	3.33	36
PR112/PBA-co-PMMA (mixture)	-	170	4.51	4.14	4.21	41
PR112/PSt-co-PBA (mixture)	-	170	4.58	4.09	4.26	39
PR112 without copolymer latex	-	170	1.67	1.65	1.47	46

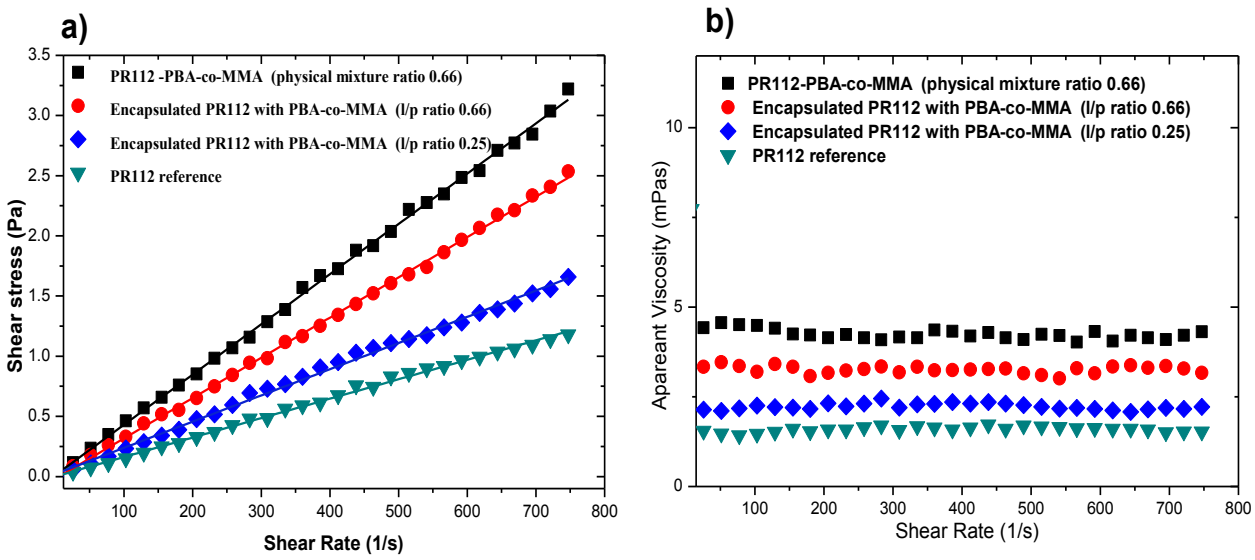

Fig. 5.8: Rheological properties of the different PR112 inkjet inks a) Shear stress developed vs. applied shear rate b) Shear viscosity of PR112 inks developed vs. applied shear rate.

The values of surface tension of the encapsulated PR112 with BA-MMA and St-BA copolymer latexes, as presented in table 5.5, ranged between 36 and 43 mNm^{-1}, where these rather low values can in general be attributed to the presence of excess surfactant (SDS), in the inks. It was observed that the surface tension of the encapsulated PR112 slightly decreases with increasing latex/PR112 ratio. In general, the surface tension of the encapsulated pigments, the separately dispersed latex/pigments and the free latex pigments have approximately similar values and their values are within the operational range of the inkjet printing. At these surface tension values, a regular droplet formation and pigment loading are expected to provide a good dot formation and limited penetration depth of the ink fluid.

5.2.6.2 Assessment of the inkjet printed cotton fabrics with the encapsulated inks.

One of our main objectives beside enhancing the ink stability by encapsulation and lowering the risk of the pigment particles agglomeration is to study the applicability of these hybrid inks in the inkjet printing of textile cotton fabrics and compare them to conventional ink recipes. We aimed to have hybrid inks with dual property; to form the final color coat and at the same time to act as binder by providing the film during the curing process and thereby avoiding possible agglomeration, which occurs occasionally between pigment and binder particles within conventional ink formulations. In this regard, we applied the encapsulated PR112 with BA-MMA and St-BA copolymer latexes, which were prepared with different latex/pigment ratios as inks for the inkjet printing of cotton fabrics. The encapsulated PR112 inks were formulated

and filtered easily with the other additives such as the humectants and silicon surfactant without addition of separate latex binder. The encapsulated hybrid inks were then jetted and printed successfully on cotton fabrics without causing agglomeration or cloaking the nozzles of the digital printer machine, which gives an indication for the excellent inkjet printing behavior of the encapsulated PR112 inks. The properties of the printed cotton fabrics with the encapsulated inks was assessed and compared to fabrics printed with non-encapsulated PR112 inks having separate polymer latex. The optimum conditions of the inkjet printing with the encapsulated PR112 was then applied for two other different pigment colors, C.I. Pigment blue (PB 15:3) and C.I. Pigment yellow (PY.155) in order to test their printability over the non-encapsulated inks.

5.2.6.2.1 Color strength and fastness properties toward rubbing and washing of the inkjet printed cotton fabrics with the encapsulated PR112 inks with PBA-co-PMMA and PSt-co-BA latexes.

Table 5.6 shows the values of color strength, rubbing and washing fastness of the inkjet printed cotton fabrics with the encapsulated PR112 inks with the BA-co-MMA and St-co-BA latexes using different latex/pigment ratios, the non-encapsulated PR112 ink containing separate PBA-co-PMMA or PSt-co-PBA latex binders and the non-encapsulated PR112 ink without binder. The color strength (K/S) of the printed fabrics with the encapsulated PR112 after washing showed comparable values to the non-encapsulated inks, which contain separate binder latexes, and better values than the non-encapsulated inks without binder regardless of the type of copolymer used for encapsulation. However, we observed that the color strength values of the printed fabrics with the encapsulated inks before washing slightly decreases with increasing latex/pigment ratio while the change in color strength before and after washing minimizes and improves with increasing latex/pigment ratio.

On the other hand, the values of the rubbing and washing fastness of the printed cotton fabrics with the encapsulated inks using the two copolymer latexes indicated that the variation of the latex/pigment ratio from 0.11 to 0.66 improves the fastness toward dry and wet rubbing as well as minimizes the color change and staining after washing. These findings may be attributed to the dependence of the degree of the pigment film formation on fabrics on the polymer latex content in the ink formulation, which finally affects the color strength especially after washing, rubbing and washing fastness.

Based on the values of rubbing and washing fastness, we observed that the printed fabrics with encapsulated PR112 inks with BA-co-MMA or St-co-BA latexes having a latex / pigment ratio of 0.66 showed better values in comparison to the non-encapsulated conventional PR112

without binder and comparable values with the non-encapsulated conventional PR112 inks that contain separate BA-MMA or St-co-BA copolymer latex binders. In general and after the evaluation of the color strength, rubbing and washing fastness of the printed fabrics, the encapsulated inks could be used as successful candidates for the inkjet printing of textile fabrics as they showed satisfying values, which meet the criteria of the standard tests. This is of course in addition to their primary task to maintain the long-term stability upon storing and reduce the aggregates and agglomeration of the pigment particles during manufacturing the inks, which affects the quality of the film formation on substrates.

Table 5.6: Color strength, rubbing and washing fastness values of the inkjet printed cotton fabrics with the encapsulated hybrid PR112 inks with different BA-co-MMA and St-co-BA latex/ pigment ratios, physical mixture of non-encapsulated PR112 and PBA-co-PMMA or PSt-co-PBA latex binders and PR112 without latex binder. PR112 concentration 2 %.

Inks	Latex / pigment ratio	Color strength (K/S)		Rubbing fastness*		Washing fastness*	
		Before washing	After washing	Dry	Wet	Color change	Staining on wool
Encapsulated PR112 with BA-co-MMA (without binder)	0.11	2.39	1.87	2	1-2	3	2-3
	0.25	2.31	2.26	2-3	2	4-5	4
	0.66	2.19	2.17	3	2-3	4-5	4-5
Non-encapsulated PR112 with PBA-co-PMMA binder	-	2.33	2.28	3-4	2-3	5	4-5
Encapsulated PR112 with St-co-BA (without binder)	0.11	2.44	1.96	2-3	1-2	2-3	2
	0.25	2.32	2.31	2-3	1-2	4-5	4
	0.66	2.27	2.25	3-4	2-3	4-5	4-5
Non-encapsulated PR112 PSt-co-PBA binder	-	2.38	2.36	4	2-3	4-5	4
Non-encapsulated PR112 without binder	-	2.64	0.67	1-2	1	2	1-2

*Rubbing and washing fastness of fabrics are divided into five levels according to the AATCC testing methods. The highest one is the fifth level, the higher the better.

5.2.6.2.2 Color strength and fastness properties toward rubbing and washing of the inkjet printed cotton fabrics with the encapsulated PB15:3 and PY155 inks.

In order to further investigate the properties of inkjet printing with the encapsulated inks, we tested the printing of cotton fabrics with the encapsulated C.I. pigment blue 15:3 (PB15:3) and C.I. pigment yellow 155 (PY155) inks with the St-co-BA copolymer latex using a fixed latex/ pigment ratio of 0.25 as presented in table 5.7. Similarly, the color strength, rubbing and washing fastness of the inkjet printed fabrics with the encapsulated PB15:3 and PY155 inks values comply with the criteria of the standard tests and are comparable to the printed fabrics with conventional ink recipes. This means that the encapsulation of pigment particles with polymer layer not only enhances the stability and dispersability of the inks as well as reduces their viscosity but also allows for successful inkjet printing behavior with satisfying color strength, rubbing and washing fastness.

Table 5.7: Color strength, rubbing and washing fastness values of the inkjet printed cotton fabrics with the encapsulated hybrid PB15:3 and PY155 inks with St-co-BA copolymer latex using fixed latex/ pigment ratio of 0.25, physical mixture of non-encapsulated PR112 and PSt-co-PBA latex binder and PR112 without latex binder. PR112 concentration 2 %.

Inks	Color strength (K/S) after washing		Rubbing fastness*				Washing fastness*			
			Dry		Wet		Color change		Staining on wool	
	PB15:3	PY155	PB15:3	PY155	PB15:3	PY155	PB15:3	PY155	PB15:3	PY155
Encapsulated inks (without binder)	3.76	3.34	2-3	3	2	2	4-5	4-5	4	4-5
Non-encapsulated inks with binder	3.82	3.57	3	3	2	2-3	4-5	5	4-5	5
Non-encapsulated inks without binder	1.09	0.55	1-2	2	1	1-2	2	2-3	1-2	2

*Rubbing and washing fastness of fabrics are divided into five levels according to the AATCC testing methods. The highest one is the fifth level, the higher the better.

5.3 Conclusion

In this chapter, we studied systematically the encapsulation of the organic pigments with a copolymer latex layer by the miniemulsion polymerization method. We aimed at reducing the tendency for pigment agglomeration as a result of the pigment particles interaction and hence improving the stability of the pigment particles in aqueous ink dispersions. Such polymer-encapsulated pigments then can be applied for inkjet printing without addition of separate binder additives, thereby reducing the risk of unfavorite interactions between the separate latex and pigment particles. We studied then the encapsulation of C.I. Pigment red 112, an organic azo-naphthalene color, systematically by a miniemulsion polymerization of pigment/butyl acrylate-co-methyl methacrylate (BA-MMA) or styrene-co-butyl acrylate (St-BA) copolymers. SDS as anionic surfactant and hexadecane as co-stabilizer stabilized the pigment dispersions before encapsulation. The ratio of monomer to pigment (latex/pigment) was varied in order to find optimum conditions for the preparation of self-curable hybrid pigment inks for the textile inkjet printing application. The particle size and polydispersity of the pigment dispersions and pigment hybrid latex particles were investigated by dynamic light scattering (DLS), a disc centrifuge particle size analyzer and transmission electron microscopy (TEM). The determined particle sizes of the encapsulated pigment particles with the different latex/pigment ratios were bigger than the non-encapsulated ones. The efficiency of the polymer encapsulation and thermal properties of the hybrid inks were studied by thermogravimetric analysis (TGA) and differential scanning calorimetry (DSC). The encapsulation efficiencies, as determined from TGA, increase when increasing the polymer content. For instance, the variation of the latex/pigment ratio from 0.11 to 0.66 using BA-MMA as copolymer latex increases the encapsulation efficiency from 20% to 37%, while the encapsulation efficiency increases from 26% to 51% using St-BA copolymer latex by increasing the same latex/pigment ratio. The TEM images showed that the encapsulated pigment particles are somehow coated with polymer layer shells, which probably indicate a successful encapsulation. The long-term stability of the encapsulated hybrid pigment inks seen by DLS can be explained by the large negative zeta potential, where a slightly better stability is seen for the St-BA case. The viscosities of the encapsulated hybrid inks were reduced when compared to conventional inks having separately dispersed polymer latex and pigment particles, which ultimately enhance the applicability of the inks. The measured surface tension of the encapsulated pigments is well suited for the inkjet printing application. The evaluation of the inkjet printing of cotton fabrics with different encapsulated and non-encapsulated pigment colors shows that the encapsulated inks without addition of separate polymer latex binder generate satisfying and comparable values in term of color strength, rubbing and washing

fastness in comparison to the non-encapsulated conventional inks, while avoiding problems of clogging and colloidal instability.

5.4 References

[1] P. Calvert. (2001). Inkjet printing for materials and devices. *Chemistry of Materials,* 13, 3299-3305.

[2] Y. Yang, V. Naarani. (2007). Improvement of the lightfastness of reactive inkjet printed cotton. *Dyes and Pigments, 74,*154-160.

[3] A. Hladnik, T. Muck. (2002). Characterization of pigments in coating formulations for high-end ink-jet papers. Dyes and Pigments, *54*, 253-263.

[4] C. T. Kosolia, E. G. Tsatsaroni. (2010). Synthesis and characterization of hetarylazo disperse colorants: preparation and properties of conventional and microemulsified inks for polyester ink-jet printing. *Journal of Applied Polymer Science*, *116*, 1422-1427.

[5] P. S. Choi, C. W. M. Yuen, S. K. A. Ku, C. W. Kwan. (2003). Ink-jet printing for textiles. *Textile Asia, 34*, 21-24.

[6] S. Mhetre, W. Carr , P. Radhakrishnaiah. (2010). On the relationship between ink-jet printing quality of pigment ink and the spreading behavior of ink drops. *The Journal of the Textile Institute, 101,* 423-430

[7] B. Richey, B. Mary. (2002). Applications for decorative and protective coatings. D. D. Urban, D. K. Takamura (Ed.), *Polymer Dispersions and Their Industrial Applications* (pp. 123−161). Weinheim, Germany: Wiley-VCH Verlag GmbH & Co. KGaA.

[8] E. Bourgeat-Lami. (2002). Organic-Inorganic Nanostructured Colloids. *J. Nanosci. Nanotechnol., 2*, 1-24.

[9] J. L. Luna-Xavier, A. Guyot, E. Bourgeat-Lami. (2002). Synthesis and Characterization of Silica/Poly (Methyl Methacrylate) Nanocomposite Latex Particles through Emulsion Polymerization Using a Cationic Azo Initiator. *J. Colloid Interface Sci., 250*, 82-92.

[10] Y. Haga, T. Watanabe, R. Yosomiya. (1991). Encapsulating polymerization of titanium dioxide. *Angew. Makromol. Chem., 189*, 23-24.

[11] L. Quaroni, G. Chumanov. (1999). Preparation of Polymer-Coated Functionalized Silver Nanoparticles. *J. Am. Chem. Soc.*, *121*, 10642-10643.

[12] S. Fua, C. Xub, C. Duc, A. Tiana, M. Zhanga. (2011). Encapsulation of C.I. Pigment blue 15:3 using a polymerizable dispersant via emulsion polymerization. *Colloids and Surfaces A: Physicochem. Eng. Aspects, 384*, 68-74.

[13] S. Lelu, C. Novat, C. Graillat, A. Guyot, E. Bourgeat-Lami. (2003). Encapsulation of an organic phthalocyanineblue pigment into polystyrene latex particles using a miniemulsion polymerization process. *Polym. Int., 52*, 542-547.

[14] N. Bechthold, F. Tiarks, M. Willert, K. Landfester, M. Antonietti. (2000). Miniemulsion polymerization: applications and new materials. *Macromol. Symp., 151,* 549-555.

[15] B. Erdem, E. D. Sudol, V. L. Dimonie, M. S. El-Aasser. (2000). Encapsulation of inorganic particles via miniemulsion polymerization. I. Dispersion of titanium dioxide particles in organic media using OLOA 370 as stabilizer. *J. Polym. Sci., Part A: Polym. Chem., 38*, 4419-4430.

[16] F. K. Hansen, J. Ugelstad. (1979). Particle nucleation in emulsion polymerization. IV. Nucleation in monomer droplets. *J. Polym. Sci. Polym. Chem. Ed., 17*, 3069-3082.

[17] B. J. Chamberlain, D. H. Napper, RG. Gilbert. (1982). Polymerization within styrene emulsion droplets. *J. Chem. Soc. Faraday Trans.1, 78,* 591-606.

[18] F. Tiarks, K. Landfester, M. Antonietti. (2001). Encapsulation of Carbon Black by Miniemulsion Polymerization. *Macromol. Chem. Phys.*, *202*, 51-60.

[19] N. Steiert, K. Landfester. (2007). Encapsulation of organic pigment Particles via miniemulsion polymerization. *Macromol. Mater. Eng., 292,* 1111-1125.

[20] Y. D. Kim, J. H. Cho, C.R. Park, J. H. Choi, C. Yoon, J.P. Kim.(2011). Synthesis, application and investigation of structure-thermal stability relationships of thermally stable water-soluble azo naphthalene dyes for LCD red color filters. *Dyes and Pigments*, *89*, 1-8.

[21] J. W. Wilkes, C. E. Summers, C. A. Daniels, M. T. Berard. (2005). *PVC Handbook*. Munich, Germany: Hanser Verlag.

[22] H. Noguchi, K. Shirota. (2006). Pigmented ink formulation. H. Ujiie (Ed.), *Digital printing of textiles* (pp. 232). Cambridge, UK: Woodhead Publishing Limited and CRC Press.

[23] N. Mandzy , E. Grulke, T. Druffel. (2005). Breakage of TiO2 agglomerates in electrostatically stabilized aqueous dispersions. *Powder Technology, 160*,121-126.

[24] F. Strubbe, F. Beunis, K. Neyts. (2006). Determination of the effective charge of individual colloidal particles. *Journal of Colloid and Interface Science, 301,* 302-309.

[25] H. K. Lee, M. K. Joyce, P. D. Fleming, J. H. Cameron. (2002).Production of a Single Coated Glossy Inkjet Paper Using Conventional Coating and Calendering Methods,

Proceedings from TAPPI Coating and Graphic Arts Conference and Trade Fair, Orlando, FL, USA, pp. 24.

[26] C. G. de Kruif, E. M. F. van Iersel, A. Vrij, W. B. Russel.(1985). Hard sphere colloidal dispersions: Viscosity as a function of shear rate and volume fraction. *J. Chem. Phys., 83*, 4717-4725.

[27] P. Macfaul. (2003). Ink technologies for inkjet printing. *Digital Printing*. London, UK: Onwards, Enfield.

6. Preparation and application of monodisperse latex nanoparticles by subsequent polymerization in nanoemulsions obtained by the low energy phase inversion composition method.

6.1 Introduction

Nanoemulsions are a class of emulsions with droplet sizes between 20-200 nm [1-5]. Unlike microemulsions which are thermodynamically stable [6, 7], nanoemulsions are only kinetically stable. However, their outstanding long time stability against coalescence, flocculation and Ostwald ripening make them unique systems and attractive candidates for practical and industrial applications, for example as reaction templates for polymerization, in personal care and cosmetics, for health care, or in agrochemicals [8-12]. In literature, they have been termed as miniemulsions [3, 13], nanoemulsions [4, 14], fine-disperse emulsions [15] or blue emulsions [16], submicron emulsions [17], unstable microemulsions [18], translucent emulsions [19], with miniemulsion and nanoemulsion being the most commonly employed names. Miniemulsions and nanoemulsions are distinguished by the method of preparation. Miniemulsions are usually prepared by the application of external energy input such as ultrasonic or high-pressure homogenization in order to generate stable miniemulsion droplets from systems consisting of oil-costabilizer/water/surfactant [20, 21]. In contrast, nanoemulsions are prepared by low energy methods, or condensation methods, which depend on the phase transition that takes place spontaneously during the emulsification as a result of the changes in the curvature of the surfactant [22]. The phase transition can be achieved at constant composition by changing the curvature of surfactants with temperature which is well known as phase inversion temperature method, (PIT) [23, 24], or at constant temperature by varying the composition of the system and is known as phase inversion composition method, (PIC) [25-29]. The low energy phase inversion composition method (PIC) is based on the evolution of the system by changing the surfactant/oil ratio in the aggregates during the emulsification pathway, which induces the disintegration of the intermediate structures into small nano-droplets. In this method, as described in figure 6.1, the stepwise addition of water to a surfactant/oil solution leads to the formation of an O/W nanoemulsion by passing a sponge-like bicontinuous microemulsion with zero curvature or alternatively a lamellar phase, in which the oil is dissolved in a single phase. The addition of water acts to hydrate the polar part of the surfactant and together with the dissolution of well water-soluble amphiphilic components increases its spontaneous curvature, which leads to the rupture and dislocation of the sponge-

like microemulsion or the lamellar structure with the result of forming spontaneously O/W nanoemulsion droplets at the catastrophic inversion point. If the nanoemulsion droplets contain a monomer, a subsequent polymerization then generates polymer nanoparticles.

The generation of nanoparticles by the polymerization in miniemulsion templates prepared by the high-energy method is widely reported in literature [20-36]. In contrast, only few reports describe the polymer nanoparticles synthesis in monomer-nanoemulsions prepared by low energy methods [37-39] and in particular ones obtained by the phase inversion composition method [40, 41], i. e., a method that relies exclusively on the principles of self-assembly. The advantage of such an approach is that not only is a very simple procedure but also a mild one, which allows incorporating delicate chemical compounds.

In this chapter, we aimed to design a new path for the synthesis of polymer and copolymer latex nanoparticles by the subsequent polymerization in monomer-nanoemulsion templates obtained by the low energy phase inversion composition method. The monomer-nanoemulsions were prepared from systems consisting of (water/ Brij 78/ monomer-hexadecane). We used styrene as monomer for the systematic study of the monomer-nanoemulsion formation and their subsequent polymerization. The phase behavior of a system consisting of water/ Brij 78/ styrene was investigated. The polymerization was studied with potassium persulfate (KPS) and azobisisobutyronitrile AIBN initiators to generate polymer nanoemulsion latex particles. Furthermore, styrene-butyl acrylate and butyl acrylate- methyl copolymer nanoemulsion particles were prepared. The nanoemulsion copolymer latexes were then tested for application as binding agents for the printing and inkjet printing of cotton fabrics and compared to their miniemulsion copolymer analogs prepared by the high-energy method. The aim then was to find systematic correlations between the composition of the nanoemulsion, the resulting mesocopic structure and how that is transferred into the nanoparticle structure. The correspondingly varied nanolatexes then are compared finally with respect to their performance in textile inkjet printing with the principal aim of optimizing them for applications.

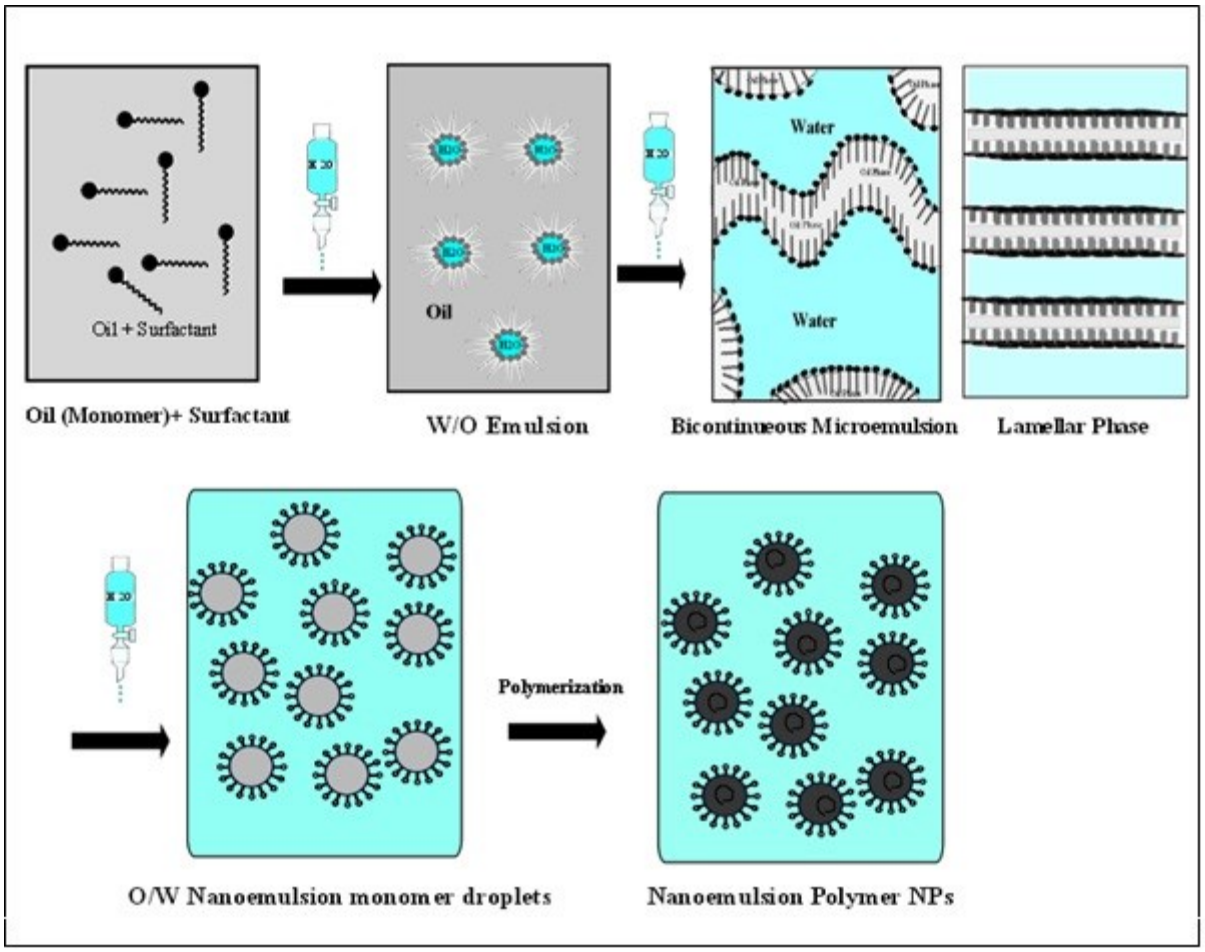

Fig. 6.1 Schematic description of the O/W nanoemulsions formation by the low energy phase inversion composition (PIC) method and the subsequent nanoparticle generation by radical polymerization.

6.2 Result and discussion:

6.2.1 Phase diagram of (Styrene/Brij 78/ water).

In order to have a systematic approach to preparing nanolatexes based on PIC nanoemulsions it is essential to study first the phase diagram of the corresponding system. Knowledge about the conditions related to the spontaneous emulsification as well as getting information and details about the different phases and intermediate structures, which occur during the evolution of the system upon dilution with water, is a key for understanding such systems. Previous studies on nanoemulsion formation by low energy methods and in particular, the phase inversion composition (PIC) method, revealed that nanoemulsion droplets can be generated if the oil is completely dissolved in a single surfactant-rich phase, which can be a bicontinuous microemulsion or a lamellar crystalline phase [42, 43]. The further evolution of the system by changing the composition of the components leads to a breaking-up of the continuous phase into small droplets.

Therefore, we studied the equilibrium phase diagram carefully in order to investigate and prove the formation of the lamellar and/or the bicontinuous microemulsion phases and their evolution to small and well-defined monomer nanoemulsion droplets. Moreover, the phase diagram study shall allow us to determine the optimum conditions at which monomer nanoemulsion droplets can be generated. To our system of styrene-hexadecane/Brij78/water hexadecane was added to the oil phase in order to prevent the growth of the large droplets at the expense of the smaller droplets via diffusion which is known as Ostwald ripening. Hexadecane acts here as an osmotic agent due to its low aqueous solubility.

The phase diagram study was restricted to styrene/Brij78 ratios between 20:80 and 90:10 as described in figure (6.2 a). The selected monomer/surfactant ratios were titrated with water under gentle stirring at room temperature. The dilution was then carried out up to a final water content of 95 wt%. In general, the equilibrium phase diagram of our system was found to be in good agreement with previous studies on related systems of water/polyoxyethylene alkyl ether nonionic surfactant/oil [26, 44-46]. As shown in figure (6.2 a), the stepwise water dilution of the different Brij 78/ styrene ratios resulted in the formation of different phases and intermediate structures. For instance, we observed that a distinct single-phase region consisting of an isotropic liquid phase (Om) is formed along the oil-surfactant axis by the dilution of styrene/Brij 78 ratios between 20:80 and 60:40 with water contents between 10-20 % depending on the surfactant/monomer ratios. The structure and composition of the Om region is usually corresponding to inverse micelles or W/O microemulsions, according to previous reports and its location in the phase diagram [46, 47]. For the relatively surfactant rich case further water

dilution of the (Om) phase leads to the formation of a lamellar liquid crystalline region (Lα). This lamellar phase region was further confirmed by optical polarizing microscopy as shown in figure 6.3, which shows Maltese crosses that are typical for lamellar phases.

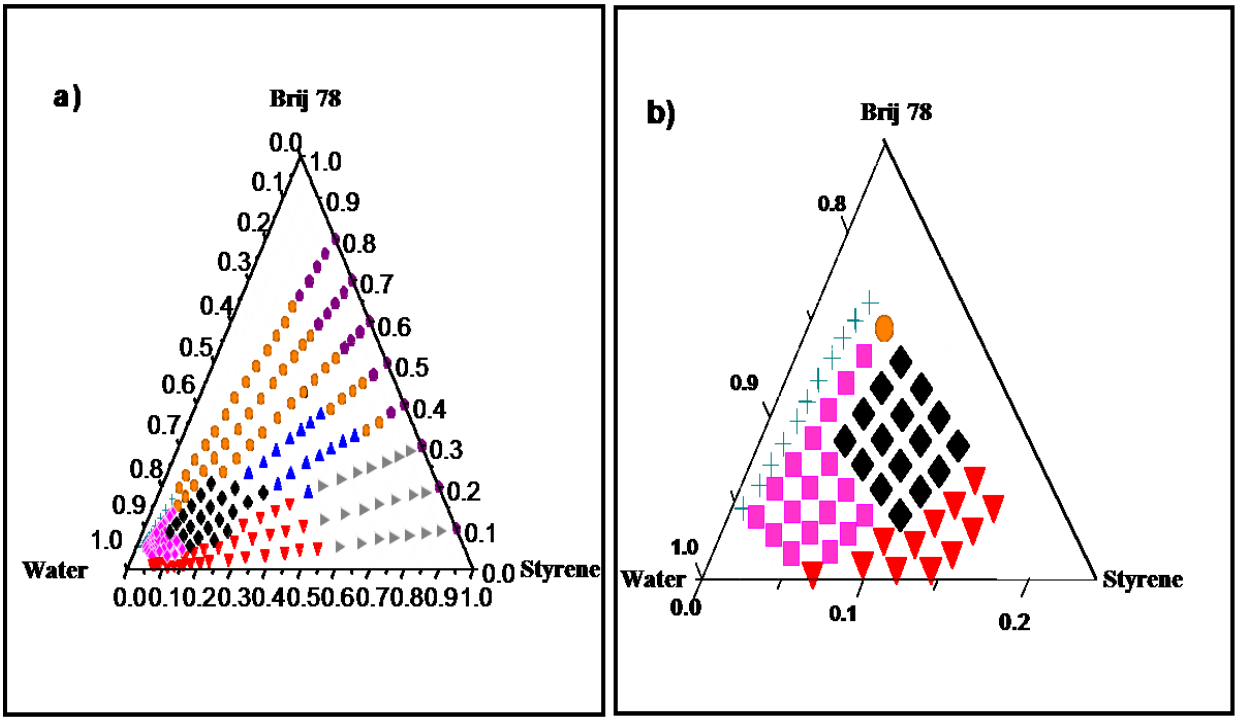

Fig.6.2: a) Equilibrium phase diagram of Brij 78/Styrene/Water system at 25 °C, b) Nanoemulsion region in the phase diagram :(⬟) Isotropic liquid phase (Om), (●) Lamellar crystalline phase (Lα) or (Lα) with (Om), (▲) gel phase, (►) two or multi-Φ, (▼) opaque milky phase, (♦) bluish O/W μE, (■) Bluish NE, (+) Wm + Lα+ O.

However, at higher dilution (more than 80 wt% water) and for higher surfactant/oil ratios of between 80:20 and 70:30, a multiphase region (Wm + Lα + O) appeared. For a lower surfactant/oil ratio a W/O gel phase is observed for water contents between 30-50 wt%. In contrast, a multiphasic region with two or more separate phases was formed at lower surfactant/oil ratio (below 30:70) and water contents up to 40%, where further dilution leads to the formation of an opaque milky phase. A transparent and clear O/W microemulsion phase appeared at water dilutions above 60 wt% for oil /surfactant ratios between 30:70 and 60:40. Its further dilution up to water contents of 95 wt% generates a bluish O/W nanoemulsion phase.

In general, the most suitable region for the formation of styrene nanoemulsion droplets could be achieved at water contents between 80-95 % (with the idea of optimizing the solid content of the latex dispersion) depending on the surfactant/monomer ratios (see also Fig. 6.2 b). This means that polymer nanoparticles with solid contents up to 20 wt% could be generated by the subsequent polymerization in the monomer-nanoemulsion droplets.

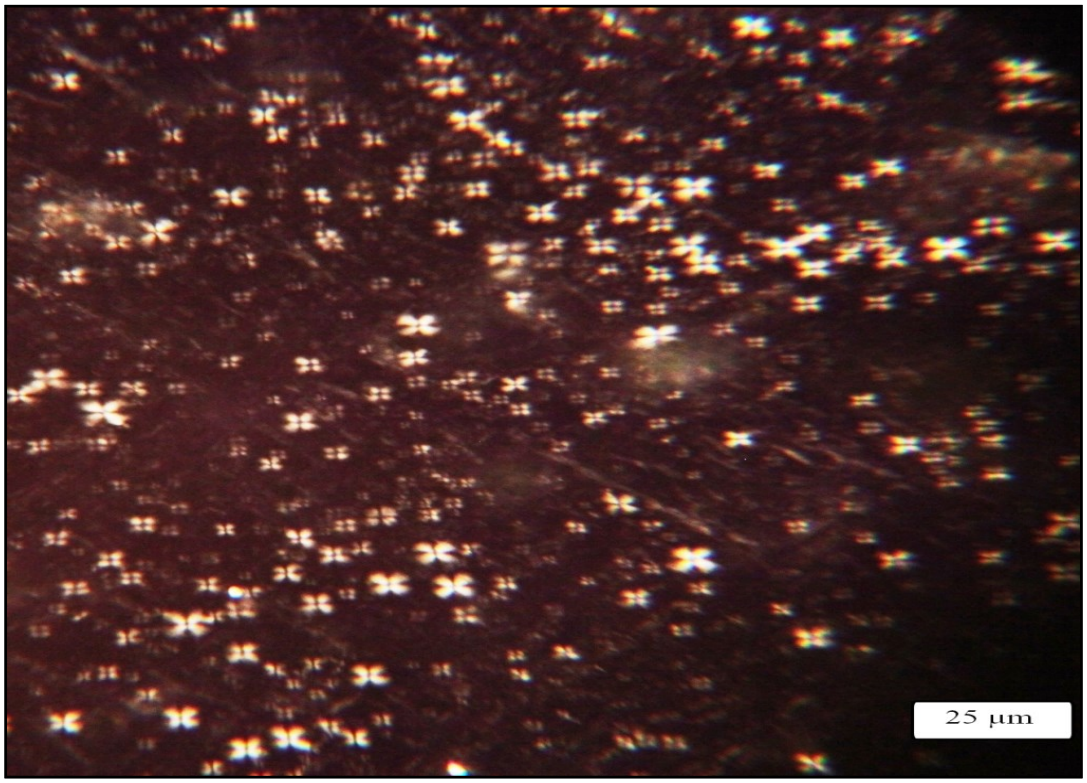

Fig.6.3: Optical micrograph from polarization microscopy of a sample (Brij 78/Styrene: 70:30) ratio in the lamellar liquid crystalline phase exhibiting typical textures of a lamellar liquid crystal (Maltese crosses).

6.2.2 Generation of polystyrene nanoparticles by polymerization of the monomer-nanoemulsions.

6.2.2.1 Monomer conversion with KPS and AIBN initiators.

The polymerization of the prepared styrene monomer–nanoemulsion by the phase inversion composition method was studied with the water-soluble potassium persulfate (KPS) and the oil soluble azo-bis-isobutyronitrile (AIBN) as initiators. Figure 6.4 shows the effect of the initiator type and concentration on the total monomer conversion of styrene as a function of polymerization time for monomer-nanoemulsions prepared with a styrene/Brij 78 mass ratio of

9 and water content of 80 wt%. We found that the final monomer conversion depends on the initiator concentration for AIBN nanoemulsion but not for KPS, where it is much higher already for lower initiator concentrations. We assume that the polymerization in nanoemulsions occurs in correspondence to the mechanism in miniemulsions, in which the particles are growing up from the monomer droplets rather than the micelles, i.e., droplet nucleation, although it should be noted that the polymerization mechanism in miniemulsion systems is not fully understood [48]. Therefore, maintaining and stabilizing the nanoemulsion droplets during the polymerization would have an influence on the overall polymerization and final conversion. In the case of KPS and during the radical polymerization, the residues of $-SO_4^-$ group of KPS may serve to stabilize the nanoemulsions by their presence at the surface of polymer particles (polymerization loci). On the other hand, the organic oil-soluble AIBN residues are housed inside the droplets-particles and do not contribute to stabilize or enhance the dispersion stability of the nanoemulsions. In addition, KPS starts polymerization in nanoemulsions from the water continuous phase, in contrast to AIBN polymerization, which starts within the droplets and could be here a problem for the radical recombination if we consider the finite size of the droplets in nanoemulsion systems. Consequently a relative faster polymerization and final monomer conversion of the nanoemulsion polymerization with the St/ Brij78/KPS was observed when compared to the St/Brij78/AIBN as shown in figure 6.4.

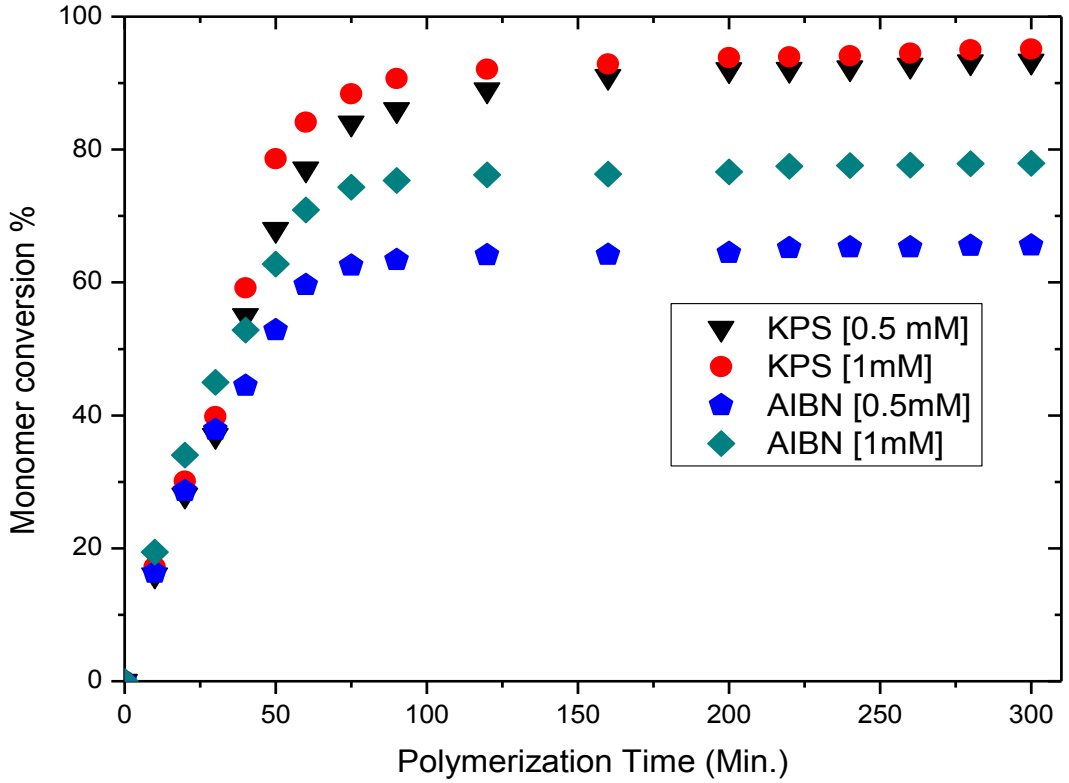

Fig.6.4: Monomer conversion of styrene using different concentrations of KPS and AIBN initiators as a function of polymerization time. Styrene/Brij 78 mass ratio = 9, hexadecane 4 wt% relative to that of styrene, polymerization temperature: 70° C.

6.2.2.2 Influence of the Styrene /Brij 78 ratio on the particle size and polydispersity of the nanolatexes.

We have varied the styrene/Brij 78 ratios in the initial preparations of the monomer-nanoemulsion templates in order to study the possibility of generating polystyrene latex nanoparticles with different monomer solid contents after polymerization. In this regard, we varied the styrene/Brij 78 ratios from 0.25 to 9 at a fixed water content of 80 wt% which changes the styrene monomer solid contents from 3.8 to 17.1 wt% as presented in table 6.1 together with the obtained structural information. The particle size and polydispersity of the polystyrene particles prepared from the different monomer/surfactant ratios were followed by DLS, while the final monomer conversion was estimated gravimetrically. It should be noted that it was not possible to measure the droplet size of the styrene monomer nanoemulsion before polymerization with the polymerized particles as the droplet size changes upon dilution. Figure 6.4 shows the intensity correlation functions and size distributions of the prepared polystyrene latex particles with different styrene/Brij 78 ratios as determined from DLS. It can be seen that

the particle size increases with increasing styrene/Brij 78 ratios, while the diameter size distributions of the styrene particles becomes narrower, i. e., less polydisperse. The mean particle diameter of the polystyrene latexes increases from 32 nm to 118 nm upon increasing the monomer/surfactant ratio from 0.25 to 9. The increase in the particle size is understood since the Brij78 concentration decreases by increasing the monomer/surfactant ration and hence only larger monomer-nanoemulsion droplets can be stabilized due to the lack of surface covering surfactant. On the other hand, the polydispersity indices, as determined from DLS, decrease from 0.26 to 0.03 as the monomer/surfactant ratio increases from 0.25 to 9.

Table 6.1: Particle diameter d and polydispersity index PDI of the polystyrene nanoparticles determined by DLS, styrene solid content (SC), and monomer conversion (MC) at varied styrene/Brij 78 ratios with fixed water content of 80 wt%, hexadecane 4 wt% relative to styrene, KPS 0.5 mM, polymerization temp. 70°C, 5h.

styrene/Brij78 mass ratio	SC (wt %)	d(nm)	PDI	MC (wt %)
0.25	3.8	32	0.26	88.1%
0.43	5.7	44	0.11	88.9%
0.67	7.6	46	0.12	91.2%
1	9.5	48	0.08	90.6%
1.5	11.4	52	0.09	90.3%
2.33	13.3	56	0.07	93.3%
4	15.2	68	0.06	94.2%
9	17.1	116	0.03	93.8%

This remarkable variation in the polydispersity index may be explained on the basis of the particle nucleation during polymerization and as the larger particles grow much longer thereby generating much more monodisperse particle through a homogeneous growth. We assume that the probability for the formation of swollen micelles of the emulsions prepared at lower monomer/surfactant ratios i.e., at higher surfactant concentration is higher than those ones prepared from higher monomer/surfactant ratios. The presence of the swollen micelles beside the emulsion droplets may change the particle nucleation mechanism of the nanoemulsion

polymerization by absorbing monomer and competing with the monomer droplets for radicals and hence changing the path of particle nucleation to proceed through a micellar or homogenous nucleation rather than a droplet nucleation. Therefore, the polymerization in the prepared monomer-nanoemulsion from lower monomer/surfactant ratios generates more polydisperse polystyrene particles.

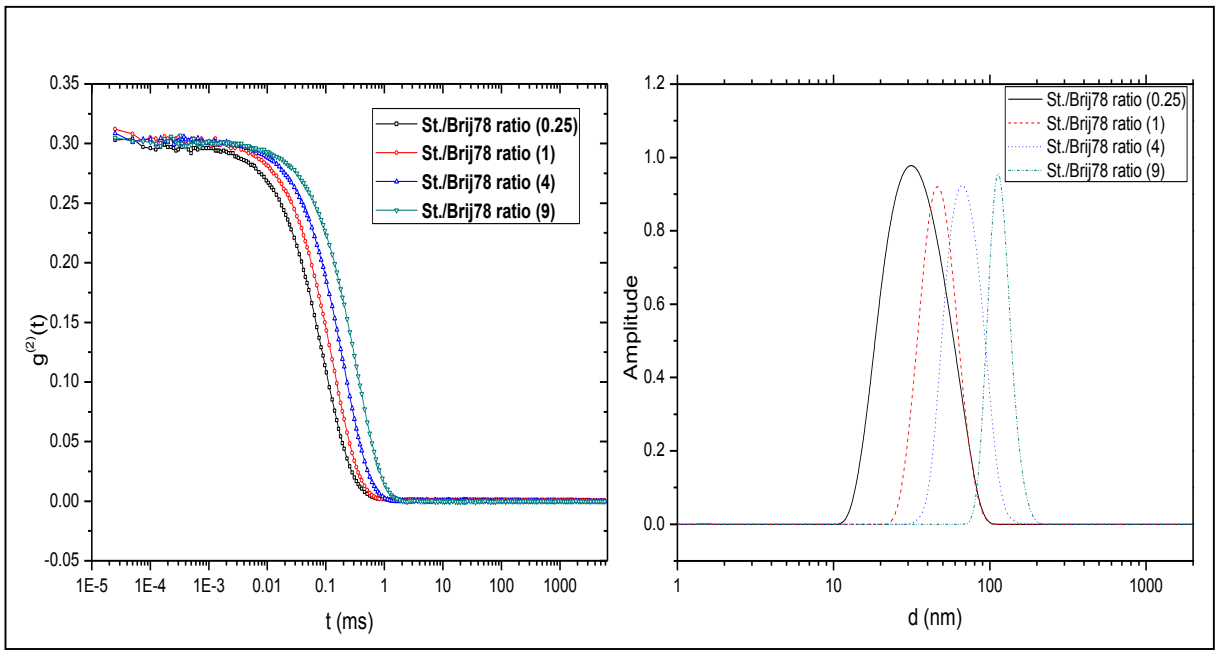

Fig. 6.5: Intensity correlation functions and corresponding hydrodynamic diameter distributions of the polystyrene nanoemulsion particles prepared at varied styrene/Brij 78 ratios, with fixed water content of 80 wt%, hexadecane 4 wt% relative to styrene, KPS 0.5 mM, polymerization temp. 70°C, 5h.

In order to further validate the obtained particle sizes from DLS, we investigated the prepared polystyrene nanoparticles by means of transmission electron microscopy as shown in figure 6.6. One can see that the polystyrene particles prepared for a monomer/surfactant ratio of 0.25 obviously have a higher polydispersity in comparison to the polymerized particles from other monomer/surfactant ratios. At the same time, the particle size increases from a mean diameter size of 30 nm to 110 nm by increasing the monomer/surfactant ration from 0.25 to 9. In general, the particle sizes and the polydispersity seen by TEM fit very well with the DLS data.

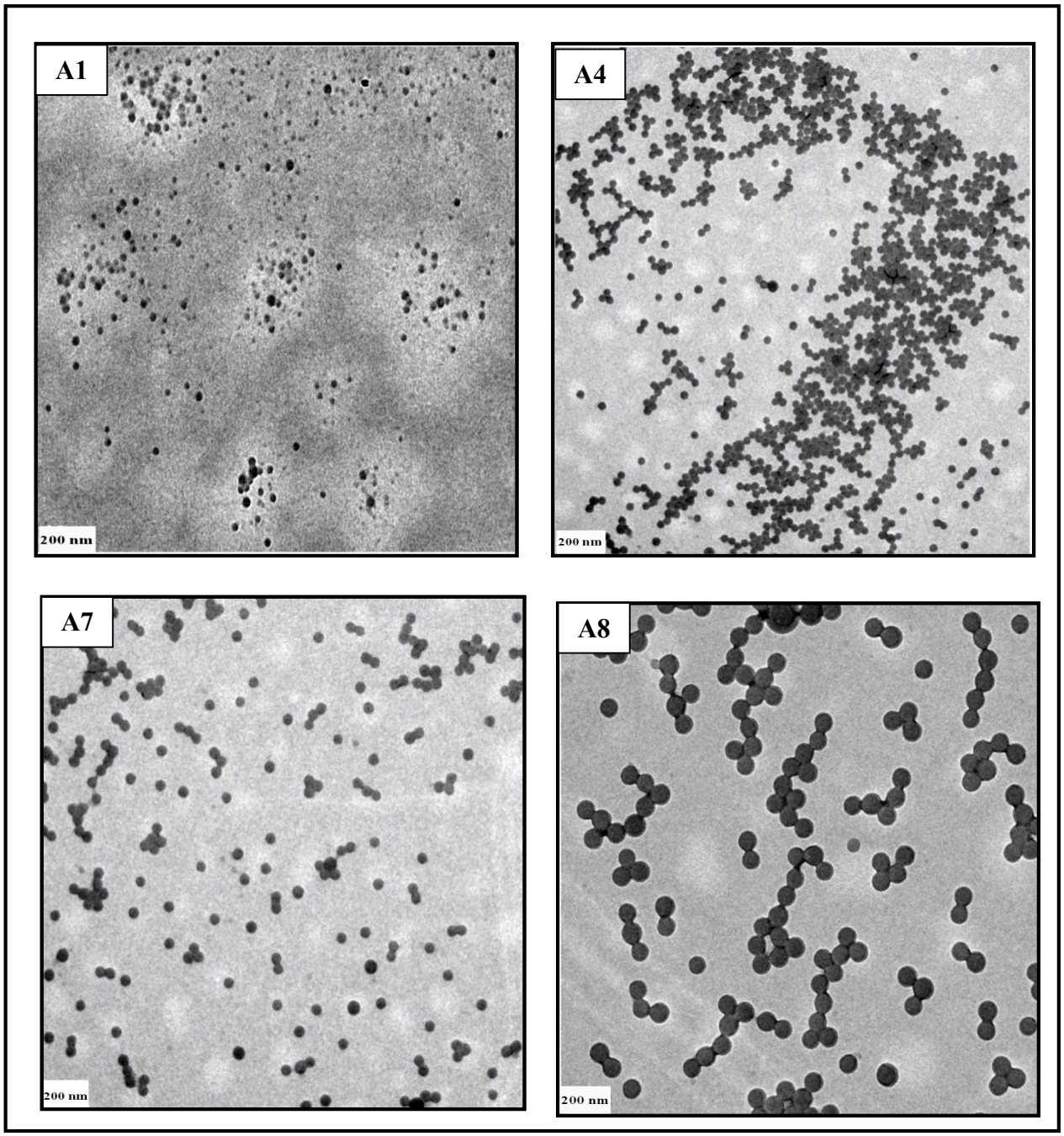

Fig.6.6: TEM images of the polystyrene latex particles prepared from PIC nanoemulsions having the following styrene/Brij 78 ratios, A1: 0.25, A4: 1, A7: 4, A8: 9 with a fixed water content of 80 wt%, hexadecane 4 wt% with respect to styrene, KPS 0.5 mM, polymerization temp. 70^{o}C, 5h.

6.2.2.3 Influence of the water dilution rate on particle size and polydispersity of the polystyrene nanoparticles.

As a further preparation parameter, we studied the influence of the water addition rate during the initial preparation of the monomer-nanoemulsions on the final particle size and polydispersity of the polystyrene particles. As seen previously for O/W nanoemulsions prepared by the PIC method of a system consisting of water–Tween20/Span20–liquid paraffin, the water addition rate plays a relevant role for droplet size and polydispersity of the nanoemulsion [49], where it was observed that the droplet size increases with the addition rate of water. Therefore, we measured by DLS the particle size and polydispersity of the polystyrene particles prepared from nanoemulsions at different water addition rates, ranging from 5 ml/h to 50 ml/h as well as addition of all water at once (which corresponds to the conventional preparation method in the case of emulsion polymerization) for a monomer/surfactant ratio of 9 and a final water content of 80 wt%. Table 6.2 shows that the particle size and polydispersity of the polystyrene particles slightly increased with the water addition rate, as found in [49]. However, the addition of water to the monomer/surfactant components at once generated polystyrene particles with a much higher polydispersity index of 0.32. In order to validate these data, TEM micrographs were obtained for the polystyrene particles prepared at a water addition rate of 5 ml/h and the ones prepared from the addition of water at once. As shown in figure 6.7, the polystyrene particles prepared on the basis of PIC nanoemulsion are nice and regular monodisperse spheres with an approximate size diameter of 110 nm, while the particles prepared by addition of water at once have obviously a much wider size distributions. In general, particle size range and polydispersity observed in figure 6.7 are in good agreement with the presented values in table 6.2. These observations demonstrate the important role of the water addition rate on the whole emulsification process during the initial preparation of the PIC nanoemulsion, where the system crosses a phase boundary as result of the change in the spontaneous curvature of surfactant to generate finally small O/W droplets which then are templated ultimately to particles by polymerization [25, 26]. Obviously, the structural transition-taking place during dilution occurs in a better-defined manner for the case of more slowly changing the spontaneous curvature of the system.

Table 6.2. Particle diameter d and polydispersity index PDI (determined by DLS) of the polystyrene nanoparticles prepared at different water addition rates using a styrene/Brij 78 ratio of 9, water content 80 wt%, hexadecane 4 wt% relative to styrene, KPS 0.5 mM, polymerization temp. 70°C, 5h.

Water Addition ratio ml/hour	d(nm)	PDI
5	**116**	**0.03**
10	**119**	**0.04**
15	**120**	**0.04**
30	**122**	**0.11**
50	**125**	**0.13**
Addition at once	**127**	**0.32**

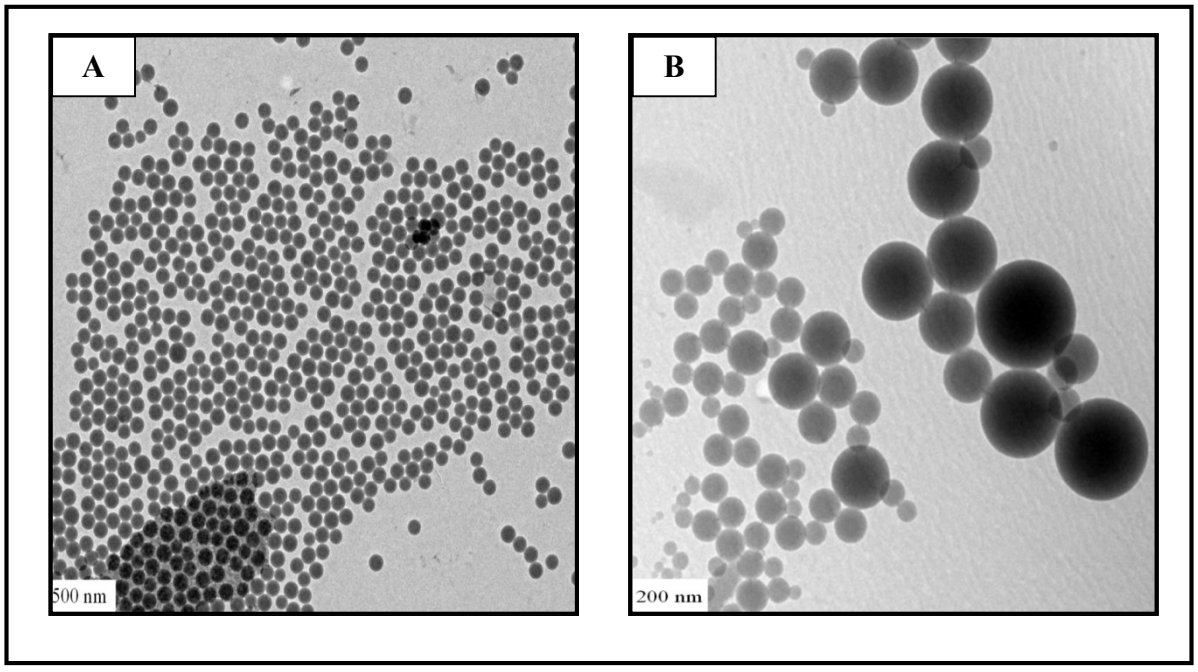

Fig.6.7: TEM images of polystyrene nanoparticles prepared using a styrene /Brij 78 mass ratio of 9, water content of 80 wt%, hexadecane 4 wt% relative to styrene. A) Water addition rate 5 ml/h, B) Water addition at once.

6.2.2.4 Colloidal stability of the nanoemulsion polystyrene particles.

The colloidal stability of the polymer particles prepared from PIC nanoemulsions is an important property for industrial practical applications, since one of our goals is the application of these polymer latexes as binders for textile printing. Therefore, we followed the change and ageing of the particle size of the polystyrene nanoemulsions prepared with different monomer/surfactant ratios as function of the storing time at 25 ^{0}C for 3 months by DLS. It should be noted that the colloidal stability of our system is mainly maintained by the steric stabilization via the non-ionic surfactant that covers the styrene particles. As shown in figure 6.8 , one can see only a negligible change in the measured hydrodynamic radius (R_h) after 3 months for the nanoemulsion particles prepared with monomer/surfactant ratios of 0.67, 2.33 and 9. Much differently, the polystyrene particles prepared from a monomer/surfactant ratio of 0.25 became a viscous gel phase after two months of storing. This may be attributed to the self-association of the excess Brij 78 with the existed latex particles since the concentration of the surfactant is 16 wt.% based on the total nanoemulsion and 4 times of monomer concentration and also to the much larger surface of the particles, which will increase its tendency for agglomeration.

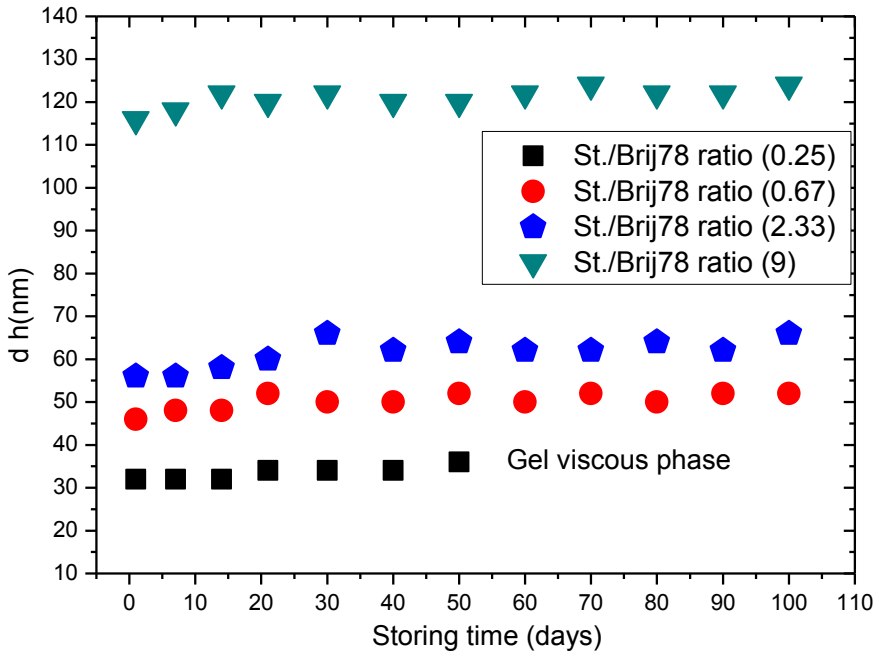

Fig.6.8: Hydrodynamic diameter d_h of the polystyrene particles as a function of the storing time (prepared at varied styrene/Brij 78 ratios, with fixed water content 80 wt%, hexadecane 4 wt% relative to styrene, KPS 0.5 mM, polymerization temp. 70^{o}C, 5h).

6.2.2.5 Synthesis of poly (styrene-co-butyl acrylate) and poly (butyl acrylate-co-methyl methacrylate) using the PIC method.

The key objectives of this work was to prepare copolymer latexes with a size range 50-100 nm and low polydispersity from monomer-nanoemulsions prepared on the basis of the low energy PIC emulsification method, which then are suitable for application in inkjet printing on textile fabrics. However, for such an application one has to have softer polymer components present than polystyrene. Therefore and to compare their applicability to the copolymer latexes prepared by the high-energy miniemulsion polymerization we prepared now corresponding copolymer latexes. For that purpose, we synthesized butyl acrylate(BA)-co-methyl methacrylate (MMA) and styrene(St.)-co-butyl acrylate(BA) using a monomer/ Brij 78 ratio of 9 with a total monomer solid content of 17 wt%. The PBA is required as it is a much softer polymer than PS and that is necessary for an efficient binder.

Table 6.3: Particle diameter d, polydispersity index PDI (determined by DLS), glass transition temperature Tg, and monomer conversion (mc) of the nanoemulsion copolymer latexes prepared with monomer/Brij 78 ratio of 9 (17 wt% monomer solid content), water content 80 wt%, hexadecane 4 wt% relative to the monomer, KPS 0.5 mM, polymerization temp. 70°C, 5h.

PIC copolymer	monomer ratio	d (nm)	PDI	Tg	mc (wt%)
BA-co-MMA	80:20	78	0.04	-32	93
St.-co-BA	50:50	105	0.06	18	95

As presented in table 6.3, we successfully prepared monodisperse (PDI ~ 0.05 from DLS) copolymer particles with size diameter of 78 nm for PBA-co-PMMA and 105 nm for PS-co-PBA in an analogous fashion as in the case of the PS nanolatexes described before. The morphology as well as the particle size and shape of the prepared copolymer latex particles were further validated by TEM images. As shown in figure 6.9 for PBA-co-PMMA and PS-co-PBA latex particles TEM corroborates the sizes and polydispersity determined by DLS.

In addition, we determined the glass transition temperature (Tg) of the two copolymer latexes because it determines the properties of the final polymer film on textile fabrics with respect to stiffness and hardness and hence its suitability for the textile application. The very low Tg of the BA-co-MMA (-32°C) in comparison to the determined Tg of the St.-co-BA (18 °C) is

attributed to the high content of the soft butyl acrylate (BA, Tg = -52 ^{O}C) in the structural composition of the copolymer.

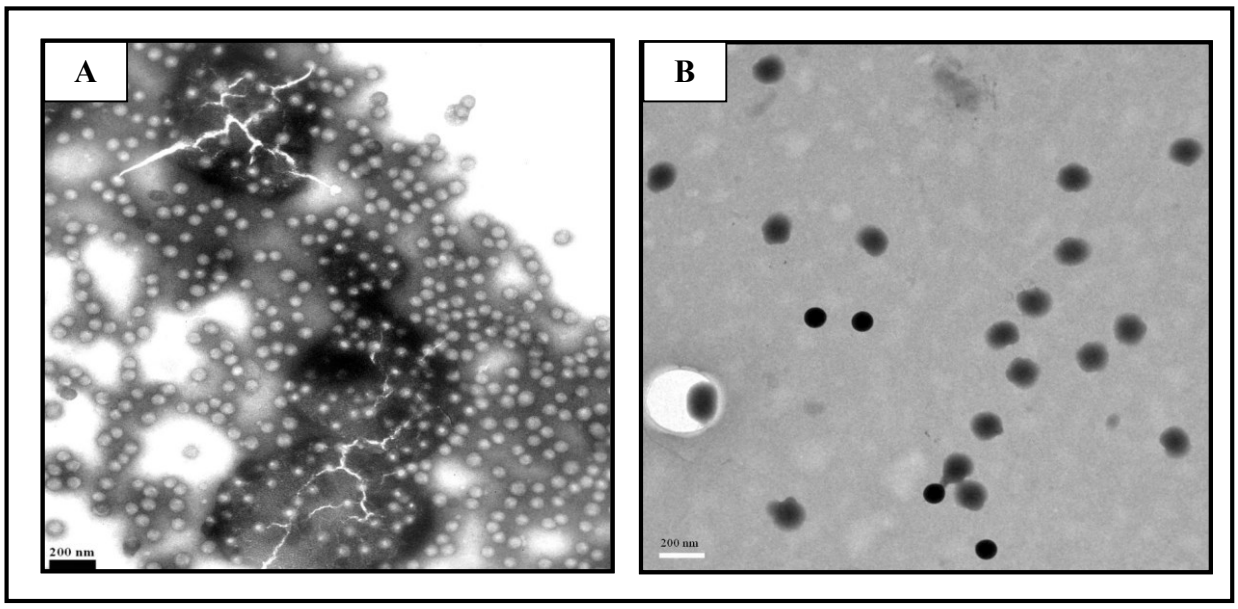

Fig.6.9: TEM images of nanoemulsion copolymer latexes prepared by using a monomer /Brij 78 ratio of 9, water content of 80 wt%, hexadecane 4 wt% relative to the monomer. A) PBA-co-PMMA /h, B) PS-co-PBA.

6.3 Application of the nanoemulsion copolymer latexes as binders for the inkjet printing process of textile cotton fabrics.

In inkjet printing, particle size and size distributions of the polymer binder and the pigment particles are of crucial importance as the main problem in this process is typically the clogging of the nozzles due to agglomeration or the presence of undesirable larger particles. Therefore, we applied our PBA-co-PMMA latexes prepared by the PIC method as binder for the inkjet printing of cotton fabrics. The PBA-co-PMMA latexes were chosen for this purpose as with their lower Tg value they are most suitable for this purpose.

The printing behavior of the formulated inks with the nanoemulsion latex as well as the assessment of the quality of the printed cotton fabrics was compared to the corresponding copolymer latex prepared by the high-energy method, i.e., the miniemulsion polymerization, and conventional emulsion latexes using the same basic copolymer structure. The different binders were formulated in pigment ink black and cyan dispersions. The nanoemulsion and miniemulsion binders were filtered easily and showed excellent printing behavior. The fastness

properties of the inkjet printed cotton fabrics towards rubbing and washing with the three different binders as well as the values of the color strength are presented in table 6.4. These results indicate that there was a slight change in the color strength of the printed fabrics with the three binders in which the miniemulsion binder that has recently been described by us [50] in chapter 4 afforded slightly better values, but the PIC binder is well comparable to the conventional commercial binder.

Table 6.4: Color strength, rubbing and washing fastness values of the inkjet printed cotton fabrics with the pigment black (PB) and cyan (PC) colors using the nanoemulsion/miniemulsion BA-co-MMA copolymer latex prepared by the low (PIC) and high-energy [50] methods.

Copolymer latex binder type	d(nm)	PDI	Color Strength (K/S)		Rubbing fastness				Washing fastness			
					dry		wet		Color change		Staining on wool	
			PB	PC	PB	PC	PB	PC	PB	PC	PB	PC
Nanoemulsion latex BA-co-MMA/Brij78	78	0.04	6.4	3.9	3	3-4	2	2	4-5	4-5	4	4-5
Miniemulsion latex BA-co-MMA/SDS	73	0.06	6.5	4.3	4	4	3	2-3	5	4-5	4-5	4-5
Conventional emulsion latex BA-co-MMA/SDS	89	0.27	6.3	4.1	3-4	3-4	2-3	2-3	4-5	4-5	4-5	4-5

The dry and wet rubbing fastness of the printed fabrics with the miniemulsion and conventional emulsion polymerization offered slightly better values, while the washing fastness was identical for all binder types. In general, inkjet printing with the nanoemulsion (PIC based) binder offered printed cotton fabrics with acceptable fastness properties and color strength, which well met the criteria of the standard tests. This means that the PIC based nanolatexes with their simple and low energy preparation method are a very suitable alternative to conventional binders that with their small particle size offer the advantage of very homogeneous film formation.

6.4 Conclusion

In this chapter, the formation of nanoemulsions based on a polymerizable oil and a nonionic surfactant (Brij 78) and their subsequent polymerization to yield nanolatexes was studied with respect to the effect of the oil/surfactant mixing ratio on the finally formed polymer latexes. The nanoemulsion here was prepared by a low energy method based on the phase inversion as a result of the concentration (composition) variation of the system components (PIC). For this purpose, the phase behavior of the surfactant/monomer system upon dilution with water was studied for the model system styrene/Brij 78. Hexadecane was added to the oil phase with a concentration 4 wt% (relative to the oil) to achieve stability against Oswald ripening. For an intermediate mixing ratio, the formation of a locally lamellar structure is observed for intermediate dilution, which upon further dilution becomes transformed into a relatively stable nanoemulsion, which is formed by the mechanism of the phase inversion concentration (PIC).

The formed monomer containing PIC nanoemulsions then can be polymerized by the addition of a radical initiator, where it was found that a water soluble initiator is more effective in yielding complete monomer conversion. The formed polymer nanolatexes are the smaller the higher the surfactant/monomer ratio, their diameter can be controlled in a systematic fashion in the range of 30 to 120 nm, and they become increasingly more polydisperse with decreasing size, which indicates a conventional homogenization of particle size with longer particle growth. It is also observed that the rate of water addition has a profound influence on the monodispersity of the particles that become more polydisperse with increasing rate of water addition, where especially a very rapid water addition leads to somewhat larger particles with much larger polydispersity

Finally, also copolymer latexes with softer polymers (PS-co-PBA and PBA-co-PMMA) were produced by the same PIC method and then applied as binders in inkjet printing on textile fabrics. Here their performance was compared to that of conventional binders and ones produced by polymerization of miniemulsions produced by a high-energy method. In general, the PIC latexes performed with a similar quality with respect to their color strength and their rubbing and washing fastness. Accordingly, they constitute a viable and interesting alternative to currently employed binders.

6.5 References:

[1] G. W. J. Lee, Th. F. Tadros. (1982). Formation and stability of emulsions produced by dilution of emulsifiable concentrates. Part I. An investigation of the dispersion on dilution of emulsifiable concentrates containing cationic and non-ionic surfactants. *Colloids Surf. A: Physicochem. Eng. Aspects, A: Physicochem. Eng. Aspects, 5,* 105-115.

[2] H. Sagitani. (1992). Phase-inversion and D-Phase emulsification. S. E. Friberg, B. Lindman (Ed.), *Organized Solutions* (pp. 259-271). New York, USA: Marcel Dekker.

[3] E. D. Sudol, M. S. El-Aasser. (1997). Miniemulsion polymerization. P. A. Lovell, M. S. El-Aasser (Ed.), *Emulsion Polymerization and Emulsion Polymers* (pp. 699-722). New York, USA: Wiley & Sons.

[4] H. Nakajima. (1997). C. Solans, H. Kunieda (Ed.). *Industrial Applications of Microemulsions*. New York, USA: Marcel Dekker.

[5] A. Forgiarini, J. Esquena, C. Gonzalez, C. Solans. (2001). Formation of nano-emulsions by low-energy emulsification methods at constant temperature. *Langmuir*, *17*, 2076-2083.

[6] T. P. Hoar, J. H. Hoar. (1943). Transparent water-in-oil dispersions: the oleopathic hydro-micelle. *Nature*, *152*, 102-103.

[7] J. Th. G. Overbeek. (1978). The First Rideal Lecture. Microemulsions, a field at the border between lyophobic and lyophilic colloids. *Faraday Discuss. Chem. Soc.*, *65*, 7-19.

[8] H. Nakajima, M. Okabe, S. Tomomasa. (1992). Emulsified composition. *U.S. Patent, 5098606.*

[9] T. Förster, S. Heinen, B. Heide. (1997). Sugar surfactant-containing o/w micro-emulsions and process for preparing the same. *European Patent Office, WO9723192 (A1)*.

[10] S. Restle, D. Cauwet-Martin. (1998). Nanoemulsion Based On Non-ionic and Cathionic Amphyphylic Lipides and Application Thereof. European Patent Office, PL323127 (A1).

[11] D. I. Jon, D. I. Prettypaul, M. J. Benning, K. S. Narayanan, R. M. Ianniello. (1999). Stabilized concentrates of water unstable AZA compounds and o/w miniemulsions thereof. *European Patent Office, WO9919256 (A2)*.

[12] M. Antonietti, K. Landfester. (2000). Osmotic stabilization of micro- or mini-emulsions for use in the production of nano-hybrid polymer particles involves using a surfactant in combination with a water-insoluble compound as co-surfactant. *European Patent Office, DE19852784 (A1)*.

[13] M. S. El-Aasser, C. D. Lack, J. W. Vanderhoff. (1988). The miniemulsification process-different form of spontaneous emulsification. *Colloids Surf. A: Physicochem. Eng. Aspects, 29*, 103-118.

[14] S. Tomomasa, M. Kochi, H. Nakajima. (1988). Microemulsion Formation in Two-phase Region Preparation Method and Stability. *J. Jpn. Oil Chem. Soc.*, *37*, 1012-1017.

[15] T. Forster, W. von Rybinski, A. Wadle. (1995). Influence of microemulsion phases on the preparation of fine-disperse emulsions. *Adv. Colloid Interface Sci.*, *58*, 119-149.

[16] T. Förster, W. von Rybinski, H. Tesmann, A. Wadle. (1994). Calculation of optimum emulsifier mixtures for phase inversion emulsification. *Int. J. Cosm. Sci.,* 16, 84-92.

[17] S. Benita, M. Y. Levy. (1993). Submicron emulsions as colloidal drug carriers for intravenous administration: Comprehensive physicochemical characterization. *J. Pharm. Sci*, *82*, 1069-1079.

[18] H. L. Rosano, T. Lan, A. Weiss, J. H. Whittam, W. E. F. Gerbacia. (1981). Unstable microemulsions. *J. Phys. Chem.,* 468-473.

[19] A. J. F. Sing, A. Graciaa, J. Lachaise, P. Brochette, J. L. Salager. (1999). Interactions and coalescence of nanodroplets in translucent O/W emulsions. *Colloids Surf. A: Physicochem. Eng. Aspects, 152*, 31-39.

[20] M. Antonietti, K. Landfester. (2002). Polyreactions in miniemulsions. *Progress in Polymer Science, 27*, 689-757.

[21] J. M. Asua. (2002).Miniemulsion polymerization. *Prog. Polym. Sci.,* 27, 1283-1346.

[22] T. Tadros, P. Izquierdo, J. Esquena, C. Solans. (2004). Formation and stability of nano-emulsions. *Adv. Colloid Interface Sci., 108–109*,303-318.

[23] K. Shinoda, H. Saito. (1969). The Stability of O/W type emulsions as functions of temperature and the HLB of emulsifiers: The emulsification by PIT-method. *J. Colloid Interface Sci.*, *30,* 258-263.

[24] N. Anton, H. Mojzisova, E. Porcher, J.P. Benoit, P. Saulnier. (2010). Reverse micelle-loaded lipid nano-emulsions: New technology for nano-encapsulation of hydrophilic materials. *Int. J. Pharm., 398,* 204-209.

[25] A. Forgiarini, J. Esquena, C. González, C. Solans. (2001). Formation of Nano-emulsions by Low-Energy Emulsification Methods at Constant Temperature *Langmuir, 17*, 2076-2083.

[26] I. Solè, A. Maestro, C. M. Pey, C. González, C. Solans, J. M. Gutiérrez. (2006). Nano-emulsions preparation by low energy methods in an ionic surfactant system. *Colloids Surf. A: Physicochem. Eng. Aspects, 288,* 138-143.

[27] K. Roger, B. Cabane, U. Olsson. (2010). Emulsification through Surfactant Hydration: The PIC Process Revisited. *Langmuir 27*, 604-611.

[28] P. Heunemann, S. Prévost, I. Grillo, C.M. Marino, J. Meyer, M. Gradzielski, Formation and structure of slightly anionically charged nanoemulsions obtained by the phase inversion concentration (PIC) method", Soft Matter 7, 5697-5710 (2011)].

[29] L. Wang, K. J. Mutch, J. Eastoe, R. K. Heenan, J. Dong. (2008). Nanoemulsions Prepared by a Two-Step Low-Energy Process. *Langmuir*, *24,* 6092-6099.

[30] K. Landfester. (2006). Synthesis of colloidal particles in miniemulsions. *Annu. Rev. Mater. Res.,* 36, 231-279.

[31] J. M. Asua. (2002). Miniemulsion polymerization. *Prog. Polym. Sci*. *27*, 1283-1346.

[32] F. J. Schork, Y. W. Luo, W. Smulders, J. P. Russum, A. Butte, K. Fontenot. (2005). Miniemulsion Polymerization. *Adv. Polym. Sci*., *175*, 129-255.

[33] C. K. Weiss, U. Ziener, K. Landfester. (2007). A route to nonfunctionalized and functionalized poly (n-butylcyanoacrylate) nanoparticles: preparation in miniemulsion. *Macromolecules*, 40, 928-938.

[34] S. Cauvin, F. Ganachaud. (2004). On the Preparation and Polymerization of p-Methoxystyrene Miniemulsions in the Presence of Excess Ytterbium Triflate. *Macromol. Symp*., *215*, 179-190.

[35] S. Cauvin, F. Ganachaud, M. Moreau, P. Hemery. (2005). High molar mass polymers by cationic polymerisation in emulsion and miniemulsion. *Chem. Commun*., 2713-2715.

[36] R. Soula, B. Saillard, R. Spitz, J. Claverie, M. F. Llaurro, C. Monnet. (2002). Catalytic Copolymerization of Ethylene and Polar and Nonpolar α Olefins in Emulsion, *Macromolecules*, *35*, 1513-1523.

[37] L. Spernath, S. Magdassi. (2007). A new method for preparation of poly-lauryl acrylate nanoparticles from nanoemulsions obtained by the phase inversion temperature process. *Polym. Adv. Technol.*, 18, 705-711.

[38] L. Spernath, O. Regev, Y. Levi-Kalisman, S. Magdassi. (2009). Phase transitions in O/W lauryl acrylate emulsions during phase inversion, studied by light microscopy and cryo-TEM. *Colloids Surf. A: Physicochem. Eng. Aspects*, *332*, 19-25.

[39] J. Galindo-Alvarez, D. Boyd, P. Marchal, C. Tribet, P. Perrin, E. Marie-Bégué.(2011) Miniemulsion polymerization templates: A systematic comparison between low energy emulsification (Near-PIT) and ultrasound emulsification methods. *Colloids Surf. A: Physicochem. Eng. Aspects*, *374*,134-141.

[40] S.Cheng, P. B. Zetterlund. (2010). Miniemulsion Polymerization Based on Low Energy Emulsification with Preservation of Initial Droplet Identity. *Macromolecules, 43*, 7905-7907.

[41] V. Sadtler, M. Rondon-Gonzalez, A. Acrement, L. Choplin, E. Marie. (2010). PEO-Covered Nanoparticles by Emulsion Inversion Point (EIP) Method *Macromol. Rapid Commun., 31*, 998-1002.

[42] K. Mohlin, K. Holmberg, J. Esquena, C. Solans. (2003). Study of low energy emulsification of alkyl ketene dimer related to the phase behavior of the system. *Colloids Surf. A: Physicochem. Eng. Aspects*, *218*, 189-200.

[43] M. J. Rang, C. A. Miller. Spontaneous Emulsification of Oils Containing Hydrocarbon, Nonionic Surfactant, and Oleyl Alcohol. *J. Colloid Interface Sci., 209*, 179-192.

[44] H. Kunieda, K.J. Shinoda. (1982). Phase behavior in systems of nonionic surfactant/water/oil around the hydrophile–lipophile-balance-temperature (HLB temperature) *J. Dispersion Sci. Technol*., *3,* 233-244.

[45] M. Kahlweit, R. Strey, G. Busse. (1991). Effect of Alcohols on the Phase Behavior of Microemulsions. *J. Phys. Chem., 95*, 5344-5352.

[46] H. Kunieda, K. Shinoda. Formation of vesicles and microemulsions in a water/tetraethylene glycol dodecyl ether/dodecane system. *Langmuir, 7*, 1915-1919.

[47] R. Strey, R. Schomacker, D. Roux, F. Nallet, U. Olsson. (1990). Dilute lamellar and L_3 phases in the binary water–$C_{12}E_5$ system. *J. Chem. Soc*., *Faraday Trans.*, *86,* 2253-2261.

[48] K. Landfester, N. Bechthold, S. Förster, M. Antonietti. (1999). Evidence for the preservation of the particle identity in miniemulsion polymerization. *Macromol. Rapid Commun.*, *20*, 81-84.

[49] C. M. Pey, A. Maestro, I. Sole, C. Gonzalez, C. Solans, J. M. Gutierrez. (2006). Optimization of nano-emulsions prepared by low-energy emulsification methods at constant temperature using a factorial design study. *Colloids Surf. A: Physicochem. Eng. Aspects, 288*,144-150.

[50] M. Elgammal, S. Prévost, R.Schweins, R. Schneider, M. Gradzielski (2014). Nanosized latexes for textile printing applications obtained by miniemulsion polymerization**.** *Colloid Polym. Sci.***,** *292*, 1487-1500.

7. Conclusion

This thesis dealt with the preparation of nanosized copolymer latexes by the polymerization in miniemulsions (nanoemulsions) prepared by the classical high energy and the low energy phase inversion concentration (PIC) methods. In addition, the encapsulation of various organic pigments with copolymer latex layers was carried out on the basis of miniemulsion polymerization. The obtained nanosized copolymer particles or encapsulated pigments have been successfully used as binders for textile printing applications.

The first part, chapter 4, we studied the preparation of nanosized copolymer latexes in a diameter size range between (50-100 nm) by the classical miniemulsion polymerization method. The copolymer latexes composed mainly of a high content of the soft butyl acrylate monomer (BA) and a low content of the hard methyl methacrylate (MMA) monomer. The addition of small amounts of functional monomers such as methacrylic acid MAA and N-methylol acrylamide NMA to some miniemulsion recipes allowed to impart cross-linking sites and functionality to the copolymer chains. The particle size analysis, structure characterization and thermal properties of the latexes were investigated by many analytical techniques such as dynamic light scattering (DLS), small angle neutron scattering (SANS), transmission electron microscopy (TEM), gel permeation chromatography (GPC), and differential scanning calorimetry (DSC). The optimized miniemulsion latexes were applied successfully as binders for the pigment printing and inkjet printing of cotton fabrics. The main objective of this part was to examine the application of the miniemulsion latexes as binders in the textile printing processes in order to reduce the risk of agglomeration and cloaking of the printer screens and nozzles during the printing process. This shortcoming might result from the undesired particle size and shape of the conventional binders and other ingredients. The evaluation of the printed fabrics showed that the miniemulsion binders with their smaller size offered technological advantages over the conventional processes for the conventional and inkjet printing processes as well as the better print properties. Accordingly, by optimized use of the miniemulsion method one is not only able to control the particle size but also to improve the properties of these latexes for textile applications.

In chapter 5, we studied systematically the encapsulation of the organic pigments with a copolymer latex layer by the miniemulsion polymerization method. We aimed at reducing the tendency for pigment agglomeration as a result of the pigment particles interaction, hence improving the stability of the pigment particles in aqueous ink dispersions. Such polymer-encapsulated pigments then can be applied for inkjet printing without addition of separate binder additives, thereby reducing the risk of unfavorable interactions between the separate

latex and pigment particles. We studied the encapsulation of C.I. Pigment red 112, an organic azo-naphthalene dye, systematically by a miniemulsion polymerization of pigment/butyl acrylate-co-methyl methacrylate (BA-MMA) or styrene-co-butyl acrylate (St-BA) copolymers. SDS as anionic surfactant and hexadecane as co-stabilizer stabilized the pigment dispersions before encapsulation. The ratio of monomer to pigment (latex/pigment) was varied in order to find optimum conditions for the preparation of self-curable hybrid pigment inks for the textile inkjet printing application.

The particle size and polydispersity of the pigment dispersions and pigment hybrid latex particles were investigated by dynamic light scattering (DLS), disc centrifugation, and transmission electron microscopy (TEM). The determined particle sizes of the encapsulated pigment particles with the different latex/pigment ratios were bigger than the non-encapsulated ones and increasing systematically with the latex content. The efficiency of the polymer encapsulation and thermal properties of the hybrid inks were studied by thermogravimetric analysis (TGA) and differential scanning calorimetry (DSC). The encapsulation efficiencies, as determined from TGA, increase when increasing the polymer content. For instance, the variation of the latex/pigment ratio from 0.11 to 0.66 using BA-MMA as copolymer latex increases the encapsulation efficiency from 20% to 37%, while the encapsulation efficiency increases from 26% to 51% using St-BA copolymer latex by increasing the same latex/pigment ratio. TEM images show that the encapsulated pigment particles are somehow coated with polymer layer shells, which probably indicate a successful encapsulation.

The long-term stability of the encapsulated hybrid pigment inks seen by DLS can be explained by the large negative zeta potential, where a somewhat higher stability is seen for the St-BA case, which can be attributed to the fact that St-BA is at room temperature below the glass transition temperature and thereby less likely to aggregate irreversibly at is surface. The viscosities of the encapsulated hybrid inks were reduced when compared to conventional inks having separately dispersed polymer latex and pigment particles, which ultimately enhance the applicability of the inks. The measured surface tension of the encapsulated pigments is well suited for the inkjet printing application. From the evaluation of the inkjet printing of cotton fabrics with different encapsulated and non-encapsulated pigment colors it can be concluded that the encapsulated inks without addition of separate polymer latex binder generate fully satisfying performance in terms of color strength, rubbing and washing fastness in comparison to the non-encapsulated conventional inks, while at the same time avoiding problems of clogging and colloidal instability. Therefore the latex encapsulation of pigments by the method of miniemulsion polymerization is a new way to employ polymer coated pigments in successful

printing on carbohydrate fibers like cotton. Due to the smaller size of the polymer/pigment hybrids employed and their colloidal stability, they offer promising perspectives for the increasingly important technique of inkjet printing.

In the last part, chapter 6, the formation of nanoemulsions based on a polymerizable oil and a nonionic surfactant (Brij 78) and their subsequent polymerization to yield nanolatexes was studied with respect to the effect of the oil/surfactant mixing ratio on the finally formed polymer latexes. For this purpose, the phase behavior of the surfactant/monomer system upon dilution with water was studied for the model system styrene/Brij 78. For an intermediate mixing ratio, the formation of a locally lamellar structure is observed which upon further dilution becomes transformed into a relatively stable nanoemulsion, which is formed by the mechanism of the phase inversion concentration (PIC).

The formed monomer containing PIC nanoemulsions then can be polymerized by the addition of a radical initiator, where it was found that a water-soluble initiator is more effective in yielding complete monomer conversion. The formed polymer nanolatexes are the smaller the higher the surfactant/monomer ratio, their diameter can be controlled in a systematic fashion in the range of 30 to 120 nm, and they become increasingly more polydisperse with decreasing size, which indicates a conventional homogenization of particle size with longer particle growth. It is also observed that the rate of water addition has a profound influence on the monodispersity of the particles that become more polydisperse with increasing rate of water addition, where especially a very rapid water addition leads to somewhat larger particles with much larger polydispersity

Finally, also copolymer latexes with softer polymers (PS-co-PBA and PBA-co-PMMA) were produced by the same PIC method and then applied as binders in inkjet printing on textile fabrics. Here their performance was compared to that of conventional binders and ones produced by polymerization of miniemulsions produced by a high energy method. In general, the PIC latexes performed with a similar quality with respect to their color strength and their rubbing and washing fastness. Accordingly, they constitute a viable and interesting alternative to currently employed binders.

Publications

[1] M. Elgammal, S. Prévost, R.Schweins, R. Schneider, M. Gradzielski (2014). Nanosized latexes for textile printing applications obtained by miniemulsion polymerization**.** *Colloid Polym. Sci.***,** *292*, 1487-1500, DOI: 10.1007/s00396-014-3192-1
Contains parts of chapter 4

[2] M. Elgammal, R. Schneider, M. Gradzielski *(2015).* Preparation of latex nanoparticles using nanoemulsions obtained bythe phase inversion composition (PIC) method and their applicationin textile printing. *Colloids and Surfaces A: Physicochem. Eng. Aspects, 470, 70–79.*
Contains chapter 6

[3] M. Elgammal, R. Schneider, M. Gradzielski, "Development of self-curable hybrid pigment inks by miniemulsion polymerization for inkjet printing of cotton fabrics", *Dyes and Pigments. Submitted.*
Contains parts of chapter 5